GW20170814 (BBH)
Sky location : 3 detectors

1160 square degrees shrinks to 60

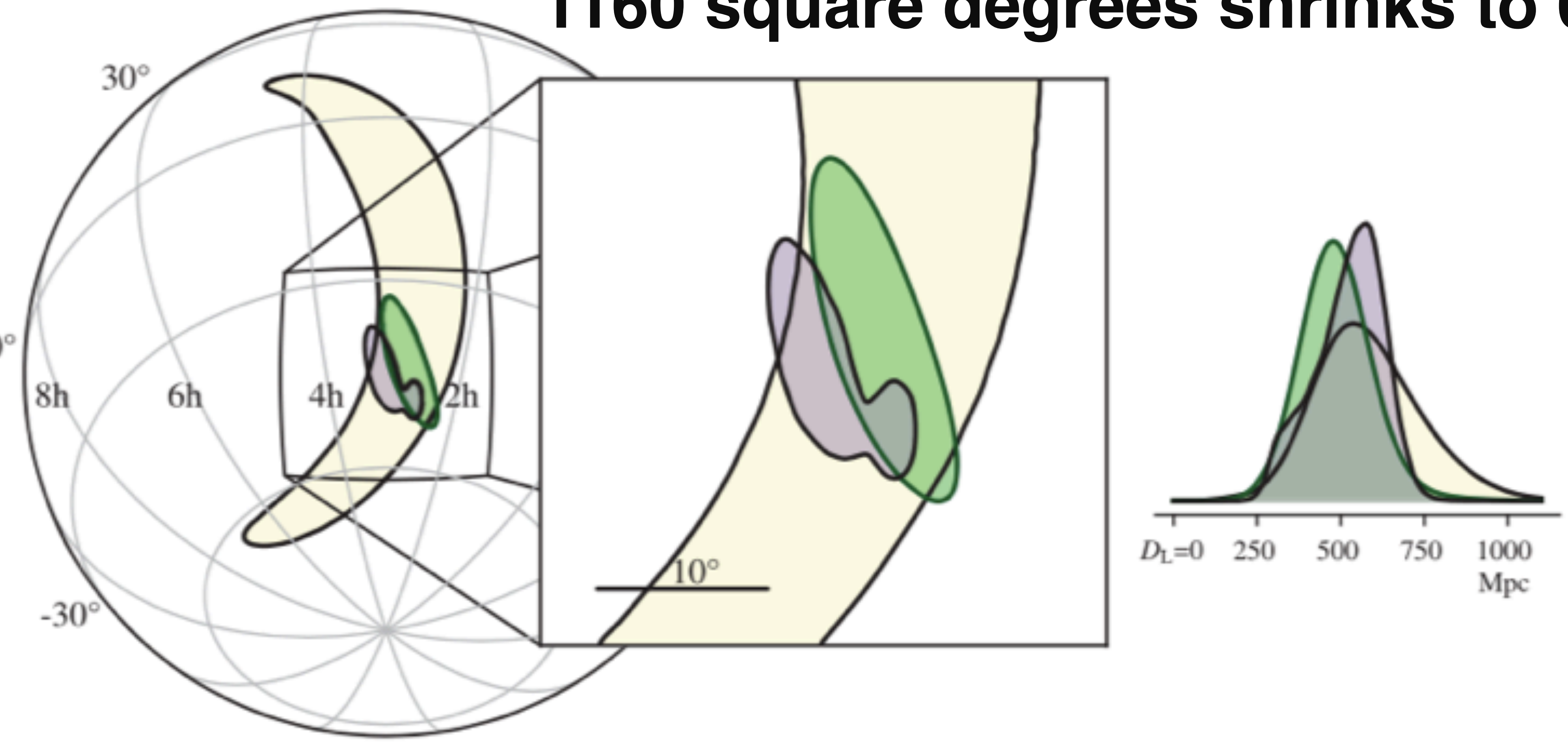

FIG. 3. Localization of GW170814. The rapid localization using data from the two LIGO sites is shown in yellow, with the inclusion of data from Virgo shown in green. The full Bayesian localization is shown in purple. The contours represent the 90% credible regions. The left panel is an orthographic projection and the inset in the center is a gnomonic projection; both are in equatorial coordinates. The inset on the right shows the posterior probability distribution for the luminosity distance, marginalized over the whole sky.

…….. as of 2017 Aug 14

Skymap movement

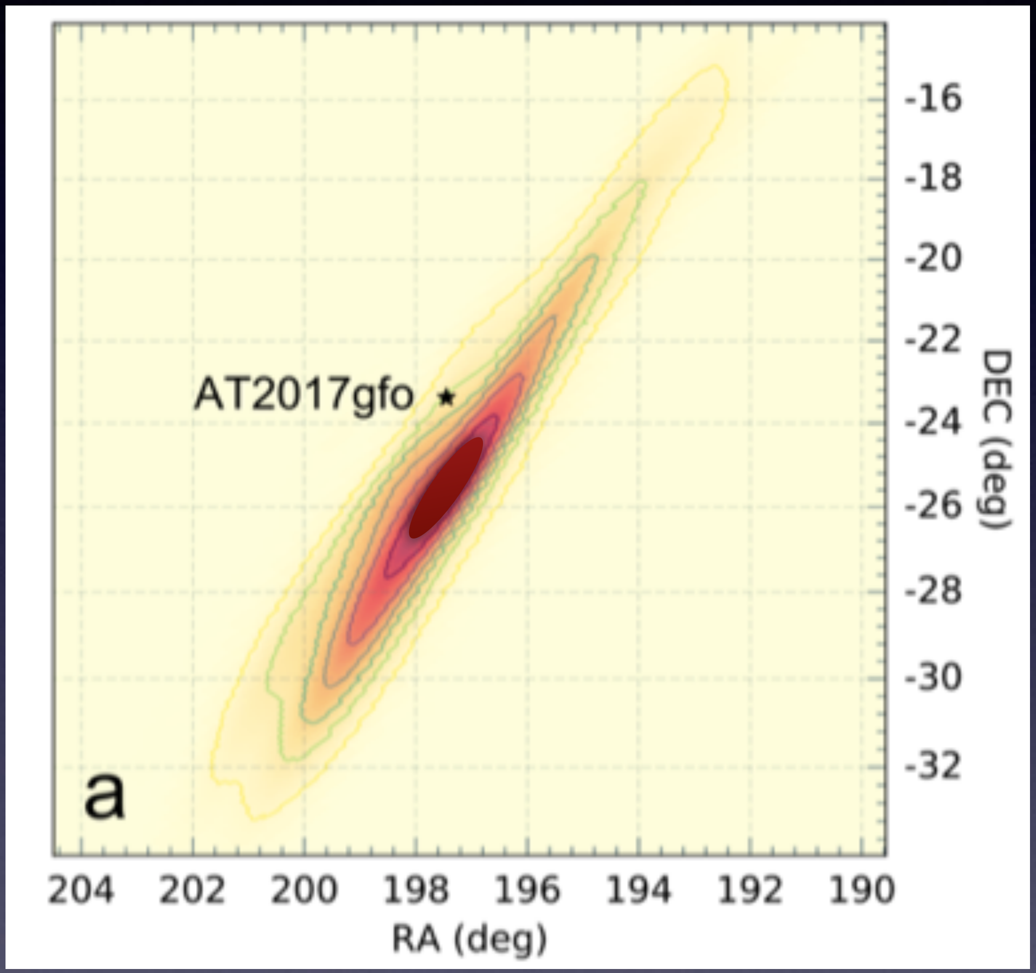

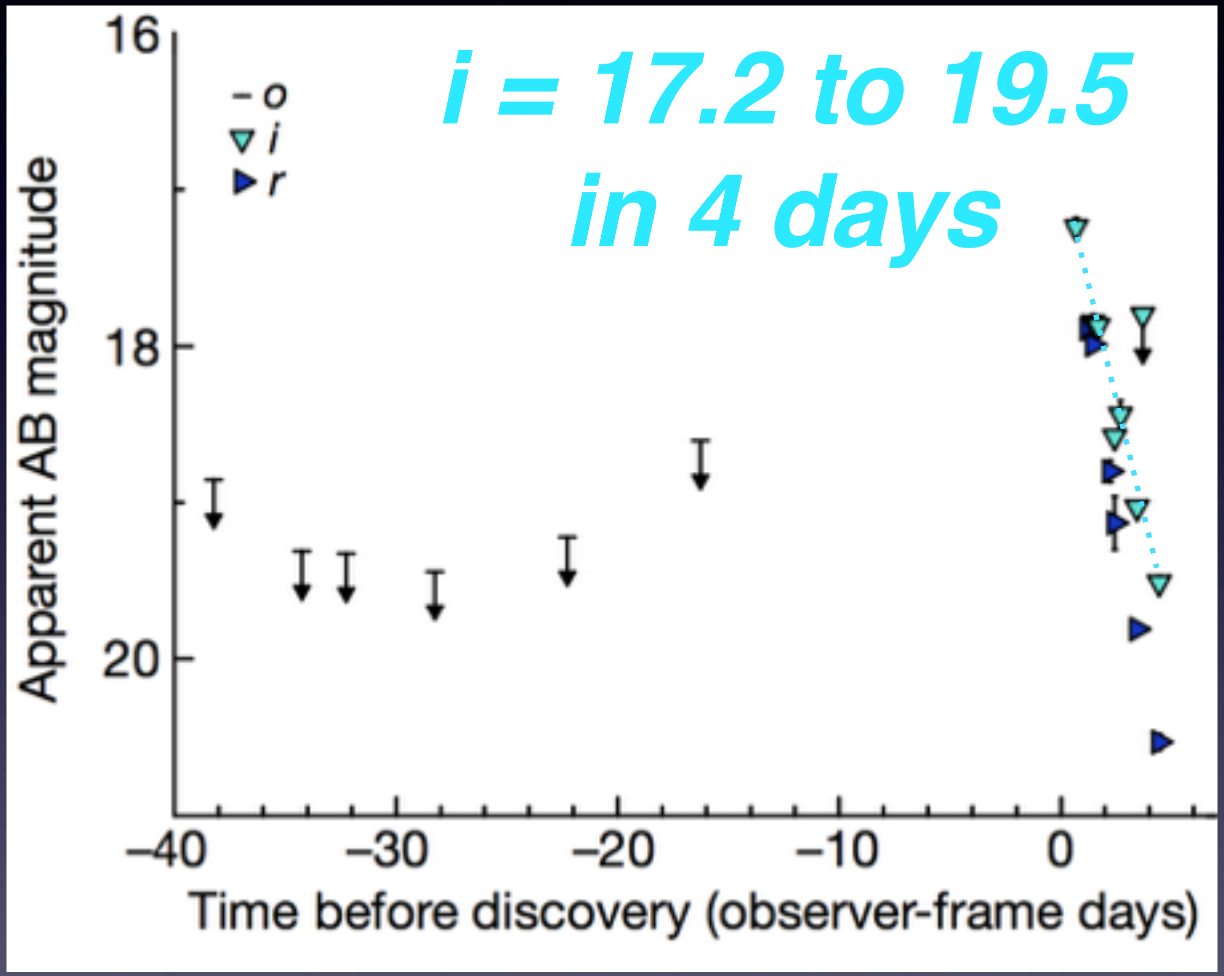

Skymap movement

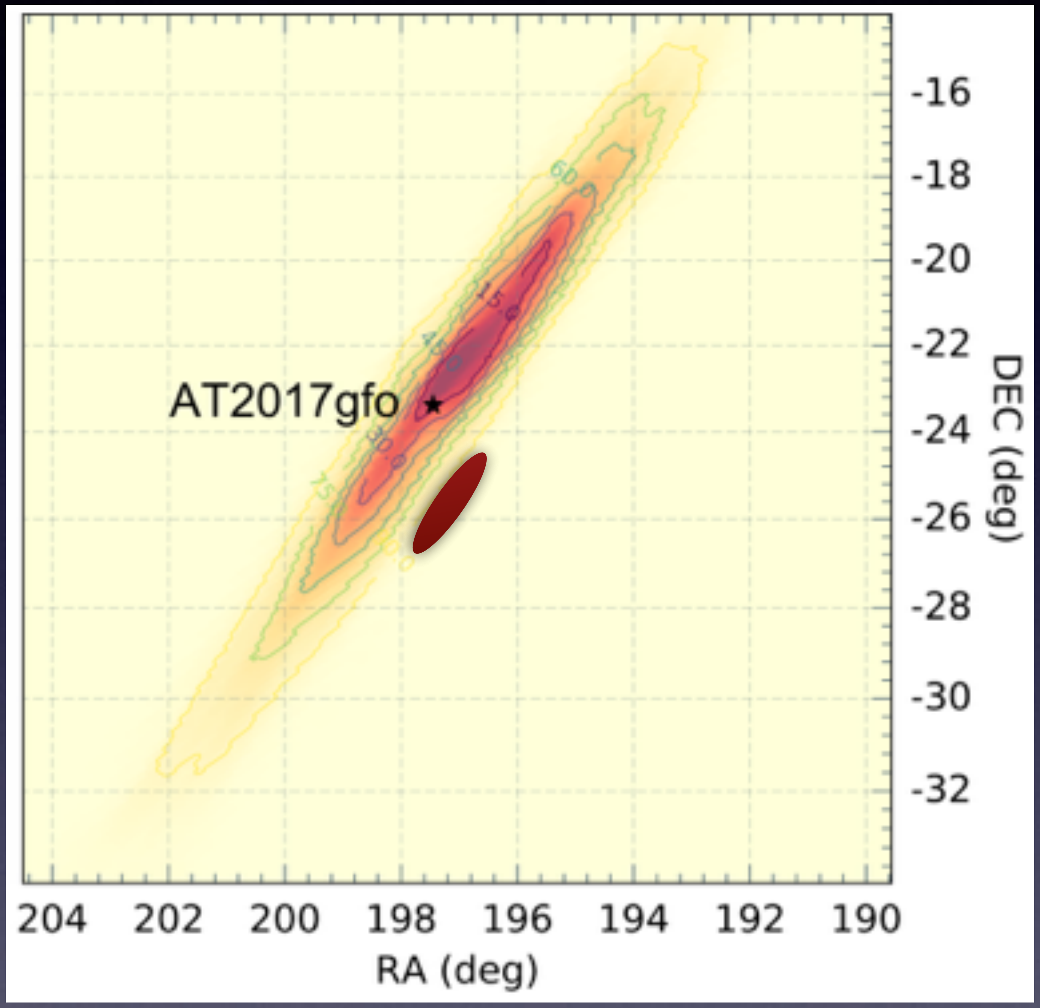

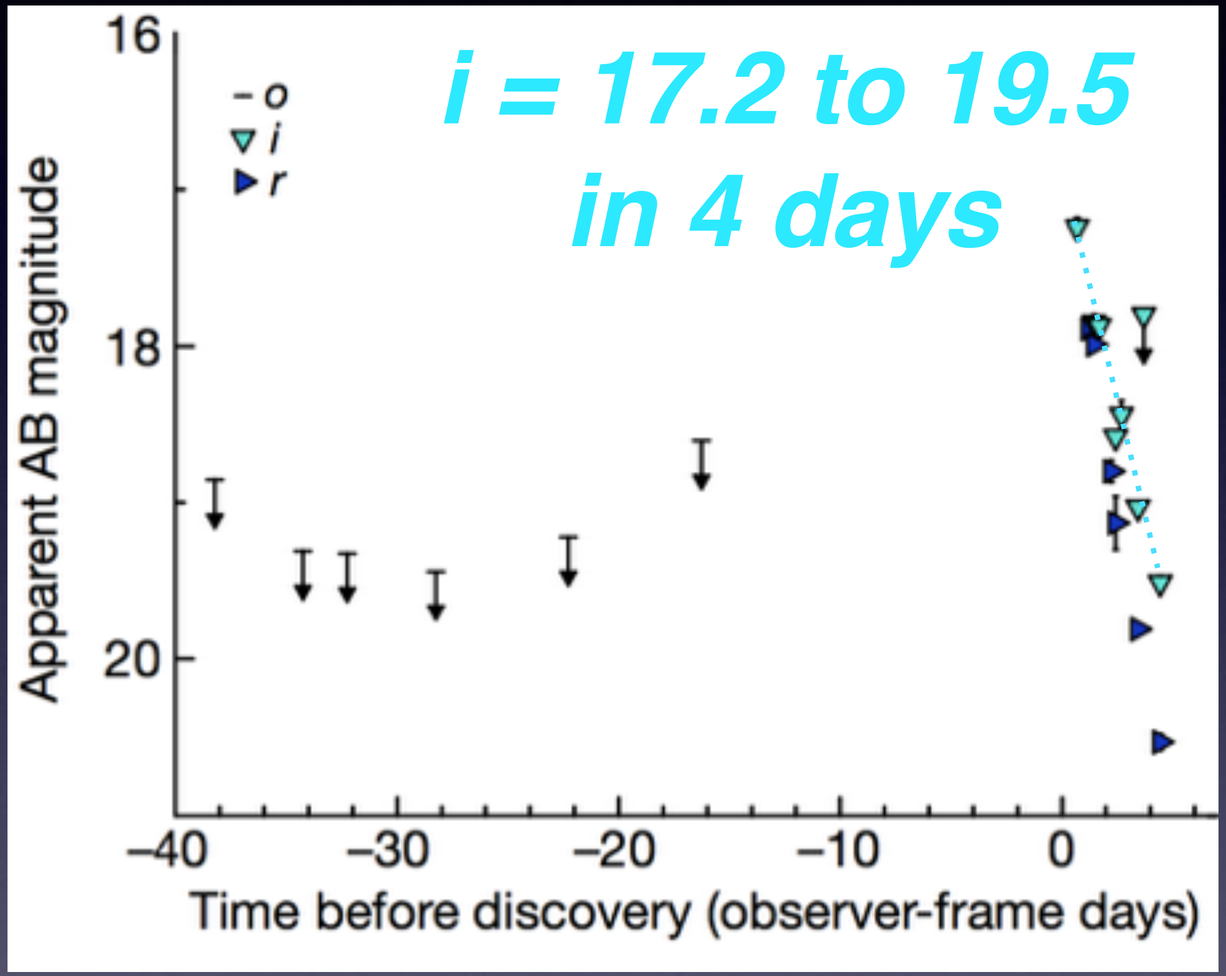

Skymap movement

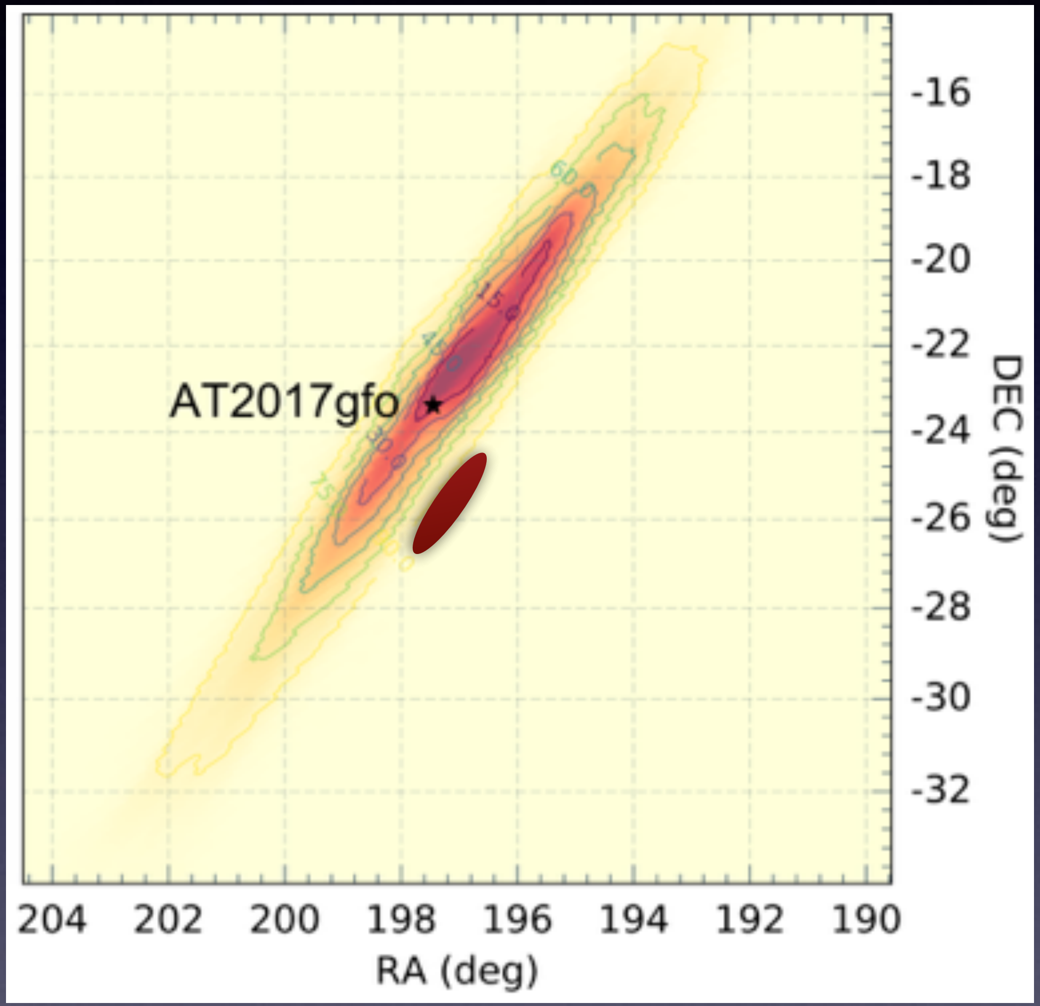

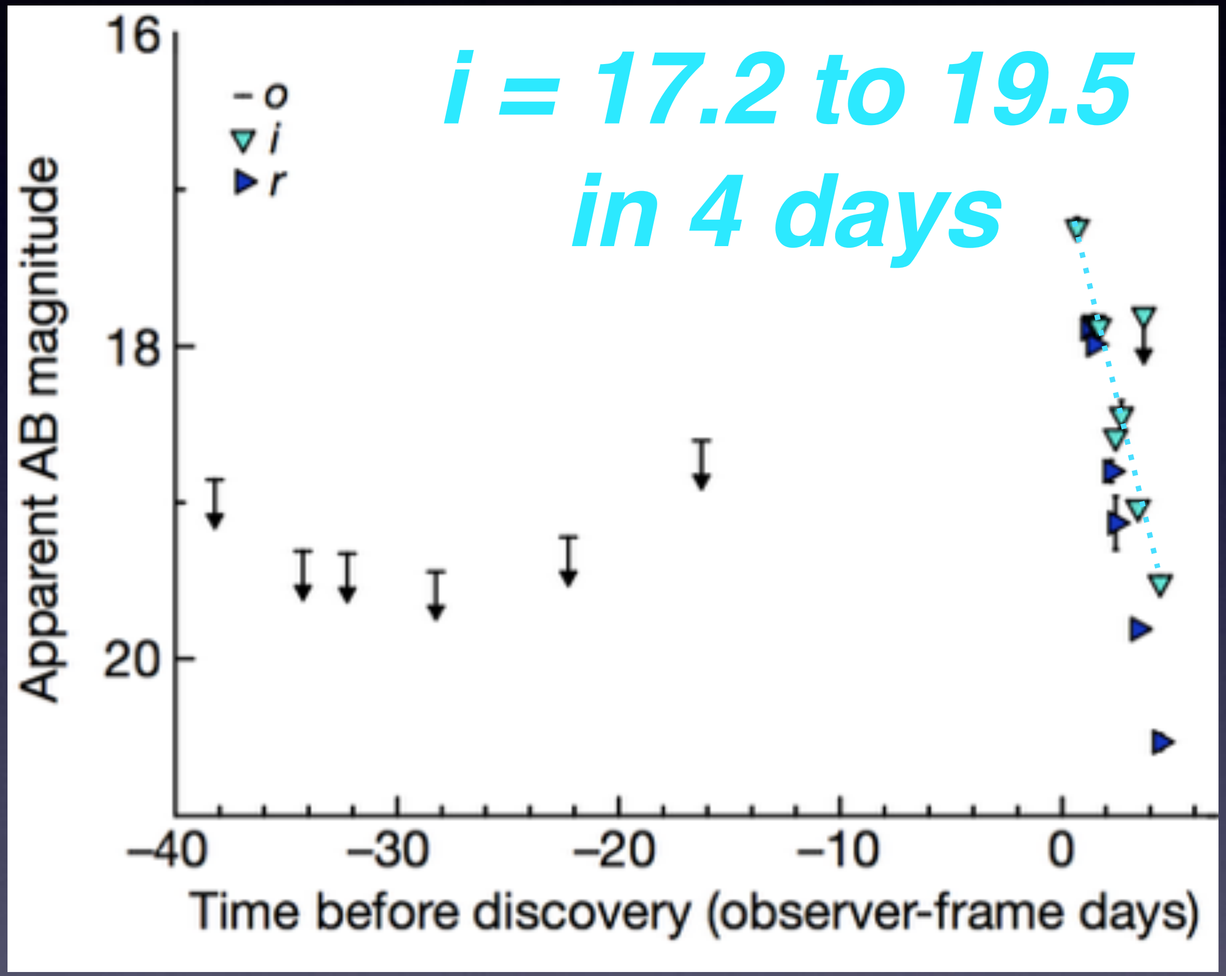

- **Skymaps from LIGO-Virgo Collaboration - 3 degree offset !**
- Smartt S.J. et al. Nature, 2017, 551, 75 : ATLAS upper limits, GROND, ESO-NTT, Pan-STARRS, 1.5m Boyden,

Optical and near-infrared kilonova emission - light r-process composition

S. Smartt, A. Jerkstrand, G. Leloudas, M. Coughlin, E. Kankare

S. J. Smartt[1], T.-W. Chen[2], A. Jerkstrand[3], M. Coughlin[4], E. Kankare[1], S. A. Sim[1], M. Fraser[5], C. Inserra[6], K. Maguire[1], K. C. Chambers[7], M. E. Huber[7], T. Krühler[2], G. Leloudas[8], M. Magee[1], L. J. Shingles[1], K. W. Smith[1], D. R. Young[1], J. Tonry[7], R. Kotak[1], A. Gal-Yam[9], J. D. Lyman[10], D. S. Homan[11], C. Agliozzo[12,13], J. P. Anderson[14], C. R. Angus[6], C. Ashall[15], C. Barbarino[16], F. E. Bauer[13,17,18], M. Berton[19,20], M. T. Botticella[21], M. Bulla[22], J. Bulger[7], G. Cannizzaro[23,24], Z. Cano[25], R. Cartier[6], A. Cikota[26], P. Clark[1], A. De Cia[26], M. Della Valle[21,27], L. Denneau[7], M. Dennefeld[28], L. Dessart[29], G. Dimitriadis[6], N. Elias-Rosa[30], R. E. Firth[6], H. Flewelling[7], A. Flörs[3,26,31], A. Franckowiak[32], C. Frohmaier[33], L. Galbany[34], S. González-Gaitán[35], J. Greiner[2], M. Gromadzki[36], A. Nicuesa Guelbenzu[37], C. P. Gutiérrez[6], A. Hamanowicz[26,36], L. Hanlon[5], J. Harmanen[38], K. E. Heintz[8,39], A. Heinze[7], M.-S. Hernandez[40], S. T. Hodgkin[41], I. M. Hook[42], L. Izzo[25], P. A. James[15], P. G. Jonker[23,24], W. E. Kerzendorf[26], S. Klose[37], Z. Kostrzewa-Rutkowska[23,24], M. Kowalski[32,43], M. Kromer[44,45], H. Kuncarayakti[38,46], A. Lawrence[11], T. B. Lowe[7], E. A. Magnier[7], I. Manulis[9], A. Martin-Carrillo[5], S. Mattila[38], O. McBrien[1], A. Müller[47], J. Nordin[43], D. O'Neill[1], F. Onori[23,24], J. T. Palmerio[48], A. Pastorello[49], F. Patat[26], G. Pignata[12,13], Ph. Podsiadlowski[50], M. L. Pumo[49,51,52], S. J. Prentice[15], A. Rau[2], A. Razza[14,53], A. Rest[54,55], T. Reynolds[38], R. Roy[16,56], A. J. Ruiter[57,58,59], K. A. Rybicki[36], L. Salmon[5], P. Schady[2], A. S. B. Schultz[7], T. Schweyer[2], I. R. Seitenzahl[57,58], M. Smith[6], J. Sollerman[16], B. Stalder[60], C. W. Stubbs[61], M. Sullivan[6], H. Szegedi[62], F. Taddia[16], S. Taubenberger[3,26], G. Terreran[49,63], B. van Soelen[62], J. Vos[40], R. J. Wainscoat[7], N. A. Walton[41], C. Waters[7], H. Weiland[7], M. Willman[7], P. Wiseman[2], D. E. Wright[64], Ł. Wyrzykowski[36] & O. Yaron[9]

nature **551,** 75–79 (2017) doi:10.1038/

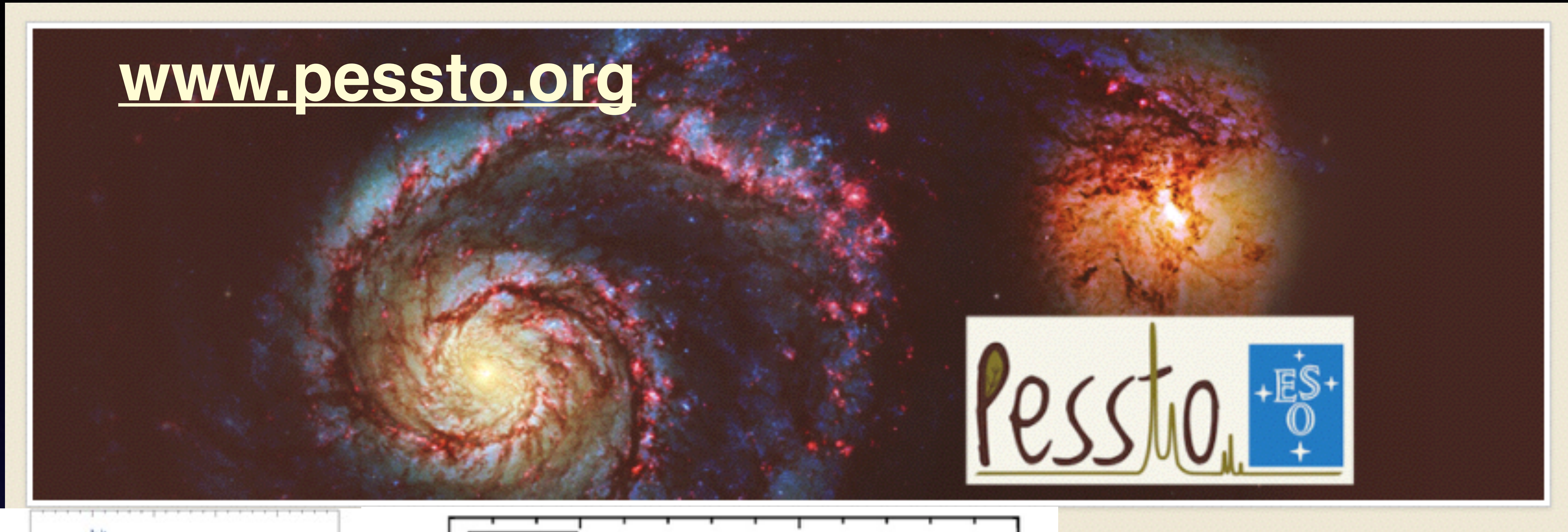

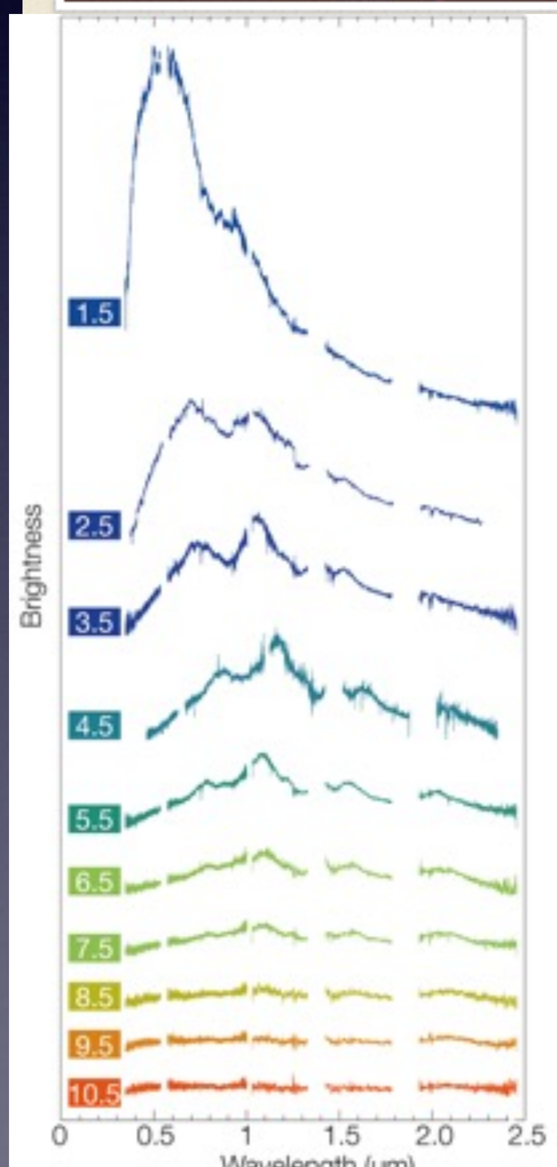

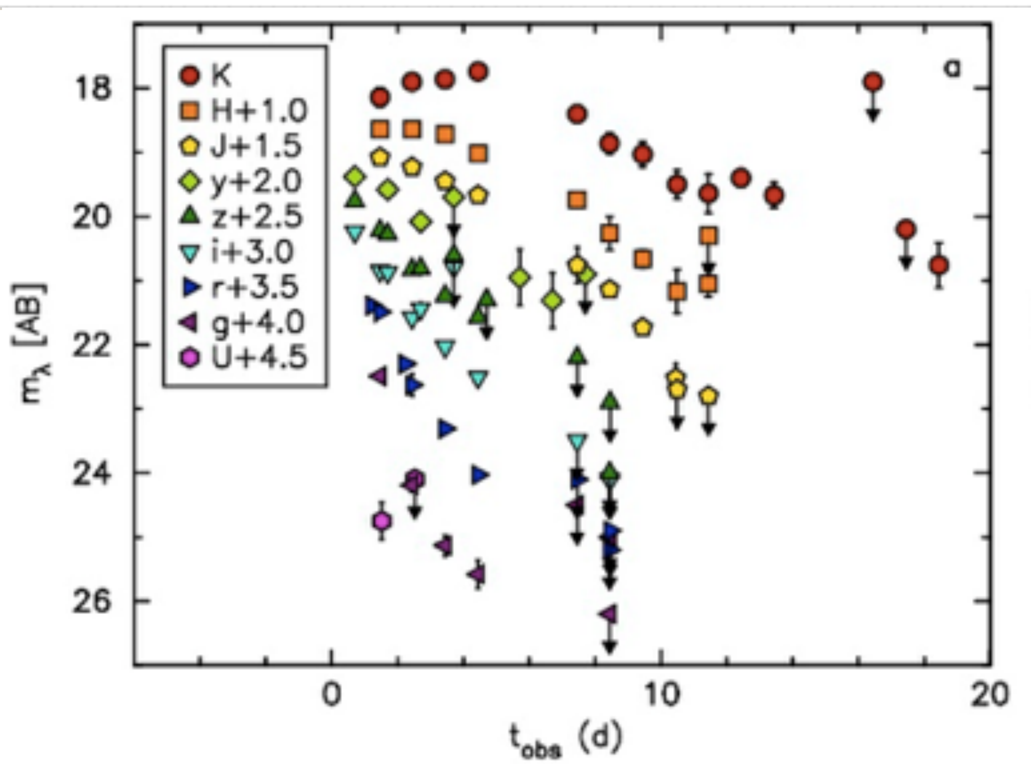

Smartt et al. 2017
Pian et al. 2017

- All data available on www.pessto.org (calibration notes)
- And https://kilonova.space/
- https://wiserep.weizmann.ac.il/

NS-NS mergers - EM radiation

- NS-NS mergers and BH-NS mergers
- Predicted to be strong emitters of EM radiation

- Short GRBs : working model is NS-NS mergers
- Gamma rays are beamed from relativistic jet

- Beam opening angle ~ 10^o (see Berger ARA&A 2014)

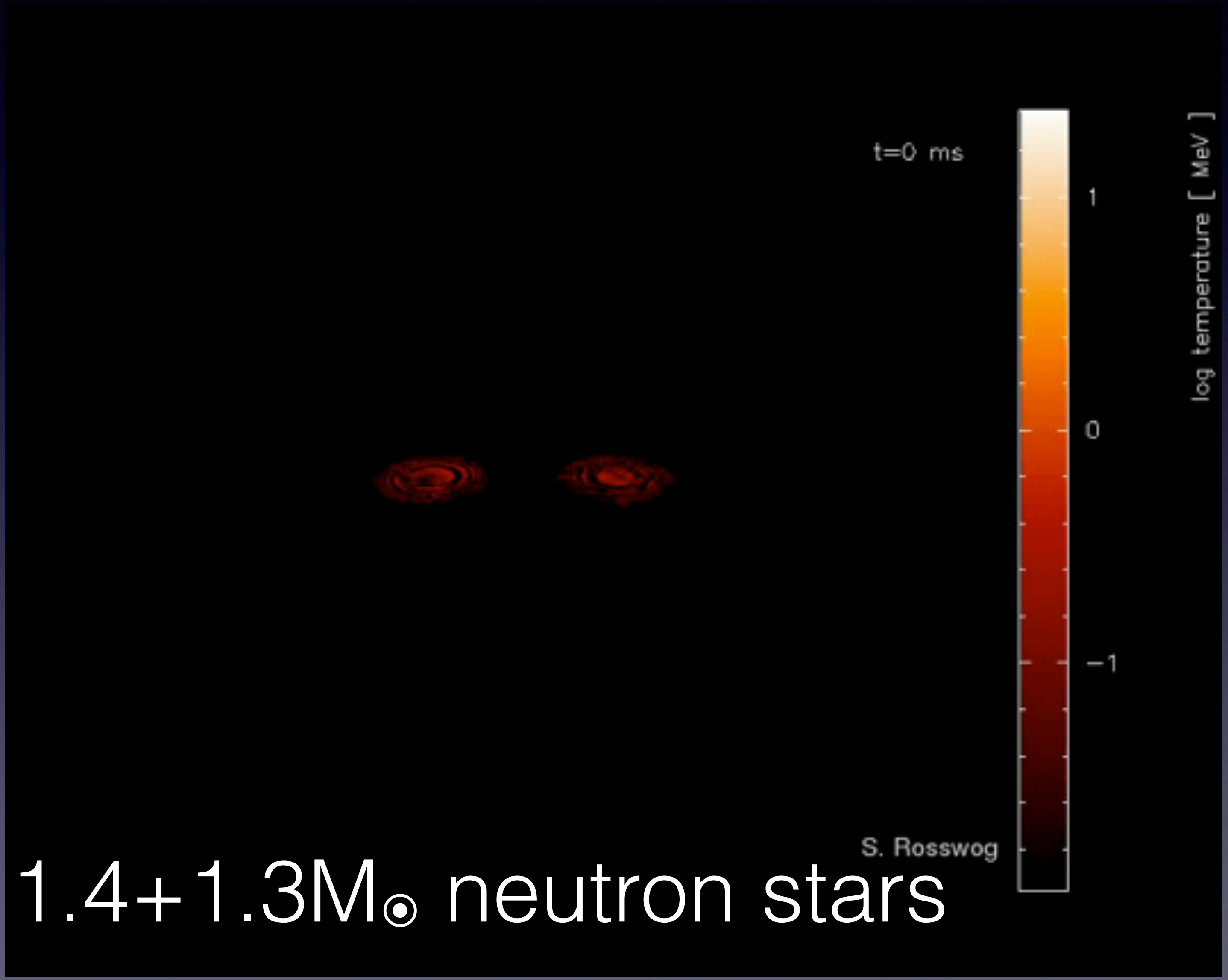

http://compact-merger.astro.su.se/

See Rosswog, Piran & Nakar 2013

NS-NS mergers - EM radiation

- NS-NS mergers and BH-NS mergers
- Predicted to be strong emitters of EM radiation

- Short GRBs : working model is NS-NS mergers
- Gamma rays are beamed from relativistic jet

- Beam opening angle ~ 10^o (see Berger ARA&A 2014)

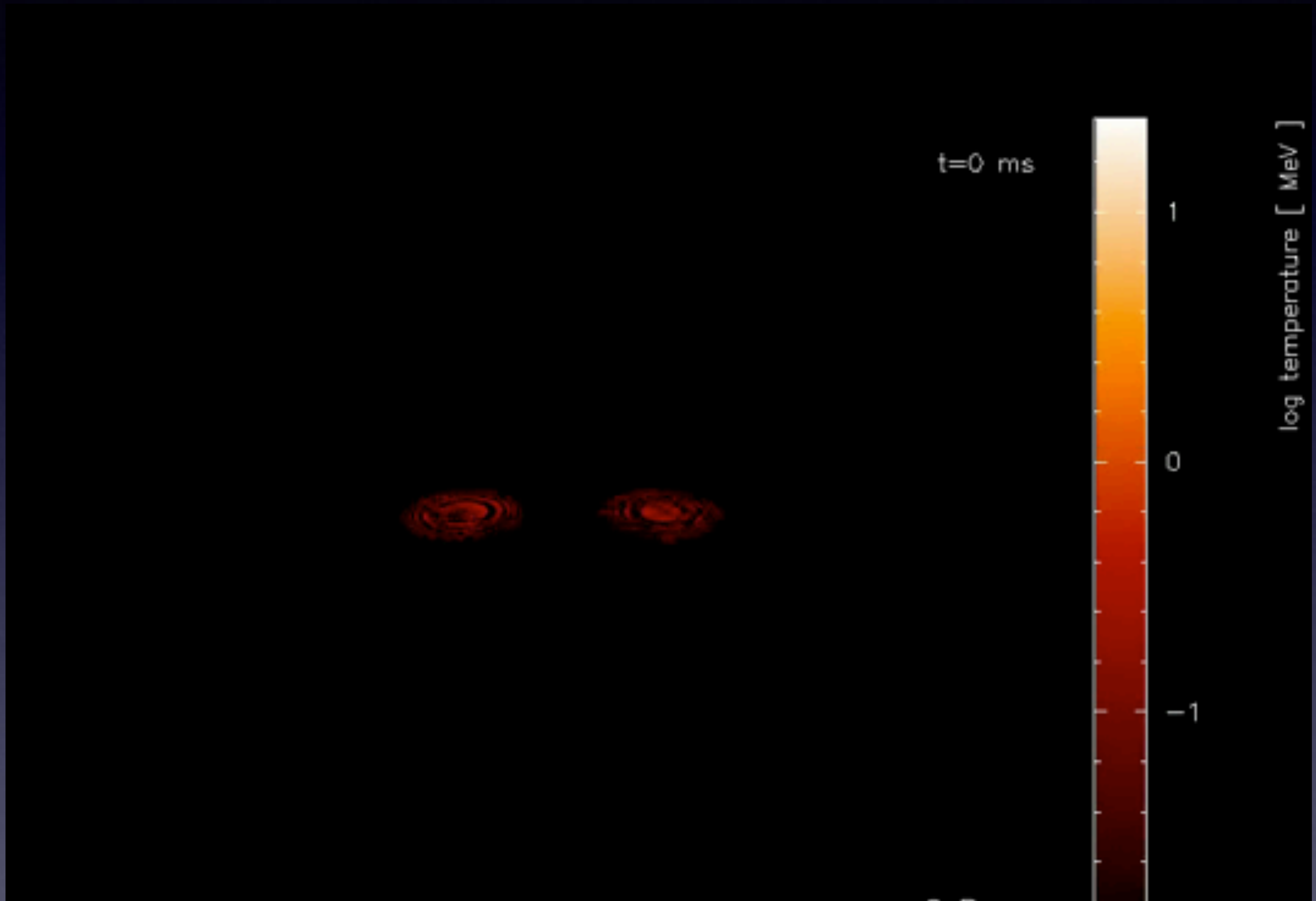

1.4+1.3M$_\odot$ neutron stars

http://compact-merger.astro.su.se/
See Rosswog, Piran & Nakar 2013

Multiple components

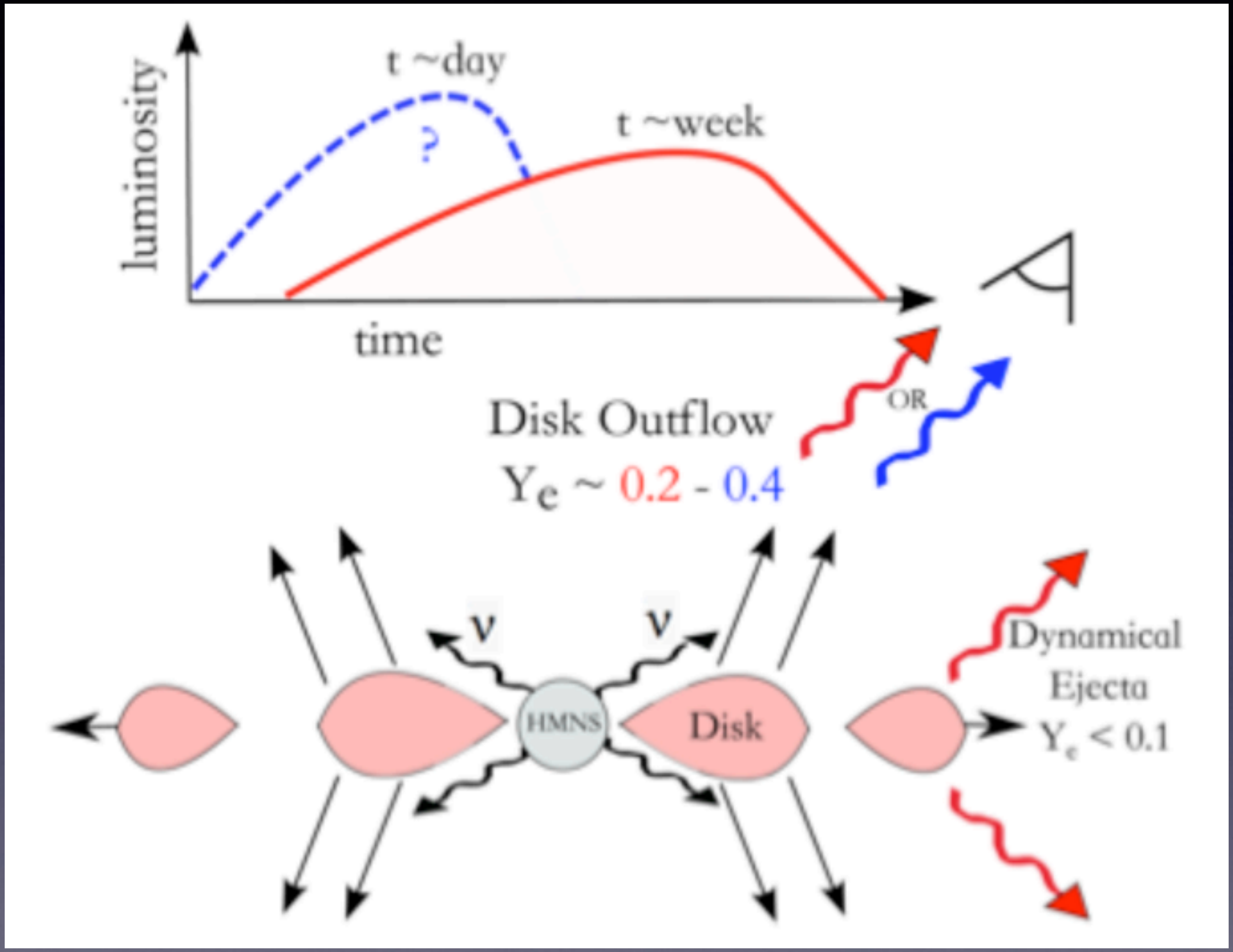

Metzger 2014

Multiple components or 1?

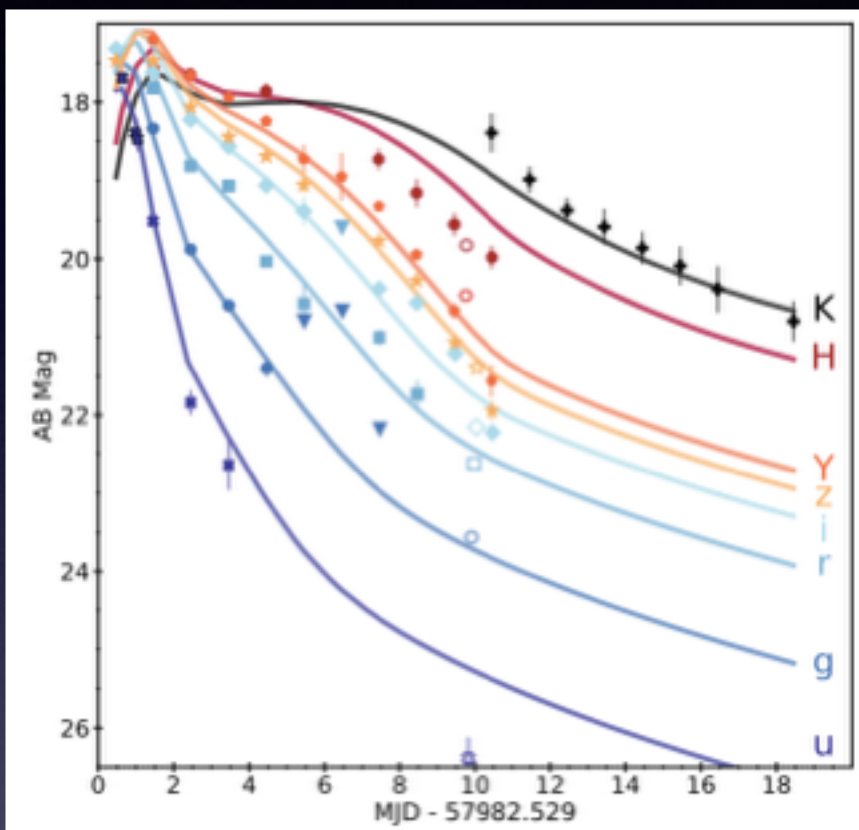

$M_{\rm ej}^{\rm blue} \approx 0.01\ M_{\odot}$ and $v_{\rm ej}^{\rm blue} \approx 0.3$ c

$M_{\rm ej}^{\rm red} \approx 0.04\ M_{\odot}$ and $v_{\rm ej}^{\rm red} \approx 0.1$ c

DECam team
Cowperthwaite et al.

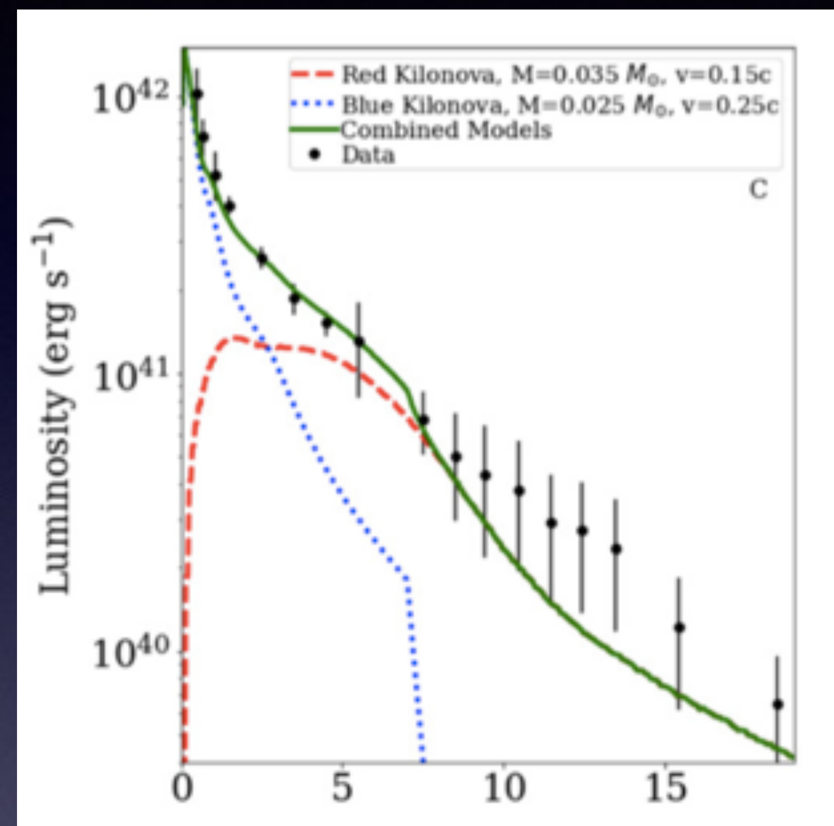

Red Kilonova, M=0.035 $M_{\odot}$, v=0.15c
Blue Kilonova, M=0.025 $M_{\odot}$, v=0.25c

Swope/Carnegie team
Kilpatrick et al. +
Drout et al.

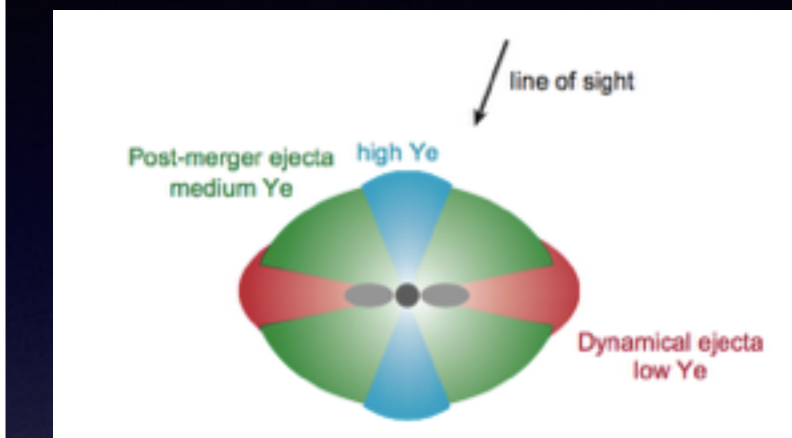

Fig. 4. Schematic picture of the ejecta of the NS merger event GW170817.

Tanaka et al.

AT2017fgo

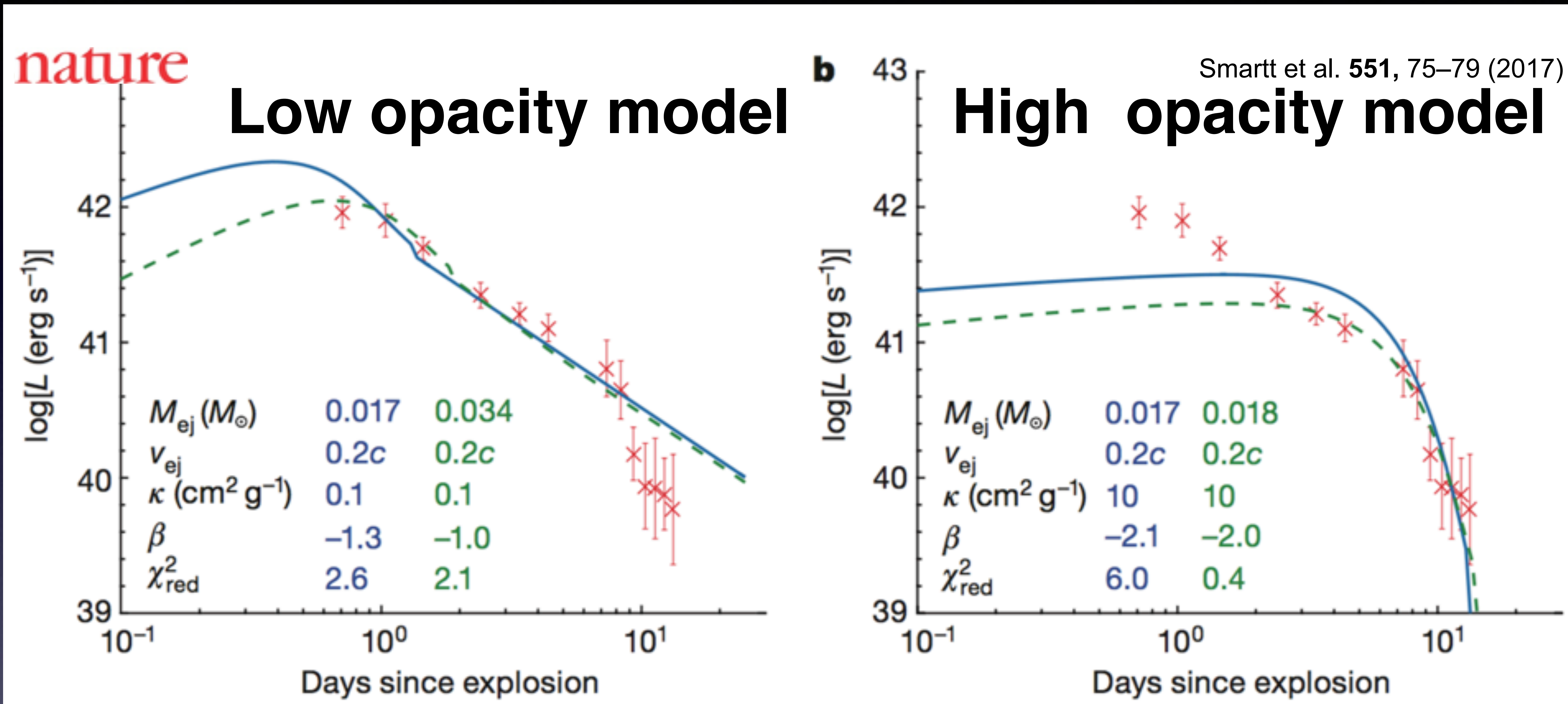

2 lightcurve models: our own Arnett formulation and Metzger

See also Rosswog et al. 2017, A&A, Waxman et al. 2017

Heating rates $P(t) = A\,t^{-\beta}$ (Lippuner & Roberts 2015)

Semi-analytic models "Arnett-Jerkstrand"

$$L_{\rm SN}(t) = e^{-(t/\tau_{\rm m})^2} \int_0^{t/\tau_{\rm m}} P(t') 2(t'/\tau_{\rm m}) e^{(t'/\tau_{\rm m})^2} \frac{dt'}{\tau_{\rm m}} \ {\rm erg\ s^{-1}}, \quad \text{(D1)}$$

where $\tau_{\rm m}$ is the diffusion timescale parameter, which in the case of uniform density ($E_{\rm k} = (3/10) M_{\rm ej} V_{\rm ej}^2$) is

$$\tau_{\rm m} = \frac{1.05}{(\beta c)^{1/2}} \kappa^{1/2} M_{\rm ej}^{3/4} E_{\rm k}^{-1/4} \ {\rm s}. \quad \text{(D2)}$$

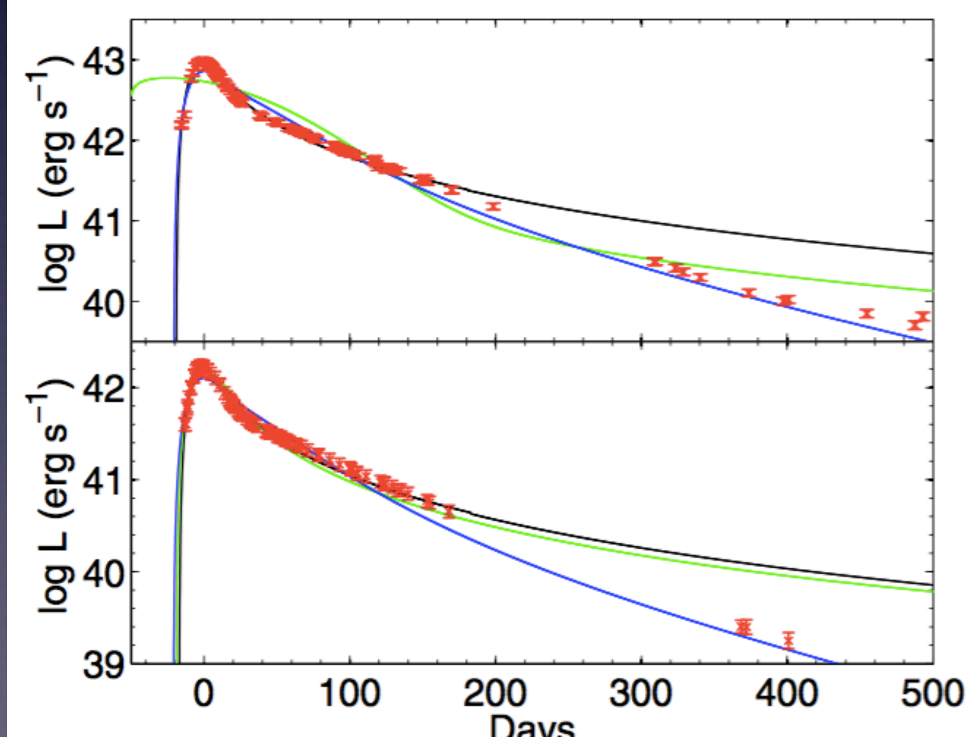

Can vary

M = mass

E = energy (velocity)

κ *= opacity*

P(t) = power source function

Inserra, Smartt, Jerkstrand et al 2013

https://star.pst.qub.ac.uk/wiki/doku.php/users/ajerkstrand/

r-process radioactivity

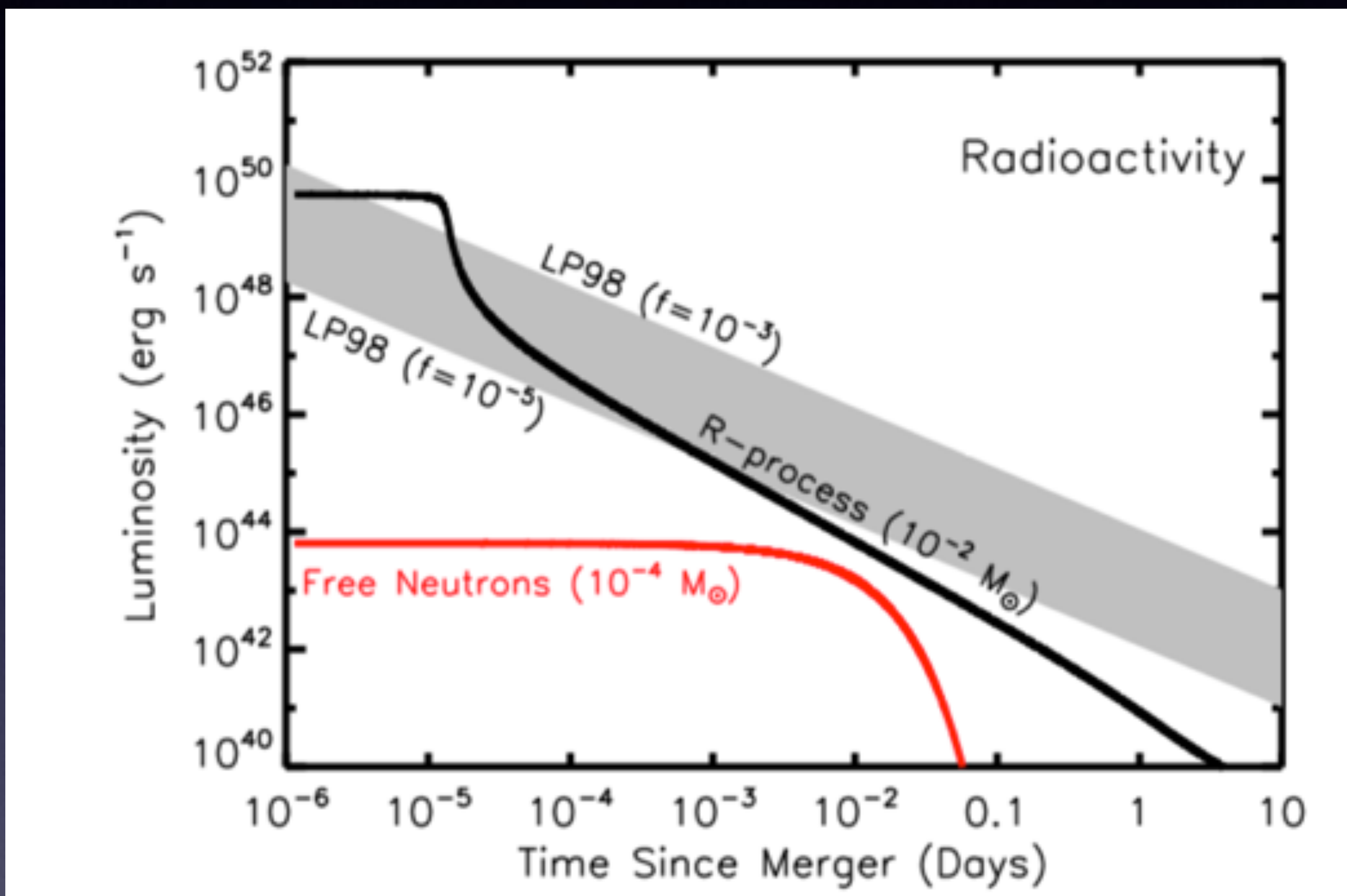

Table 1. Properties of the dominant β-decay nuclei at $t \sim 1$ d.

Isotope	$t_{1/2}$ (h)	Q^a (MeV)	ϵ_e^b	ϵ_ν^c	ϵ_γ^d	$E_\gamma^{\mathrm{avg}\,e}$ (MeV)
^{135}I	6.57	2.65	0.18	0.18	0.64	1.17
^{129}Sb	4.4	2.38	0.22	0.22	0.55	0.86
^{128}Sb	9.0	4.39	0.14	0.14	0.73	0.66
^{129}Te	1.16	1.47	0.48	0.48	0.04	0.22
^{132}I	2.30	3.58	0.19	0.19	0.62	0.77
^{135}Xe	9.14	1.15	0.38	0.40	0.22	0.26
^{127}Sn	2.1	3.2	0.24	0.23	0.53	0.92
^{134}I	0.88	4.2	0.20	0.19	0.61	0.86
^{56}Ni^f	146	2.14	0.10	0.10	0.80	0.53

^{a}Total energy released in the decay.
^{b,c,d}Fraction of the decay energy released in electrons, neutrinos and γ-rays.
^{e}Average photon energy produced in the decay.
^{f}Note: ^{56}Ni is not produced by the *r*-process and is only shown for comparison [although a small abundance of ^{56}Ni may be produced in accretion disc outflows from NS–NS/NS–BH mergers (Metzger et al. 2008b)].

- **Metzger 2017, Living Reviews in Relativity, 20, 3 "*Kilonovae*"**
- **Metzger et al. 2010, MNRAS, 406, 2650, "EM counterparts of compact object mergers powered by the radioactive decay of r-process material"**
- **Heating rates $P(t) = A\, t^{-\beta}$: also see Lippuner & Roberts 2015**

Spectra : light r-process elements

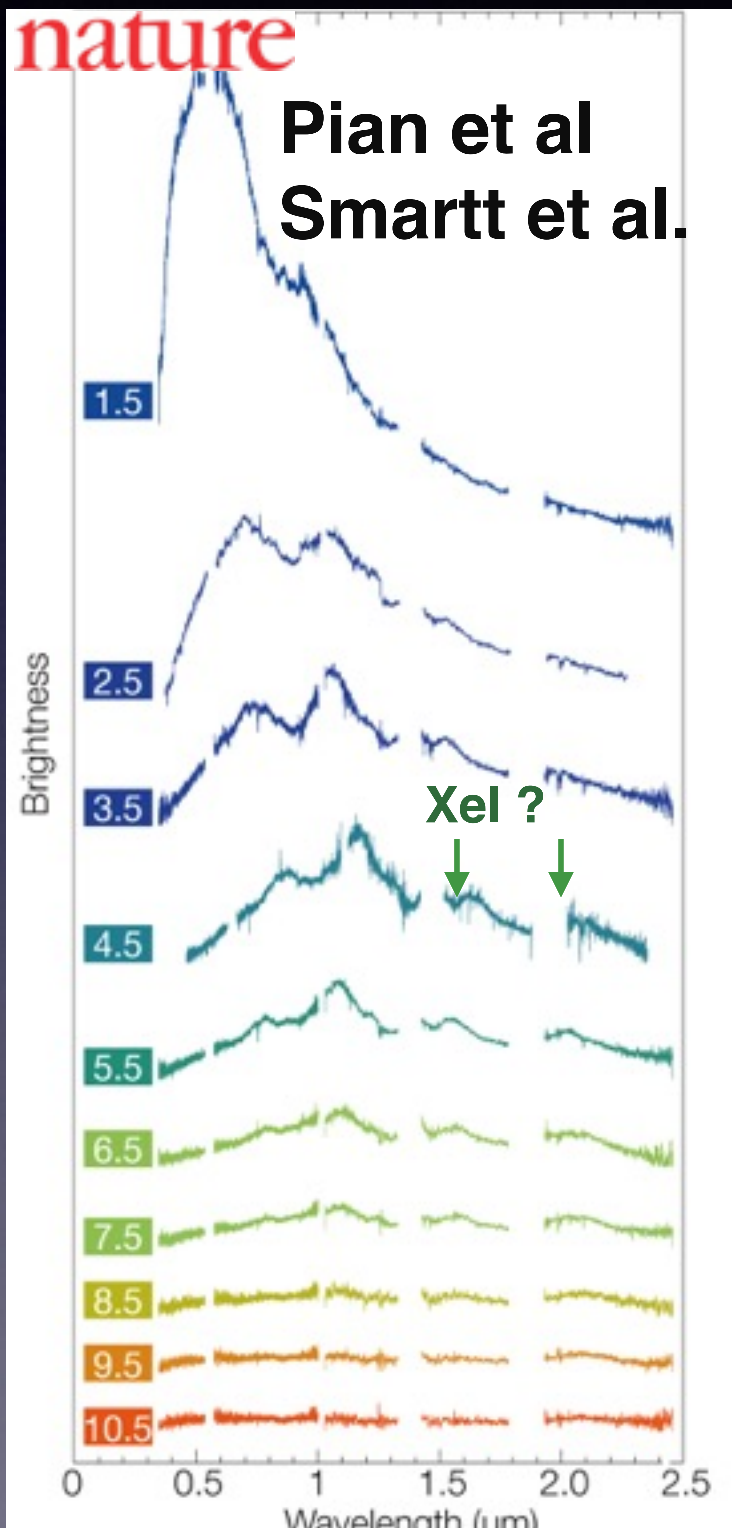

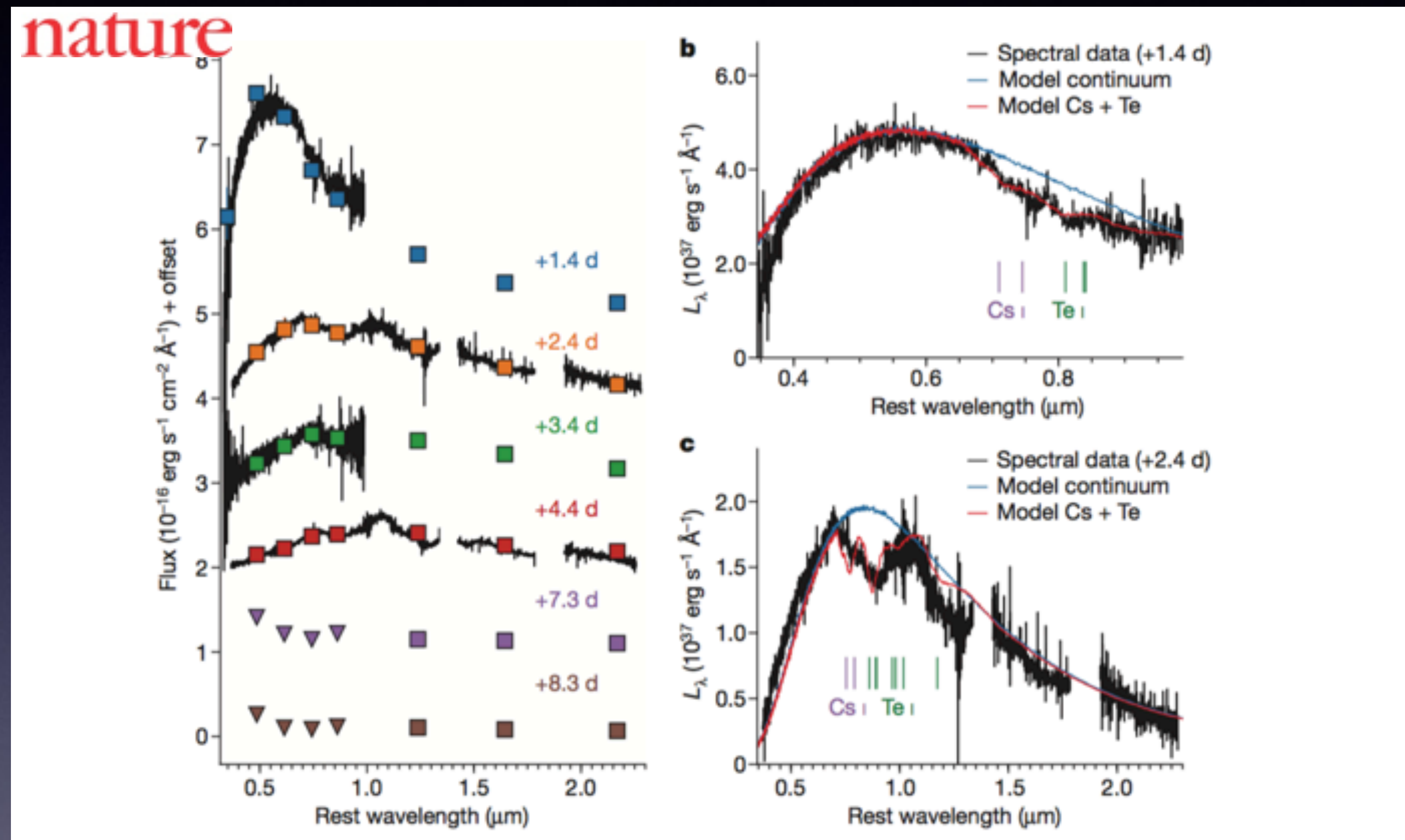

TARDIS ! Exploring supernovae made easy

Temperature and radiative diffusion in supernovae (Sim & Kerzendorf)

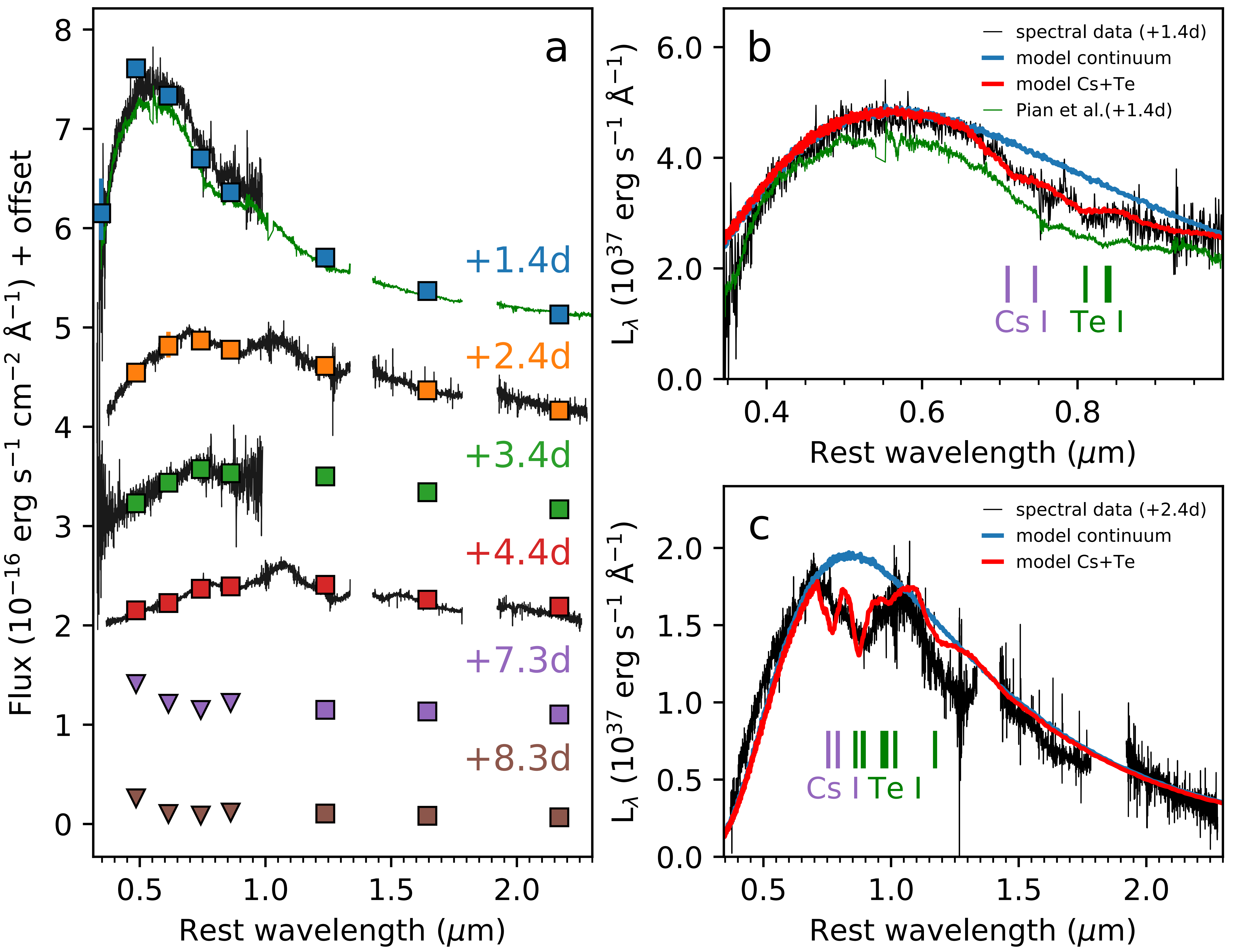

a
Flux (10^{-16} erg s^{-1} cm^{-2} Å^{-1}) + offset
+1.4d
+2.4d
+3.4d
+4.4d
+7.3d
+8.3d
Rest wavelength (μm)
b
spectral data (+1.4d)
model continuum
model Cs+Te
Pian et al.(+1.4d)
Cs I
Te I
L_λ (10^{37} erg s^{-1} Å^{-1})
Rest wavelength (μm)
c
spectral data (+2.4d)
model continuum
model Cs+Te
Cs I
Te I
L_λ (10^{37} erg s^{-1} Å^{-1})
Rest wavelength (μm)

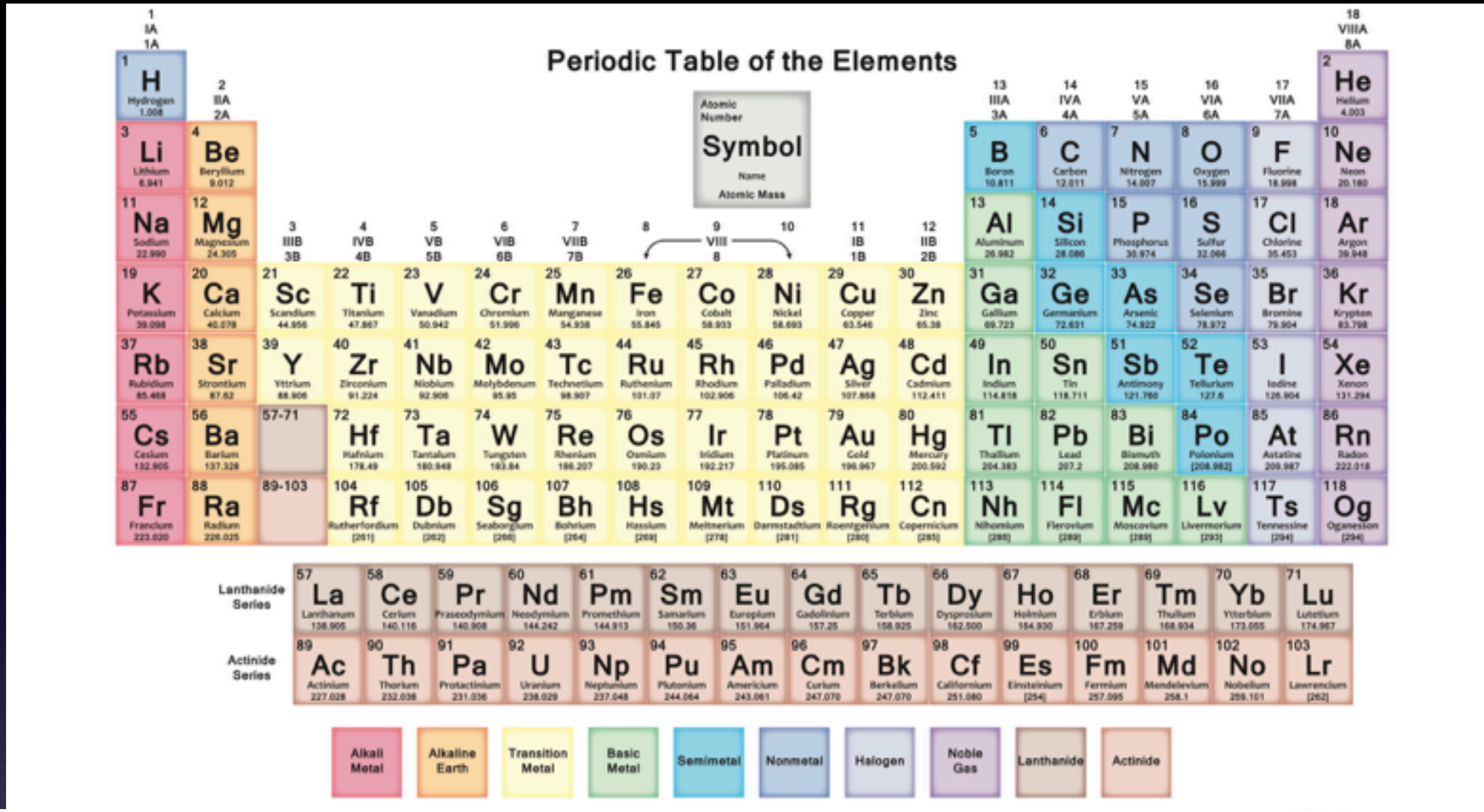
Periodic Table of the Elements
Atomic Number
Symbol
Name
Atomic Mass
Lanthanide Series
Actinide Series
Alkali Metal
Alkaline Earth
Transition Metal
Basic Metal
Semimetal
Nonmetal
Halogen
Noble Gas
Lanthanide
Actinide

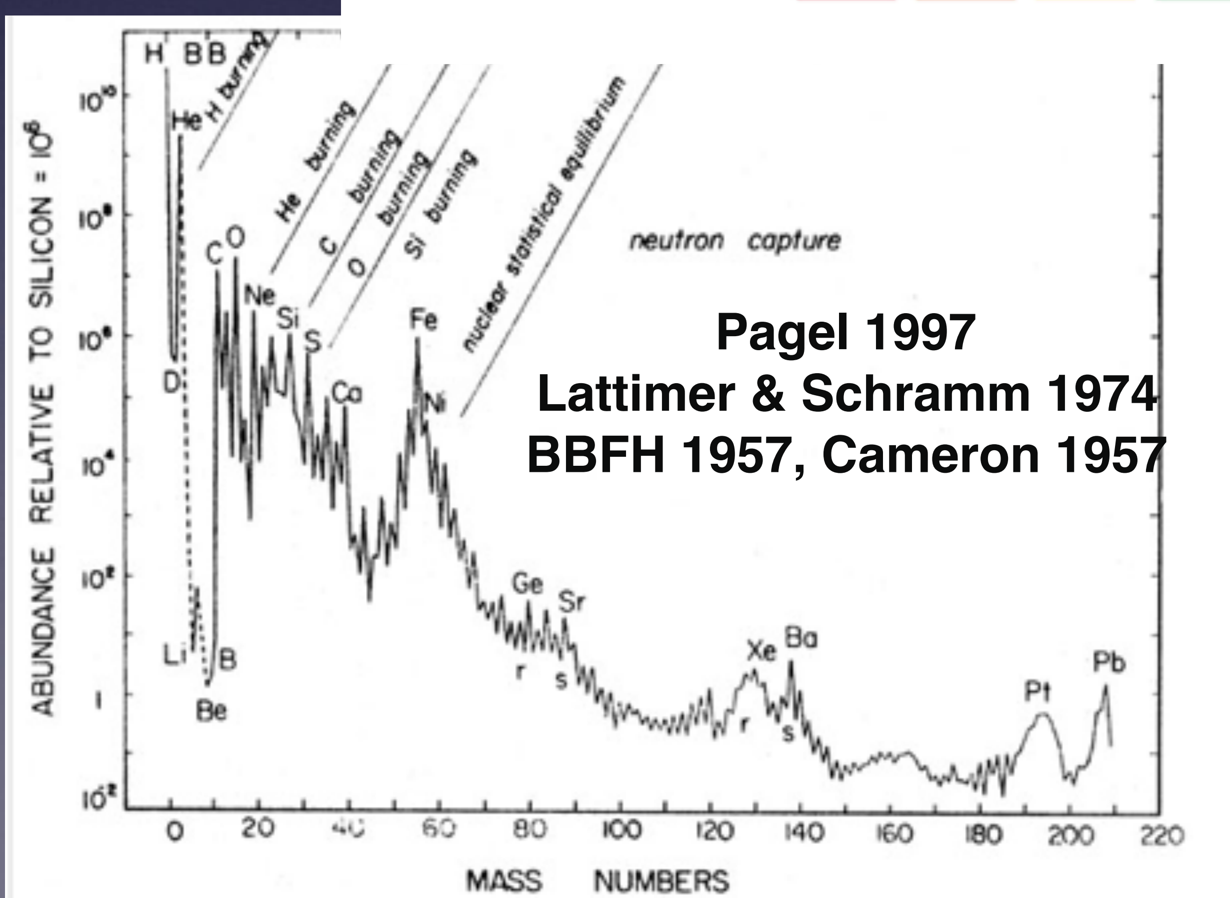
ABUNDANCE RELATIVE TO SILICON = 10^6
MASS NUMBERS
H burning
He burning
C burning
O burning
Si burning
nuclear statistical equilibrium
neutron capture
Pagel 1997
Lattimer & Schramm 1974
BBFH 1957, Cameron 1957

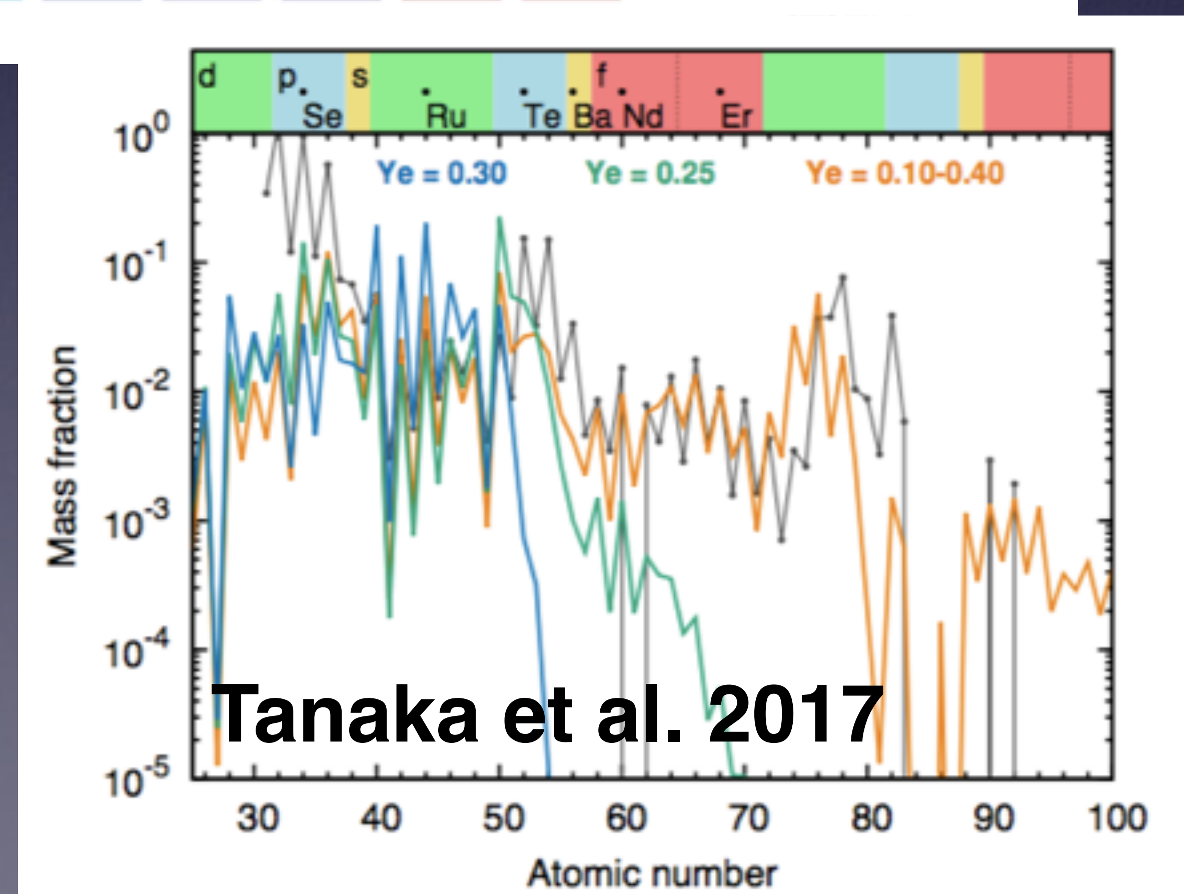
Ye = 0.30
Ye = 0.25
Ye = 0.10-0.40
Mass fraction
Atomic number
Se
Ru
Te
Ba
Nd
Er
Tanaka et al. 2017

Reasonable criticisms

- Our models are too simple - Metzger 2017 “toy model” and Arnett-Jerkstrand semi-analytic model
- We do not use the SED/spectral information available when fitting the lightcurve (L_{bol} only)
- We have underestimated K-band at > 10d. Therefore underestimated the contribution to a high opacity component
- We have only integrated our L_{bol} out to 2.5microns, there is clearly **(*some*)** flux beyond that. Therefore underestimated the contribution to a high opacity component
- **The *thermalisation function and/or heating rate* we apply for radioactive decay particles (leptons) are either wrong or unknown**

K-band issue with our data

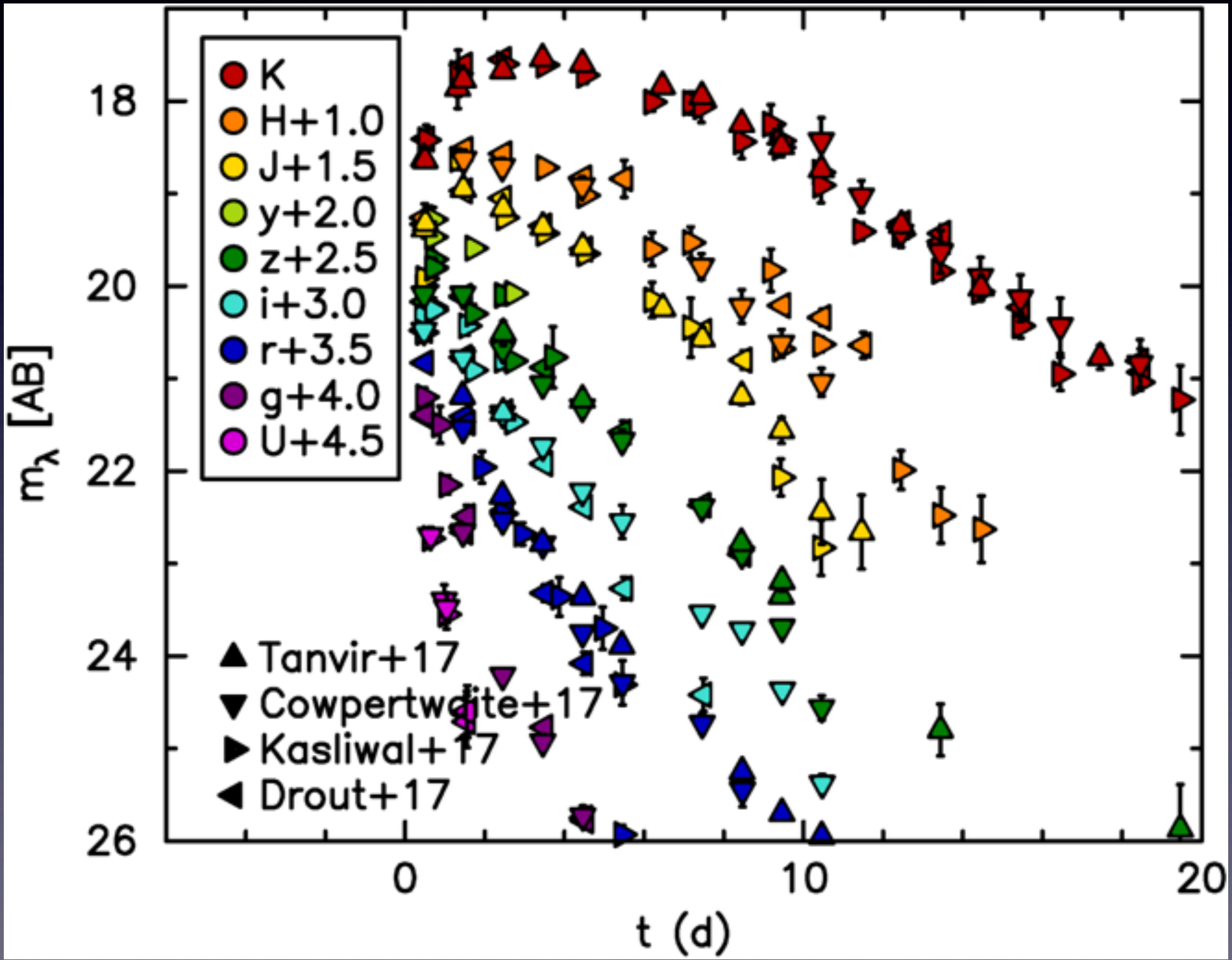

K-band issue with our data

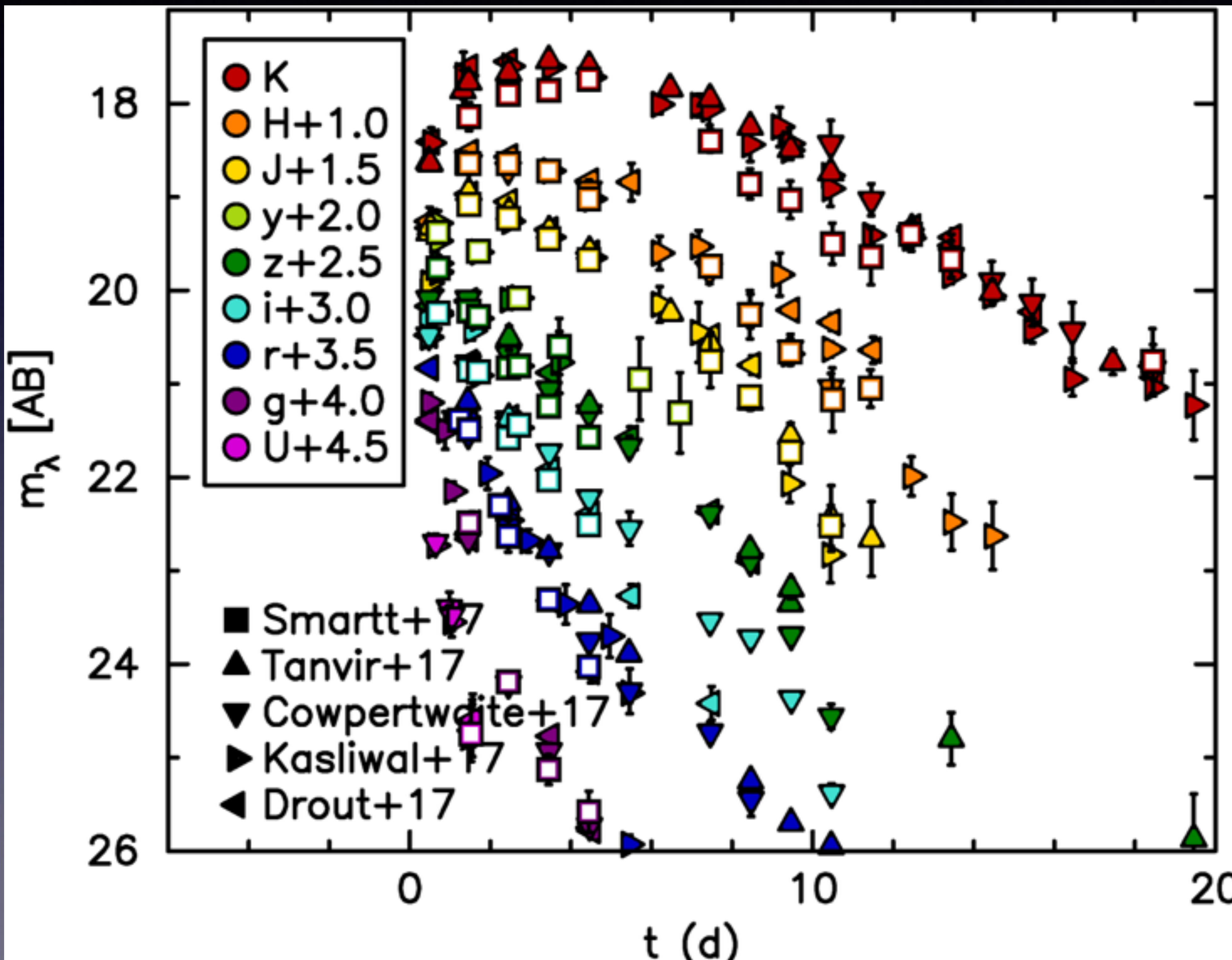

As pointed out in Villar et al. 2017

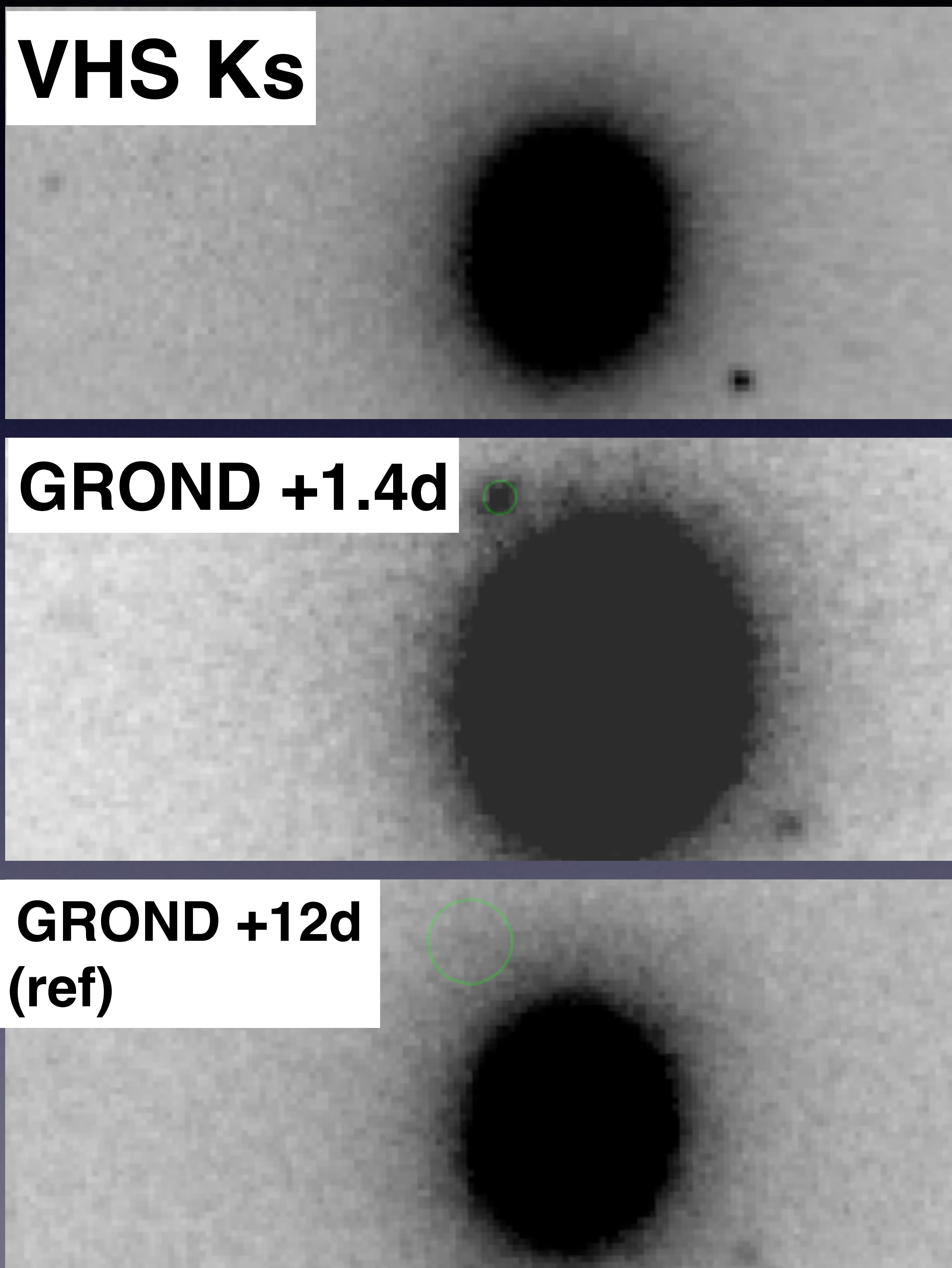
VHS Ks
GROND +1.4d
GROND +12d
(ref)

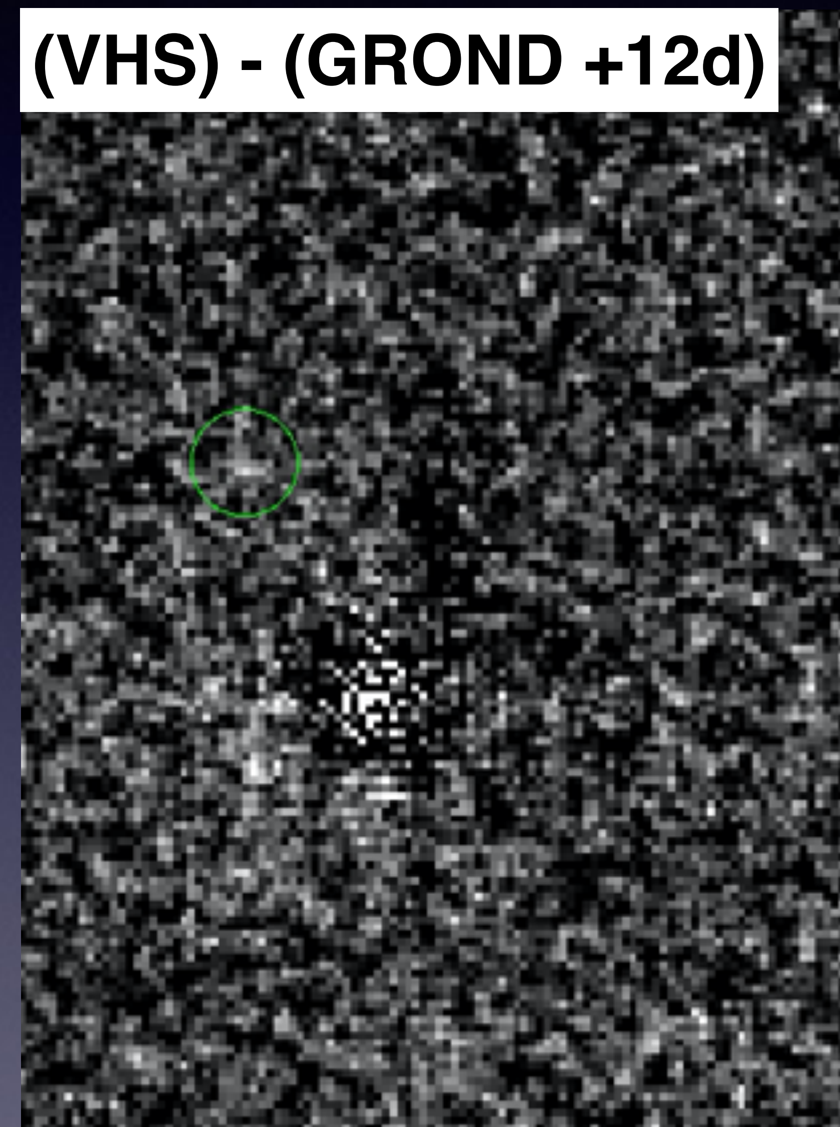
(VHS) - (GROND +12d)

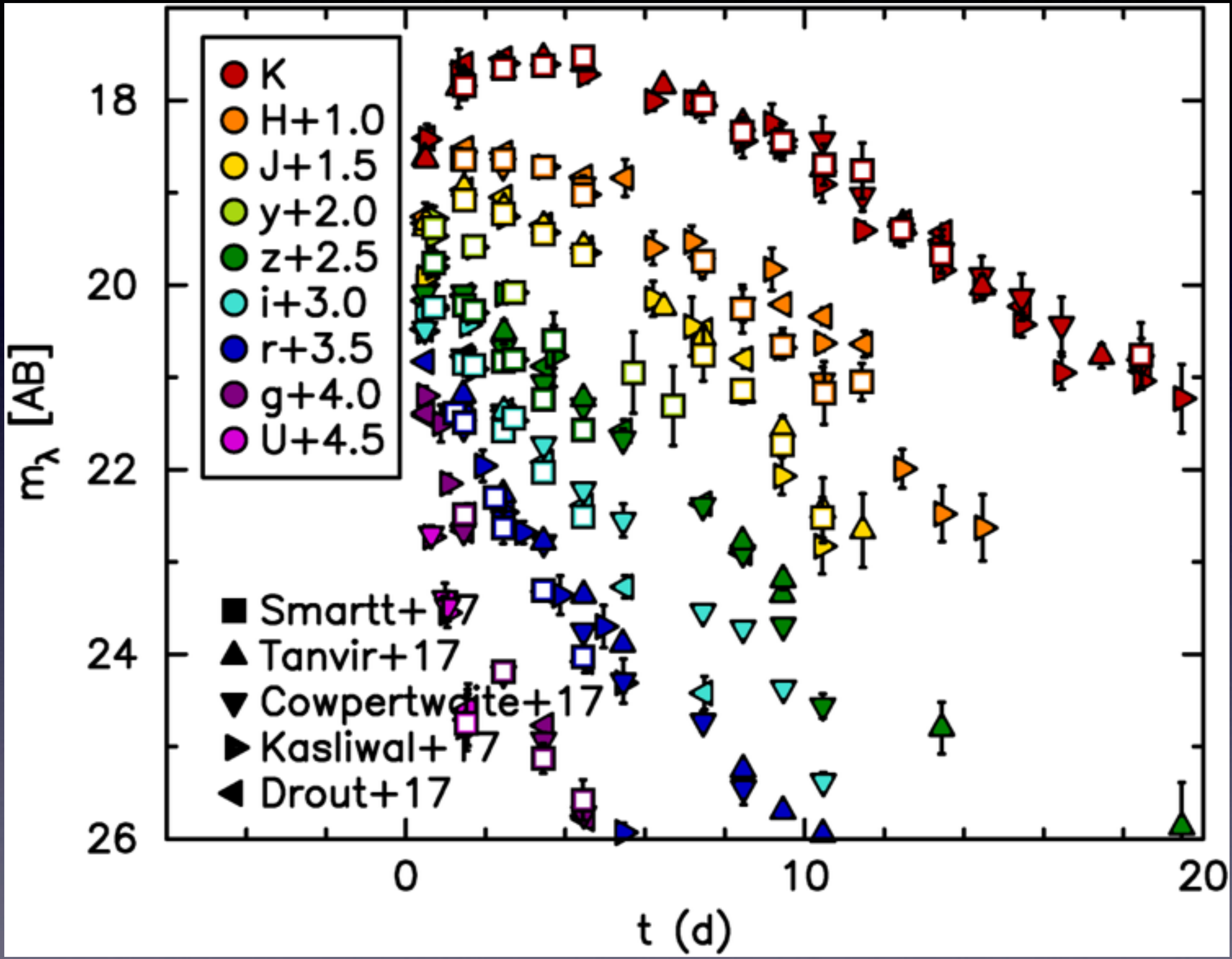
K
H+1.0
J+1.5
y+2.0
z+2.5
i+3.0
r+3.5
g+4.0
U+4.5
Smartt+17
Tanvir+17
Cowpertwaite+17
Kasliwal+17
Drout+17
m_λ [AB]
t (d)
18
20
22
24
26
0
10
20

1-component or 2 ?

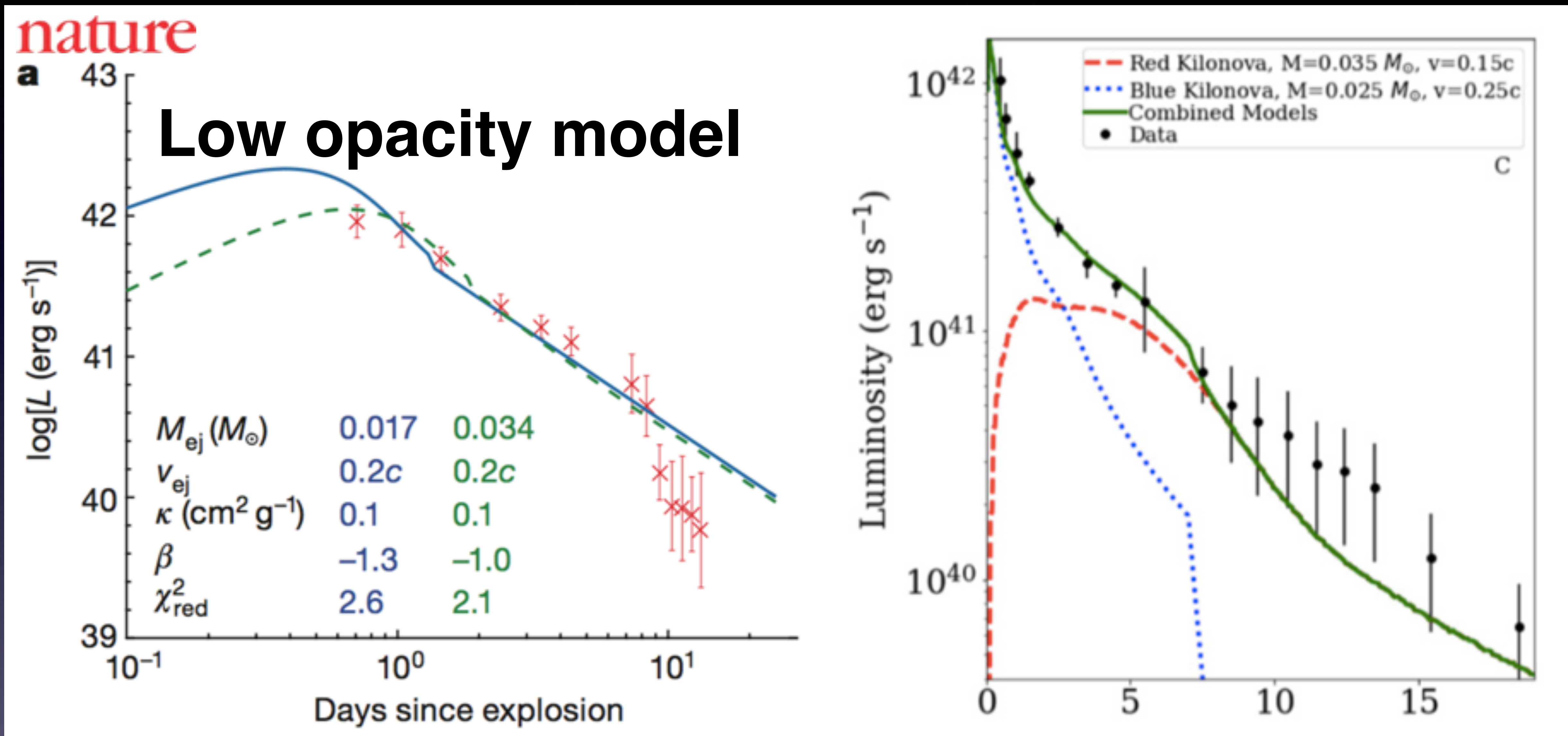

See also Rosswog et al. 2017, A&A,
Waxman et al. 2017, submitted
P(t) = A t

Kilpatrick et al. 2017
Drout et al. 2017

Combined photometry for SED fitting +0.47d to +14.3d

MJD	Phase	U	U_err	g	g_err	r	r_err	i	i_err	z	z_err	y	y_err	Tel	Phase	J	J_err	H	H_err	K_s	K_err	Telescope
57983.0	0.467	NaN	NaN	17.41	0.02	17.56	0.04	17.48	0.03	17.59	0.03	17.46	0.01	various		17.88	0.03	18.26	0.15	18.62	0.11	4star/VISTA/GS
57983.23125	0.696	NaN	NaN	NaN	NaN	NaN	NaN	17.24	0.06	17.26	0.06	17.38	0.10	PS1		NaN	NaN	NaN	NaN	NaN	NaN	
57983.42	0.88	NaN	NaN	17.46	0.08	17.32	0.07	17.42	0.05	NaN	NaN	NaN	NaN	Skymapper		NaN	NaN	NaN	NaN	NaN	NaN	
57983.75833	1.218	NaN	NaN	18.05	0.12	17.89	0.03	NaN	NaN	NaN	NaN	NaN	NaN	1.5B/LCO		17.51	0.03	17.64	0.04	17.91	0.05	Sirius
57983.96875	1.427	NaN	NaN	18.49	0.04	17.99	0.01	17.85	0.05	17.72	0.03	17.32	0.03	GROND/DECam	1.427	17.58	0.07	17.64	0.08	18.14	0.15	GROND
57984.04811	1.505	20.25	0.29	NaN	NaN	NaN	NaN	NaN	NaN	NaN	NaN	NaN	NaN	NTT		NaN	NaN	NaN	NaN	NaN	NaN	
57984.23125	1.686	NaN	NaN	NaN	NaN	NaN	NaN	17.87	0.06	17.78	0.07	17.58	0.11	PS1		NaN	NaN	NaN	NaN	NaN	NaN	
57984.37	1.82	NaN	NaN	19.28	0.17	18.34	0.11	18.32	0.14	NaN	NaN	NaN	NaN	Skymapper/LCO		NaN	NaN	NaN	NaN	NaN	NaN	
57984.76111	2.211	NaN	NaN	19.87	0.21	18.80	0.07	18.3	0.15	18.25	0.3	NaN	NaN	1.5B/LCO		17.69	0.04	17.52	0.04	17.61	0.04	Sirius
57984.96892	2.417	19.6	9999	20.19	0.11	19.13	0.17	18.58	0.04	18.33	0.06	17.77	0.03	GROND	2.417	17.73	0.09	17.64	0.08	17.90	0.10	GROND
57985.23125	2.676	NaN	NaN	NaN	NaN	NaN	NaN	18.44	0.09	18.31	0.07	18.08	0.11	PS1		NaN	NaN	NaN	NaN	NaN	NaN	
57985.38	2.83	NaN	NaN	20.43	0.16	19.34	0.09	18.62	0.07	NaN	NaN	NaN	NaN	Skymapper/LCO		NaN	NaN	NaN	NaN	NaN	NaN	
57985.77639	3.216	NaN	NaN	NaN	NaN	19.64	0.13	18.80	0.2	18.42	0.34	NaN	NaN	1.5B/LCO		17.78	0.05	17.57	0.04	17.55	0.05	Sirius
57985.97433	3.412	NaN	NaN	21.13	0.16	19.81	0.02	19.03	0.01	18.74	0.02	18.05	0.03	GROND/DECam	3.413	17.95	0.07	17.72	0.07	17.86	0.10	GROND
57986.23556	3.671	NaN	NaN	NaN	NaN	NaN	NaN	17.8	9999	18.10	0.30	17.7	9999	PS1		NaN	NaN	NaN	NaN	NaN	NaN	
57986.71	4.14	NaN	NaN	NaN	NaN	20.30	0.31	NaN	NaN	NaN	NaN	NaN	NaN	LCO		18.13	0.12	17.77	0.04	17.57	0.07	SIRIUS
57986.97426	4.402	NaN	NaN	21.58	0.22	20.53	0.05	19.51	0.04	19.07	0.06	18.35	0.03	GROND	4.403	18.17	0.07	18.02	0.10	17.74	0.11	GROND
57987.98	5.4	NaN	NaN	NaN	NaN	20.79	0.24	19.55	0.18	19.17	0.11	18.83	0.18	DECcam		NaN	NaN	NaN	NaN	NaN	NaN	
57988.99	6.4	NaN	NaN	22.08	0.52	20.95	0.35	NaN	NaN	NaN	NaN	19.06	0.31	DECam	6.4	18.74	0.04	NaN	NaN	17.84	0.03	VISTA
57990.00	7.4	NaN	NaN	23.28	0.34	21.23	0.11	20.54	0.05	19.89	0.05	19.44	0.05	DECam	7.383	19.26	0.28	18.74	0.06	18.40	0.12	GROND
57991.00	8.4	NaN	NaN	NaN	NaN	21.95	0.18	20.72	0.06	20.40	0.06	20.06	0.07	DECam	8.358	19.64	0.11	19.26	0.26	18.86	0.16	GROND
57992.00	9.4	NaN	NaN	NaN	NaN	22.2	0.04	21.37	0.06	21.19	0.07	20.78	0.11	DECam/VIMOS	9.350	20.23	0.10	19.66	0.14	19.03	0.20	GROND
57993.00	10.4	NaN	NaN	NaN	NaN	22.45	0.07	22.38	0.10	22.06	0.13	21.67	0.21	DECam/VIMOS	10.386	21.02	0.22	20.17	0.34	19.50	0.22	GROND
57993.94	11.3	NaN	NaN	24.1	0.2	23.0	0.2	22.5	0.2	NaN	NaN	NaN	NaN	HST	11.322	NaN	NaN	20.05	0.20	19.64	0.30	NTT/GROND
57994.97	12.31	NaN	NaN	NaN	NaN	NaN	NaN	NaN	NaN	NaN	NaN	NaN	NaN			NaN	NaN	20.57	0.19	19.40	0.14	NTT/GS
57995.97	13.21	NaN	NaN	NaN	NaN	NaN	NaN	NaN	NaN	22.3	0.28	NaN	NaN	VIMOS		NaN	NaN	21.01	0.14	19.67	0.20	GS/NTT
57996.99	14.32	NaN	NaN	NaN	NaN	NaN	NaN	NaN	NaN	23.34	0.37	NaN	NaN	FORS		NaN	NaN	21.63	0.36	20.02	0.13	GS/VISTA
57997.979	15.30	NaN	NaN	NaN	NaN	NaN	NaN	NaN	NaN	NaN	NaN	NaN	NaN			NaN	NaN	NaN	NaN	20.17	0.08	GS/Magellan (average)
57999.98	17.28	NaN	NaN	NaN	NaN	NaN	NaN	NaN	NaN	NaN	NaN	NaN	NaN			NaN	NaN	NaN	NaN	20.77	0.13	HAWKI
58000.966	18.26	NaN	NaN	NaN	NaN	NaN	NaN	NaN	NaN	NaN	NaN	NaN	NaN			NaN	NaN	NaN	NaN	20.76	0.35	NTT
58003.969	21.23	NaN	NaN	NaN	NaN	NaN	NaN	NaN	NaN	NaN	NaN	NaN	NaN			NaN	NaN	NaN	NaN	21.46	0.08	HAWKI
58007.969	25.19	NaN	NaN	NaN	NaN	NaN	NaN	NaN	NaN	NaN	NaN	NaN	NaN			NaN	NaN	NaN	NaN	22.06	0.22	HAWKI

+0.47d Chile

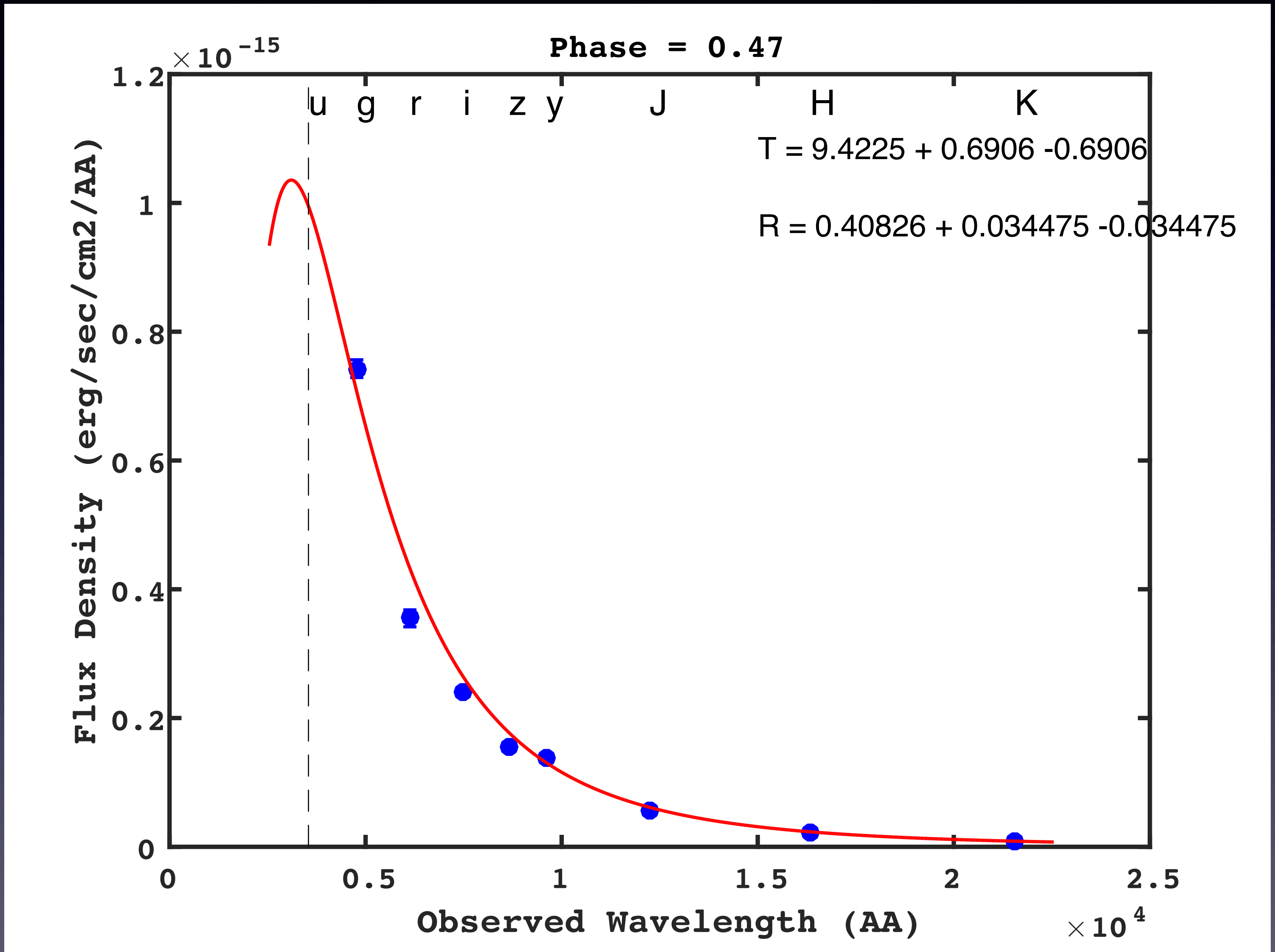

Opt:
LCO, Magellan, DECam

IR:
Magellan, VISTA, GS

Arcavi et al, 2017
Drout et al. 2017
Cowperthwaite et al./Soares-Santos et al. 2017

Tanvir et al. 2017
Drout et al. 2017
Kasliwal et al. 2017

+0.64d Space - Swift

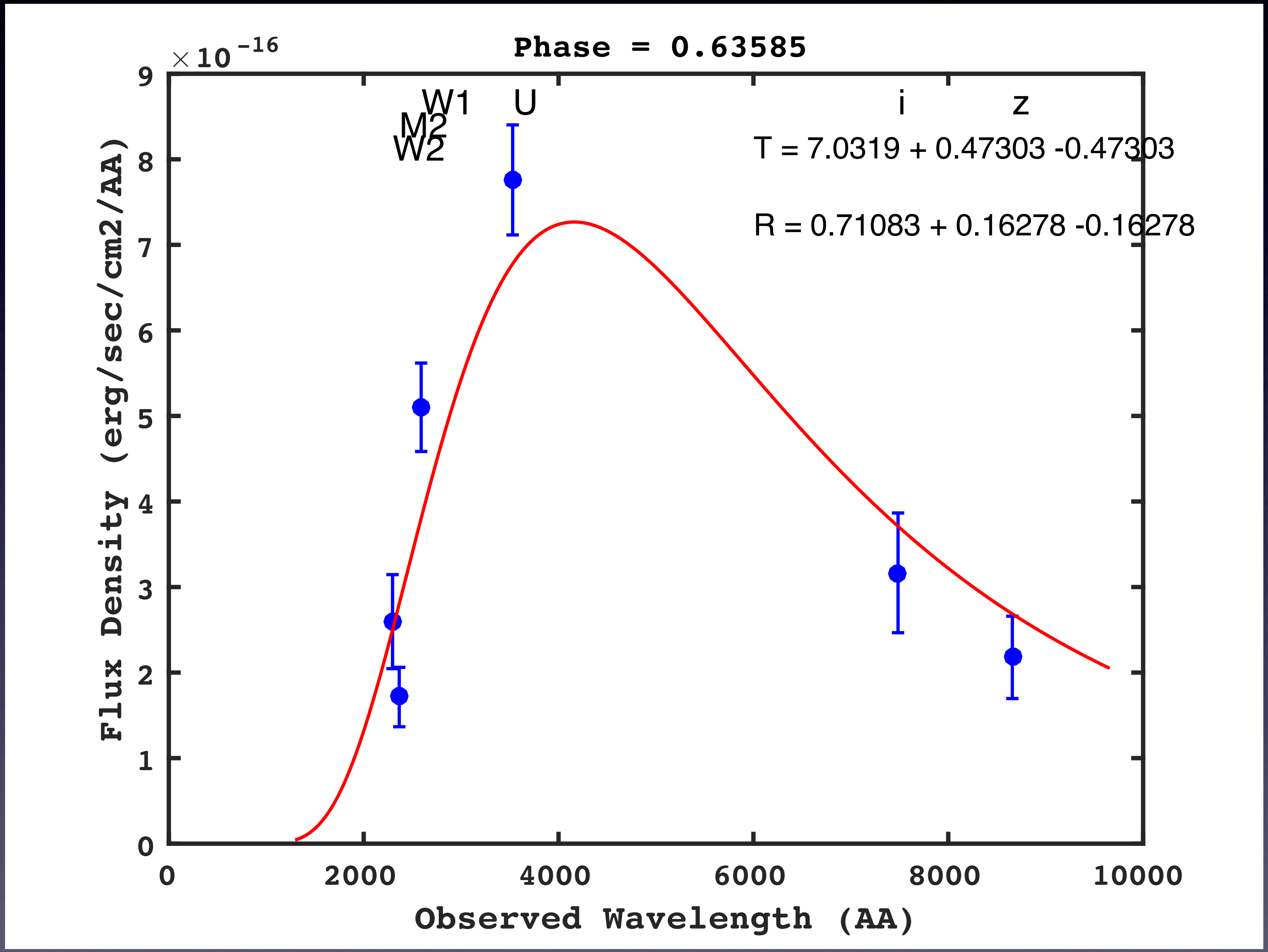

UV:
Swift

Evans et al. 2017

Optical:
Interpolated Pan-STARRS/DECam

Smartt et al. 2017
Soares-Santos et al. 2017

+0.70d Hawaii

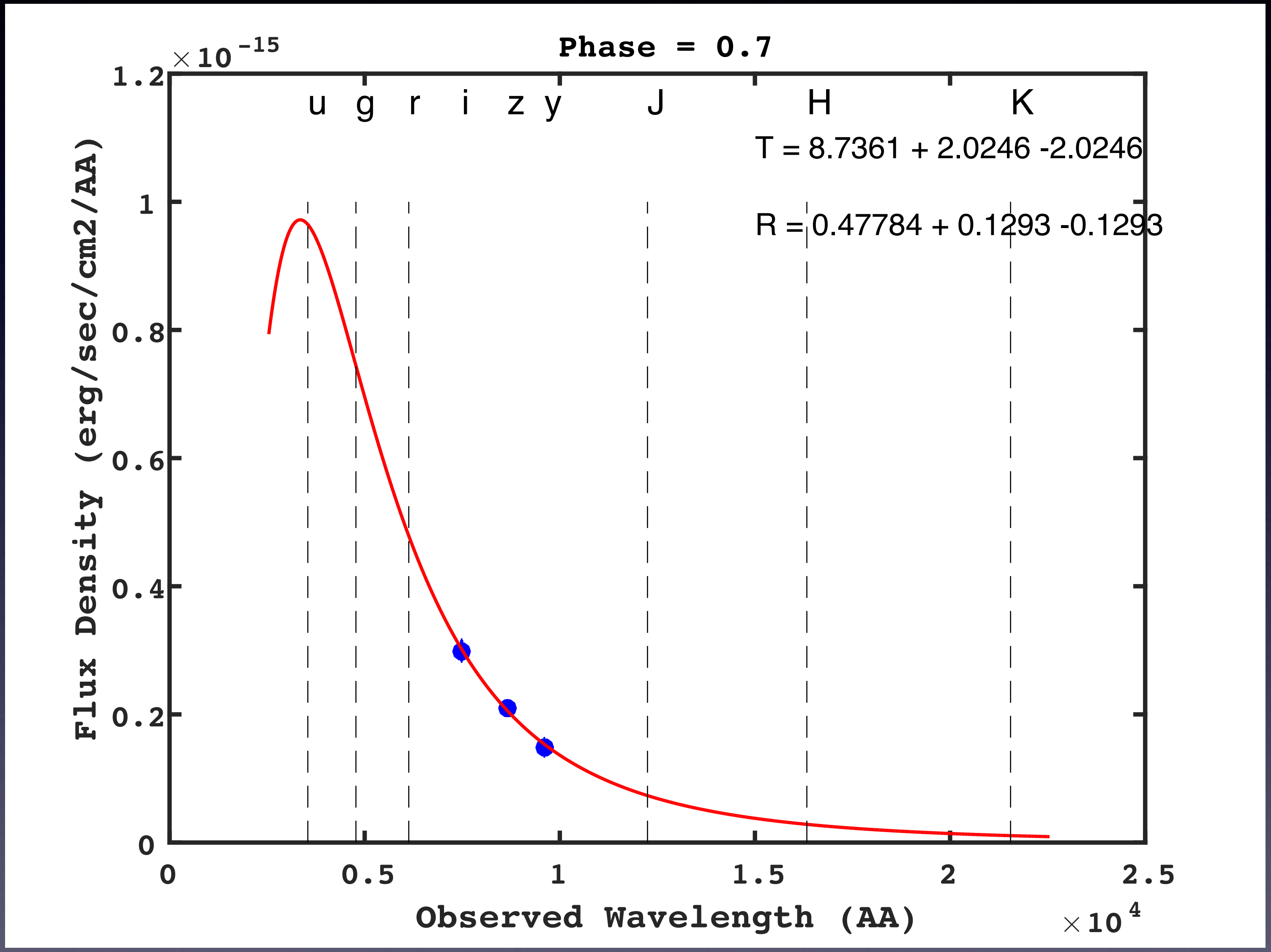

Optical/NIR: Pan-STARRS

Smartt et al. 2017

+0.88d Australia

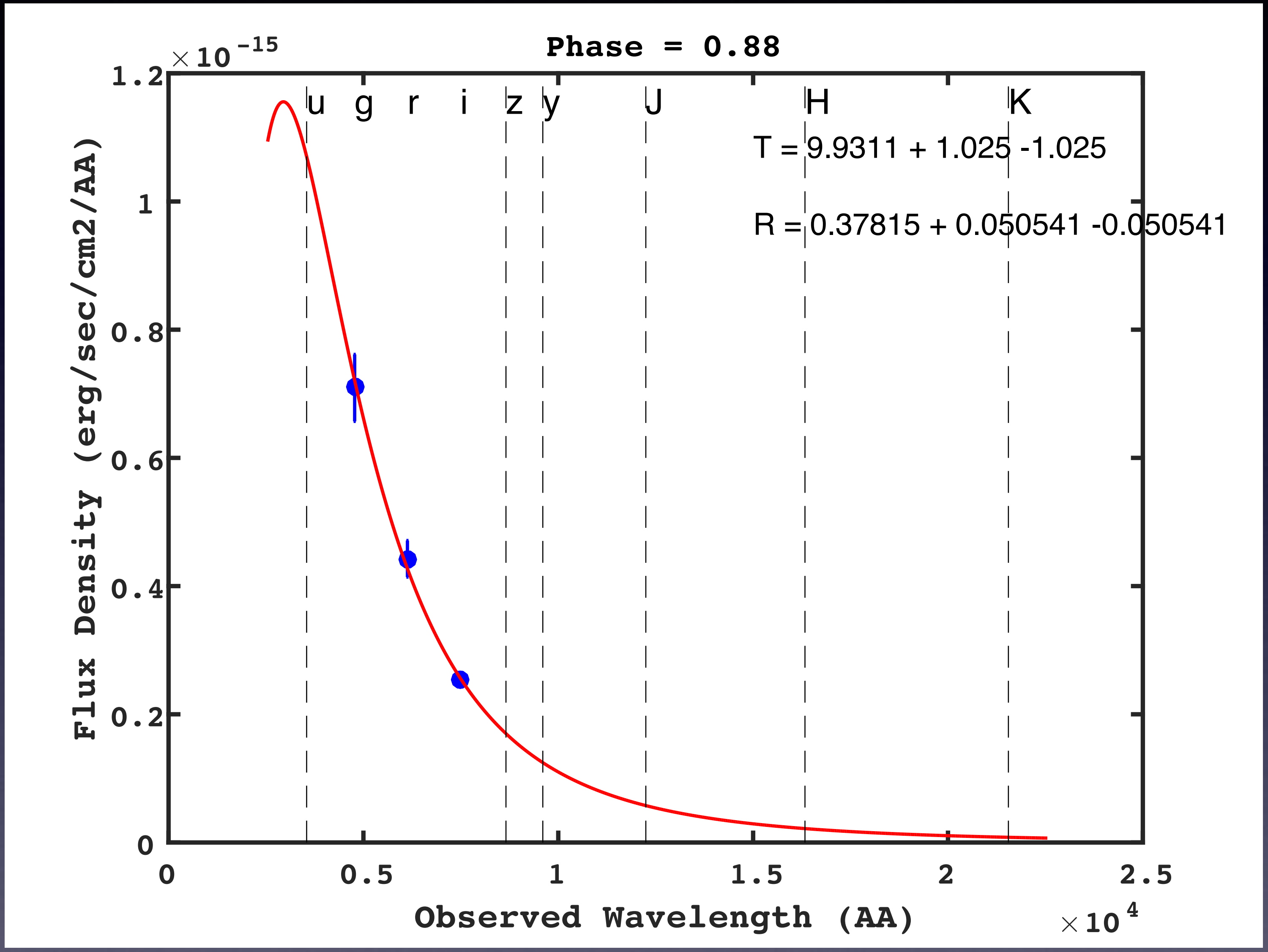

Opt: SkyMapper

Andreoni et al. 2017

+1.05d Space - Swift

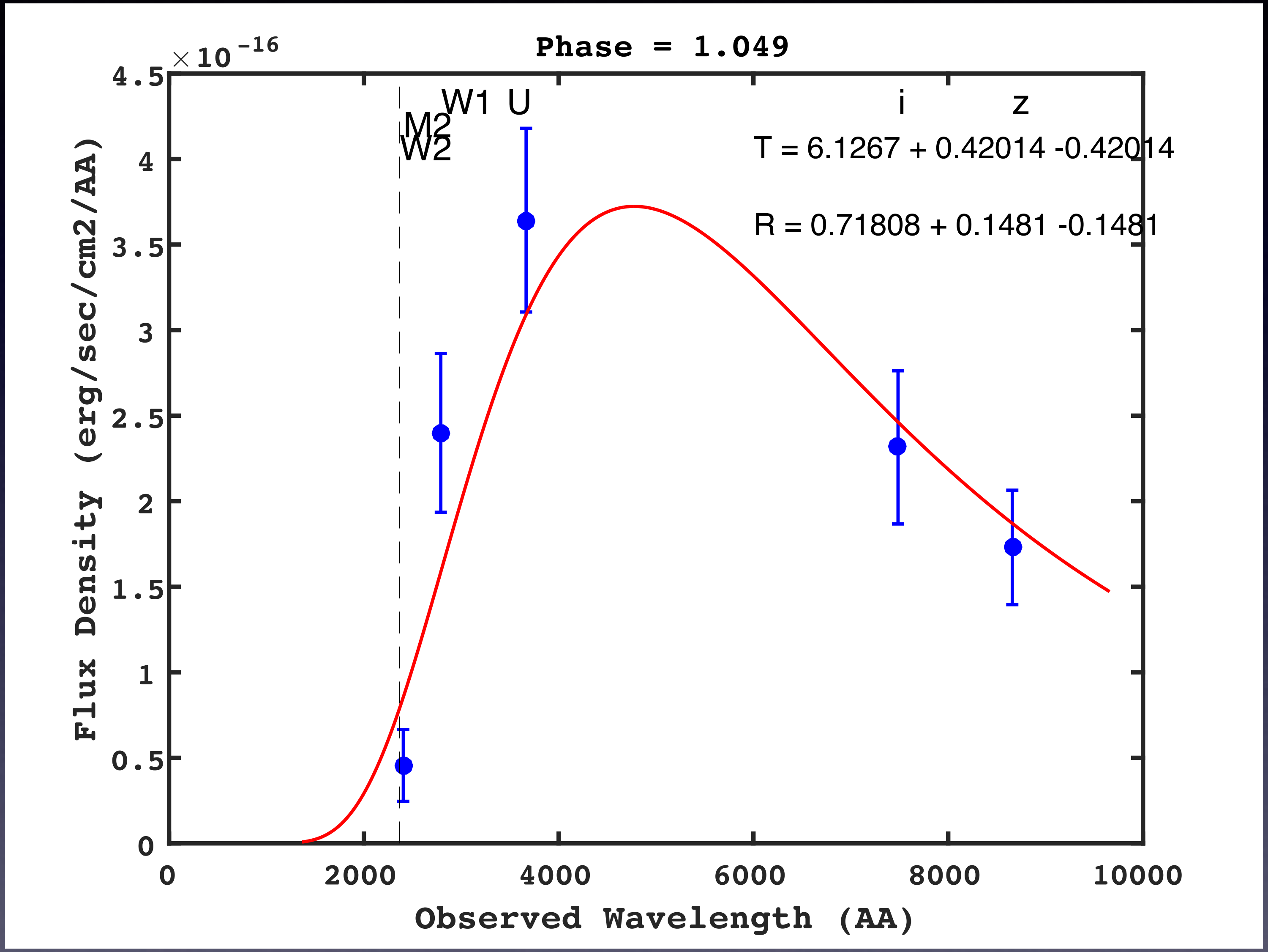

UV: Swift

Optical/NIR: Pan-STARRS (interpolated)

Evans et al. 2017

Smartt et al. 2017

+1.22d South Africa

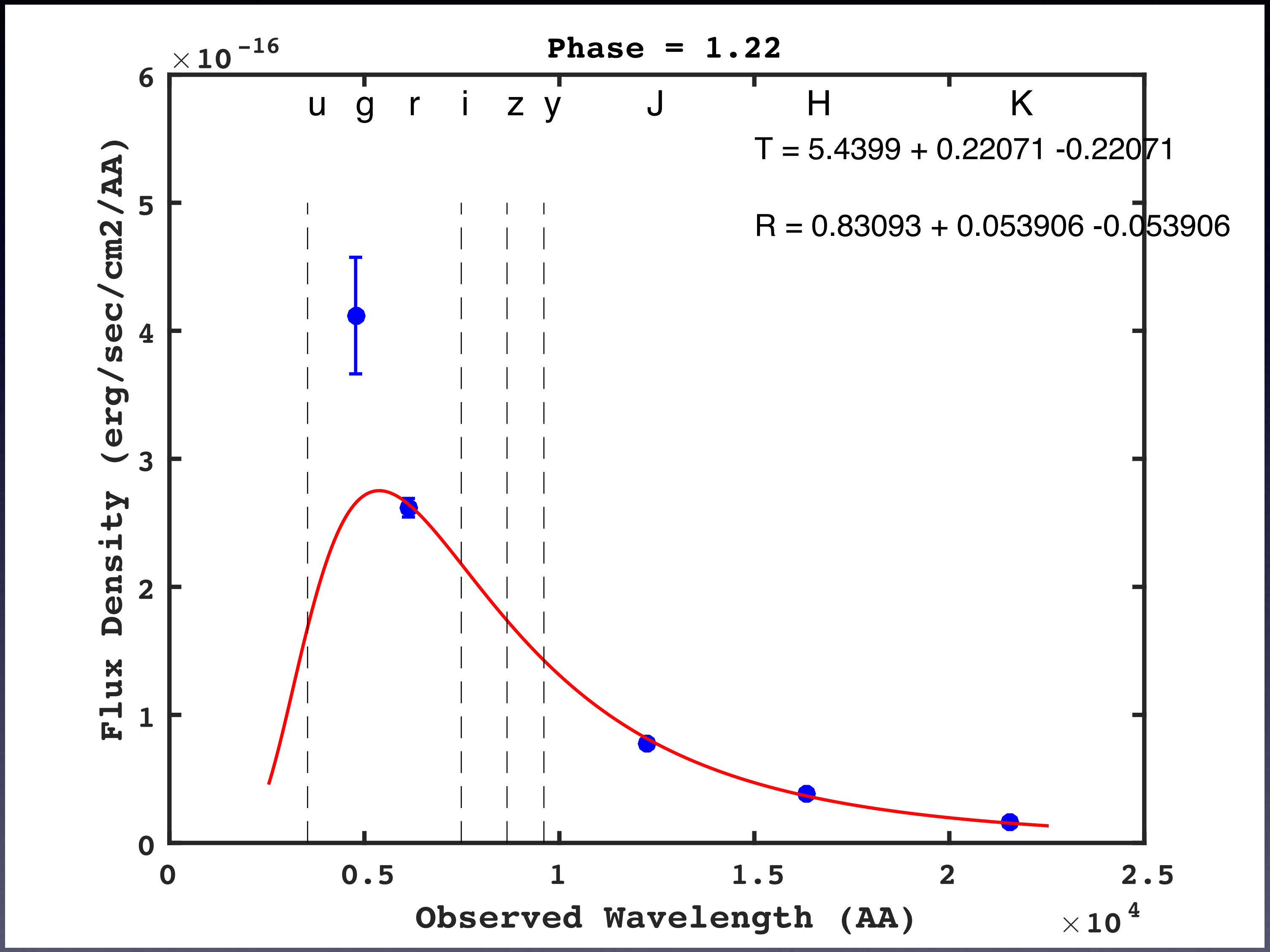

Optical : LCO, 1.5m Boyden

NIR: IRSF

Arcavi et al, 2017
Smartt et al, 2017

Utomi et al. 2017

+1.43d Chile

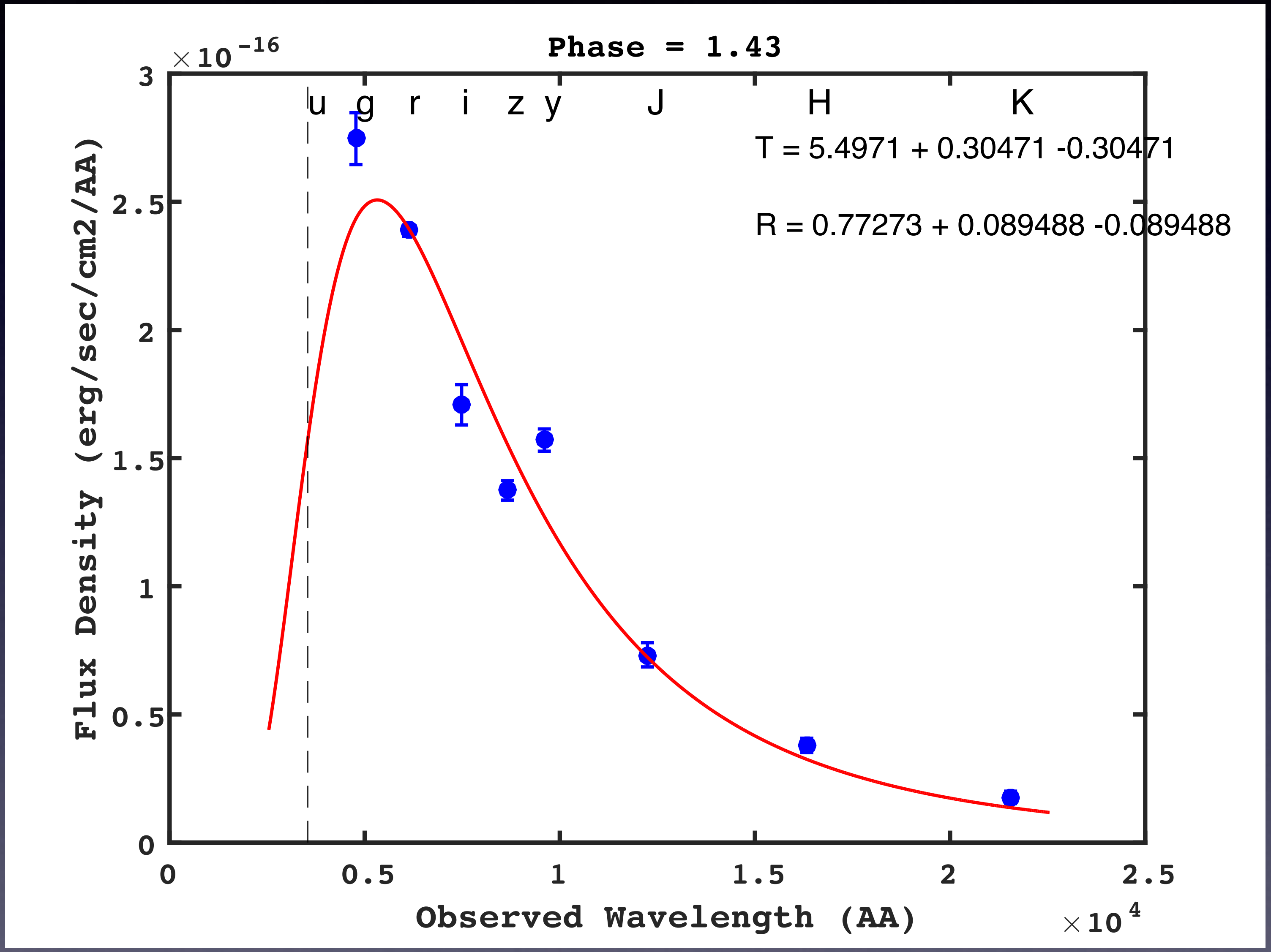

Opt: GROND, DECam

NIR: GROND

Smartt et al. 2017
Cowperthwaite et al./Soares-Santos et al. 2017

Smartt et al. 2017

+1.69d Hawaii

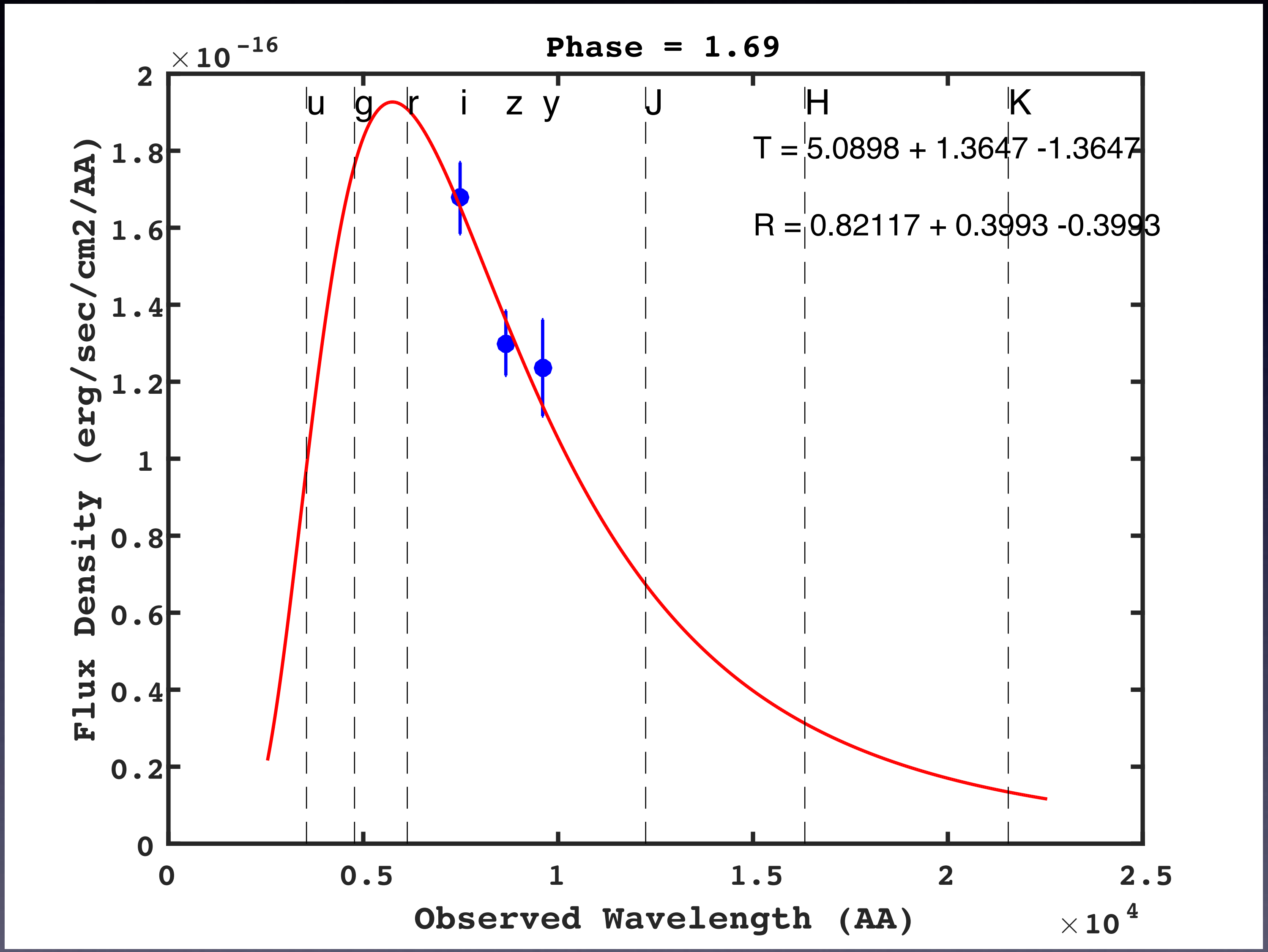

Optical/NIR: Pan-STARRS

Smartt et al. 2017

+1.82d Australia

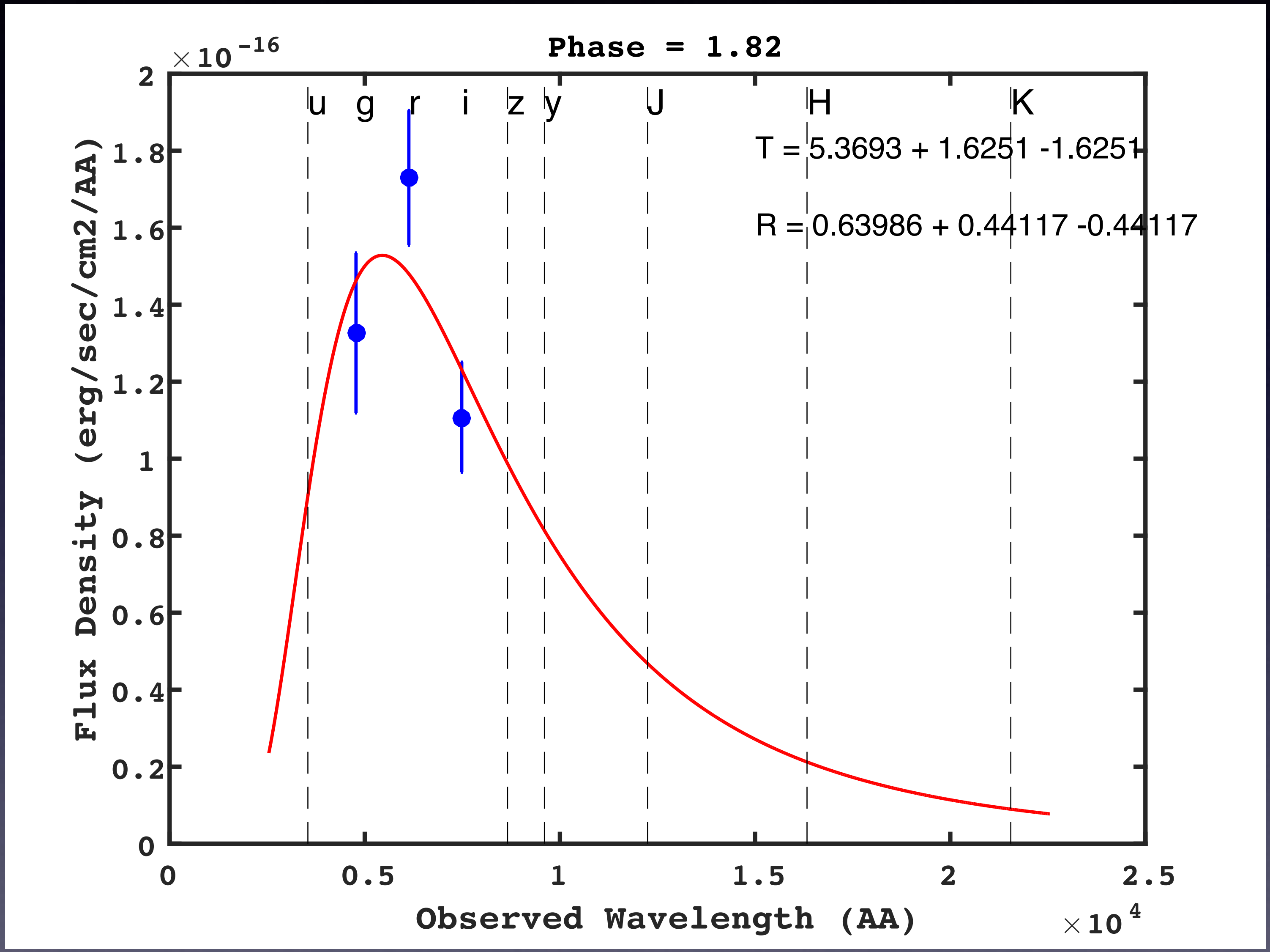

Opt: SkyMapper

Andreoni et al. 2017

+2.21d South Africa

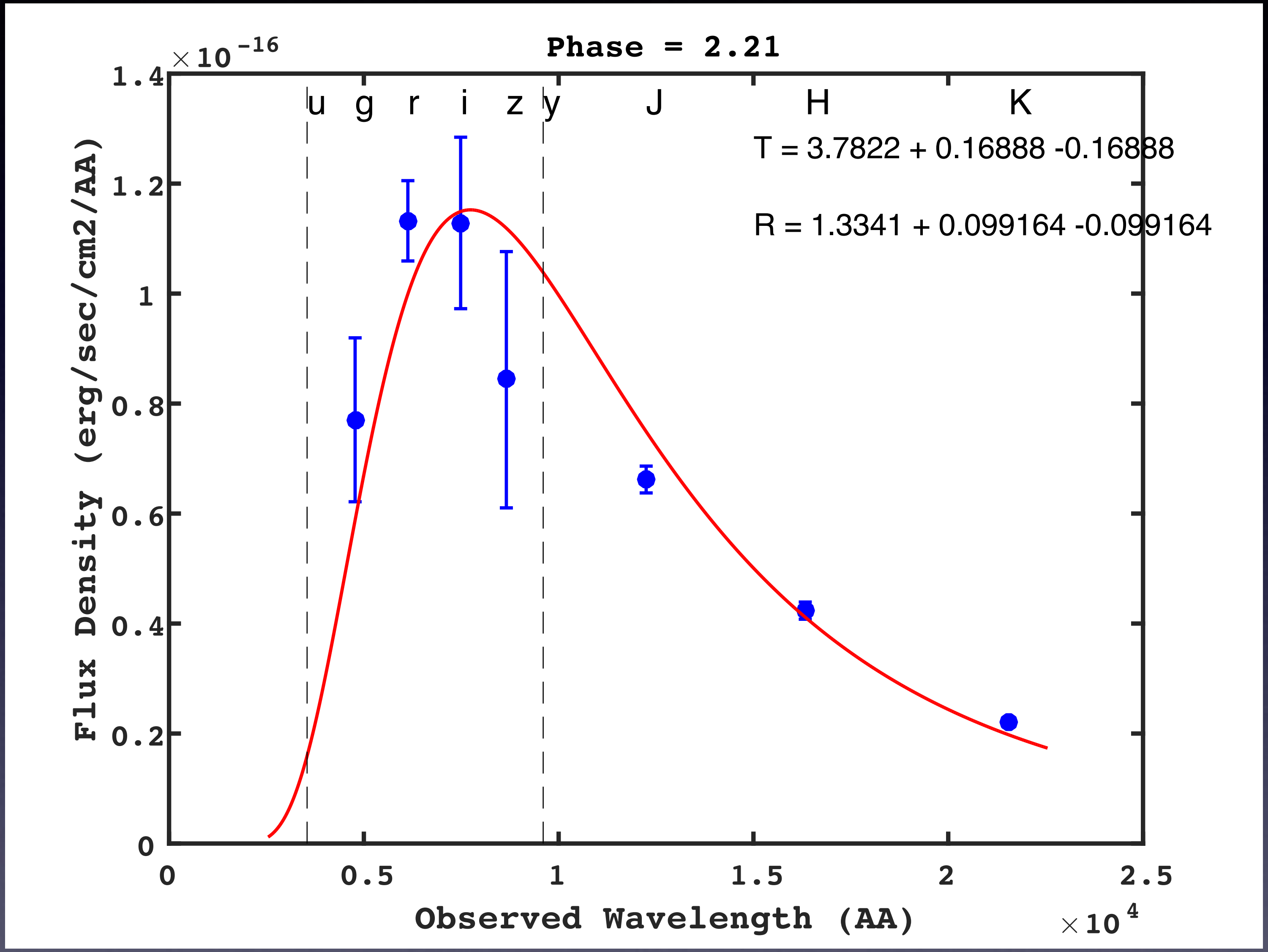

Optical : LCO, 1.5m Boyden

Arcavi et al, 2017
Smartt et al, 2017

NIR: IRSF

Utomi et al. 2017

+2.42d Chile

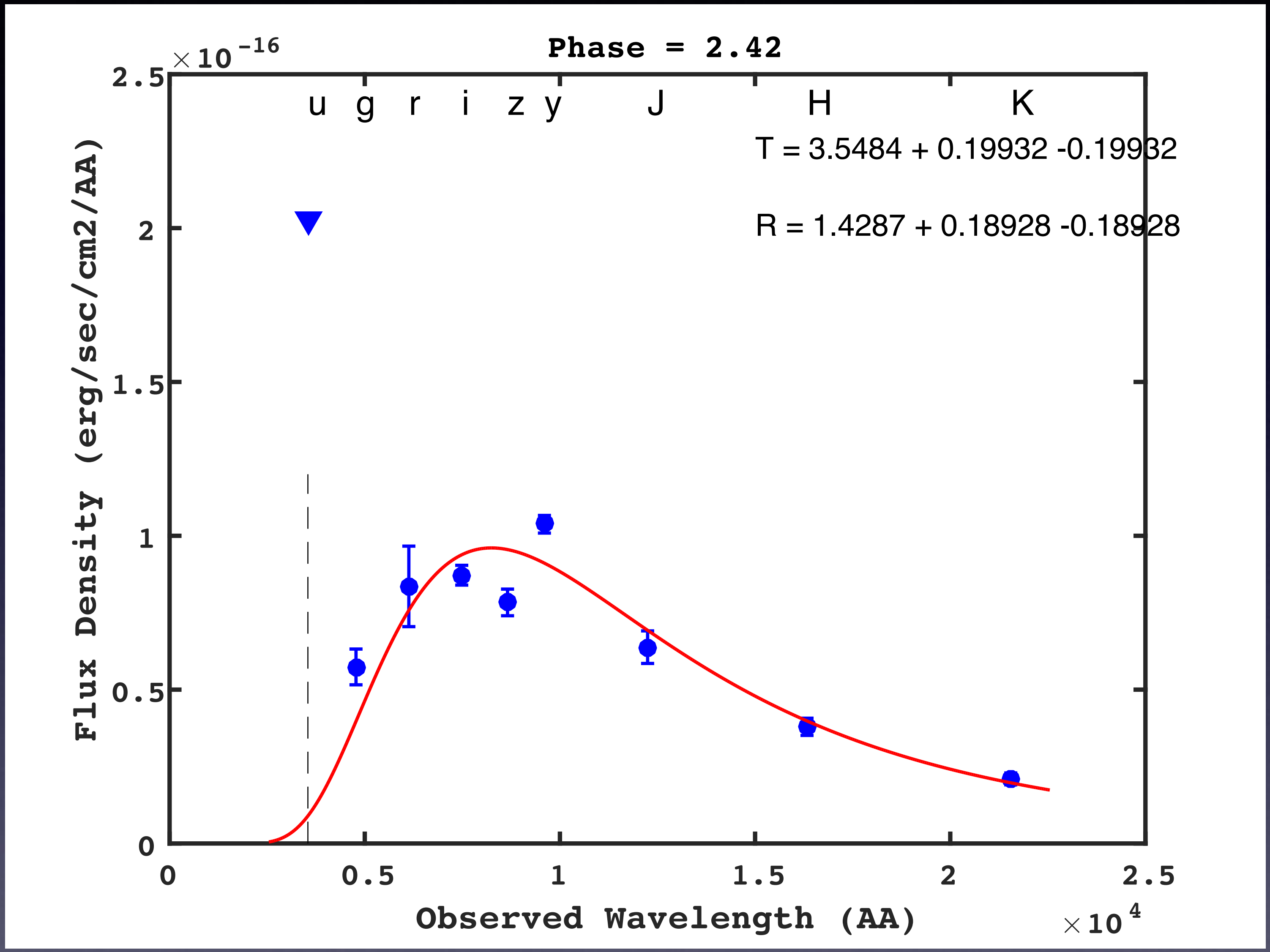

Opt: GROND, DECam

Smartt et al. 2017
Cowperthwaite et al./Soares-Santos et al. 2017

NIR: GROND

Smartt et al. 2017

+2.68d Hawaii

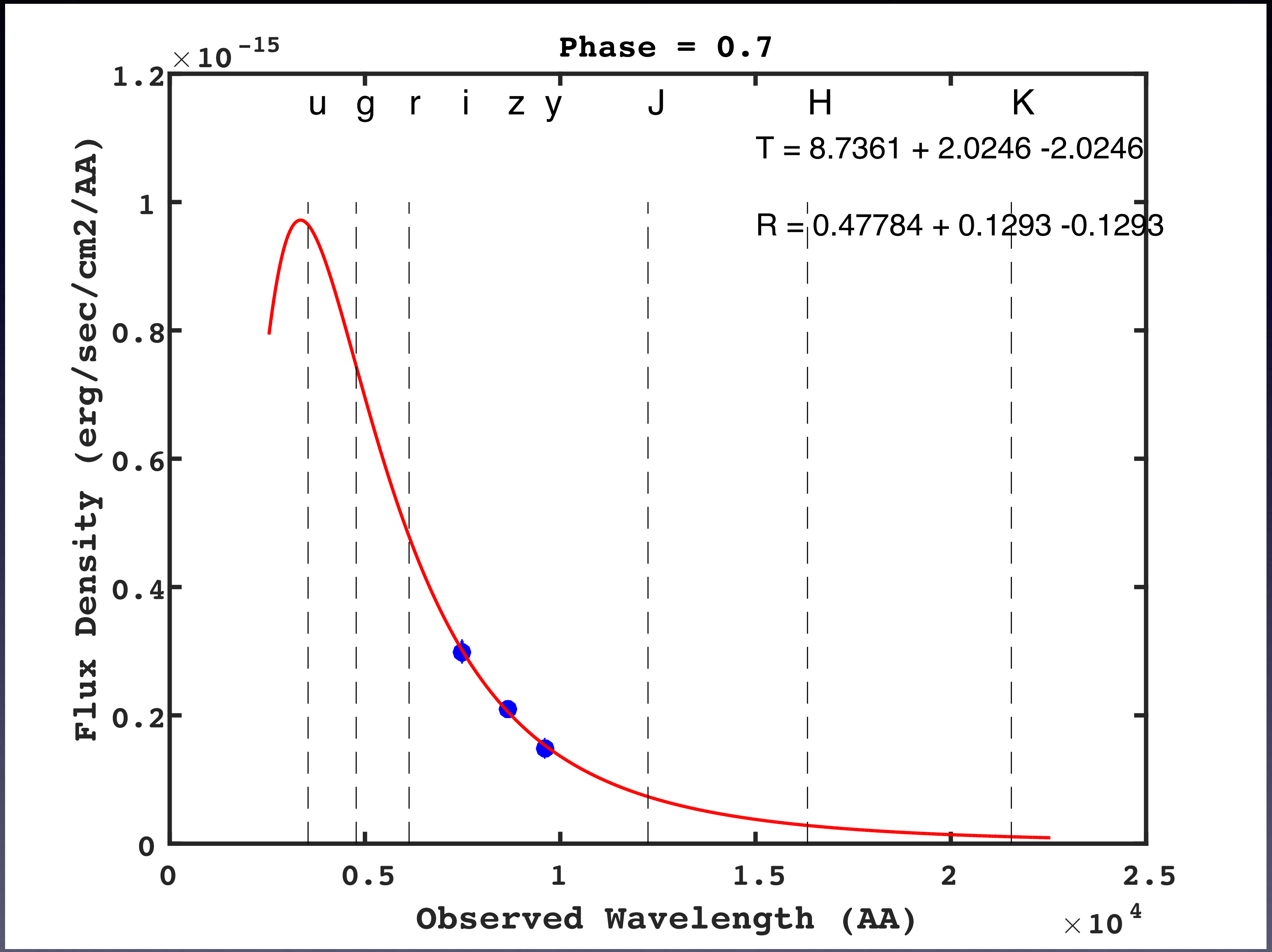

Optical/NIR: Pan-STARRS

Smartt et al. 2017

+2.83d Australia

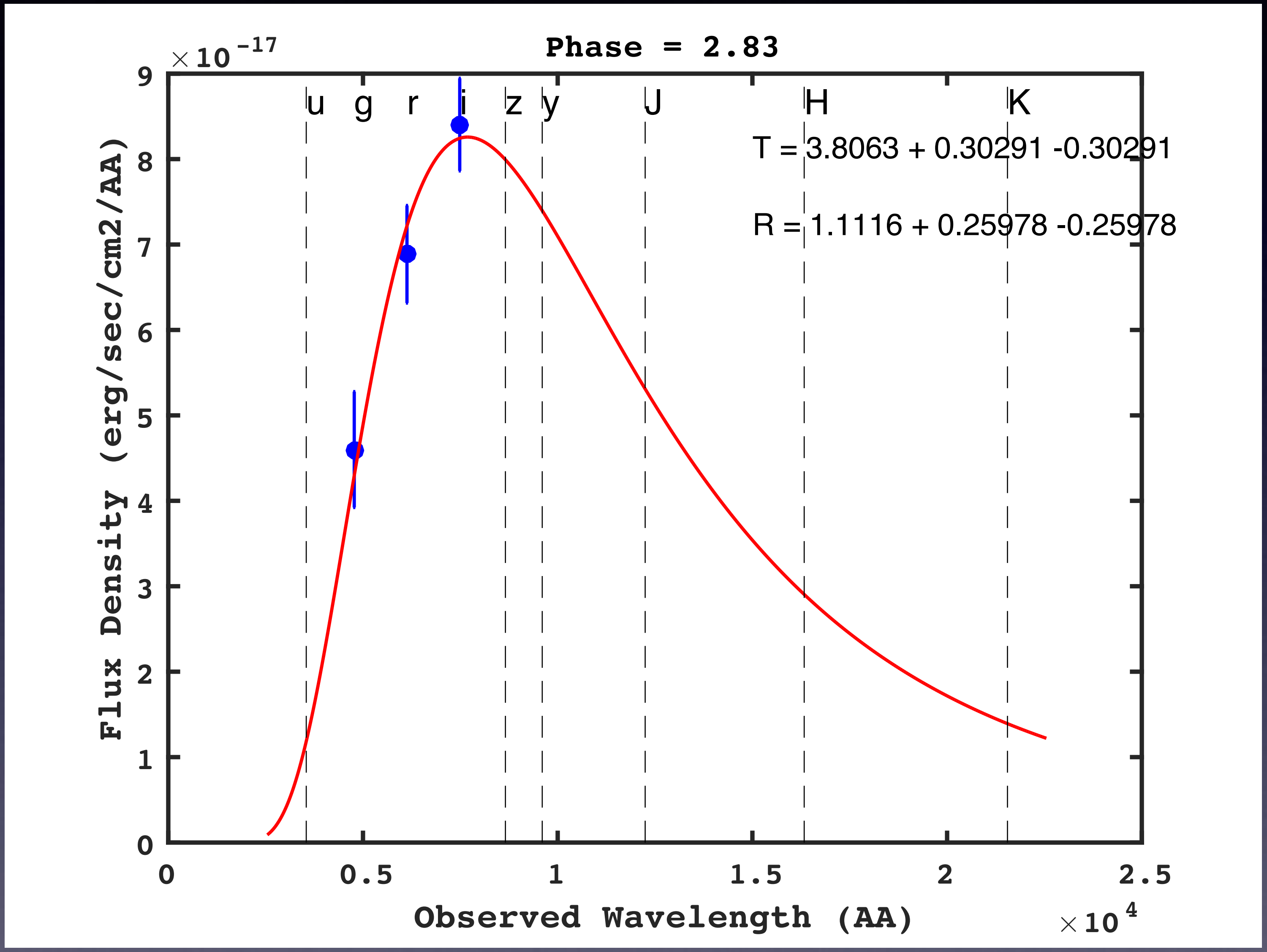

Opt: SkyMapper

Andreoni et al. 2017

+3.22d South Africa

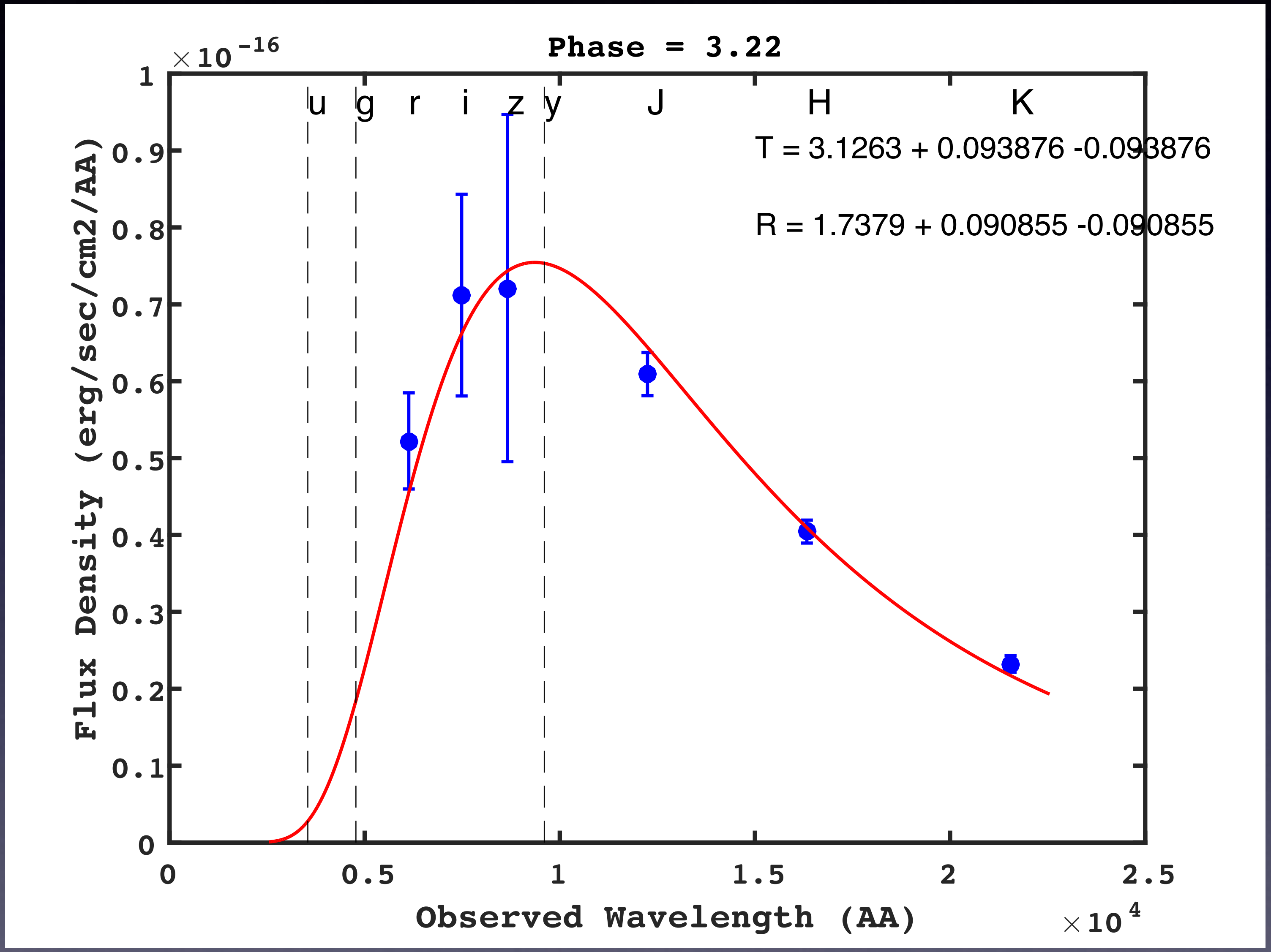

Optical : LCO, 1.5m Boyden

NIR: IRSF

Arcavi et al, 2017
Smartt et al, 2017

Utomi et al. 2017

+3.41d Chile

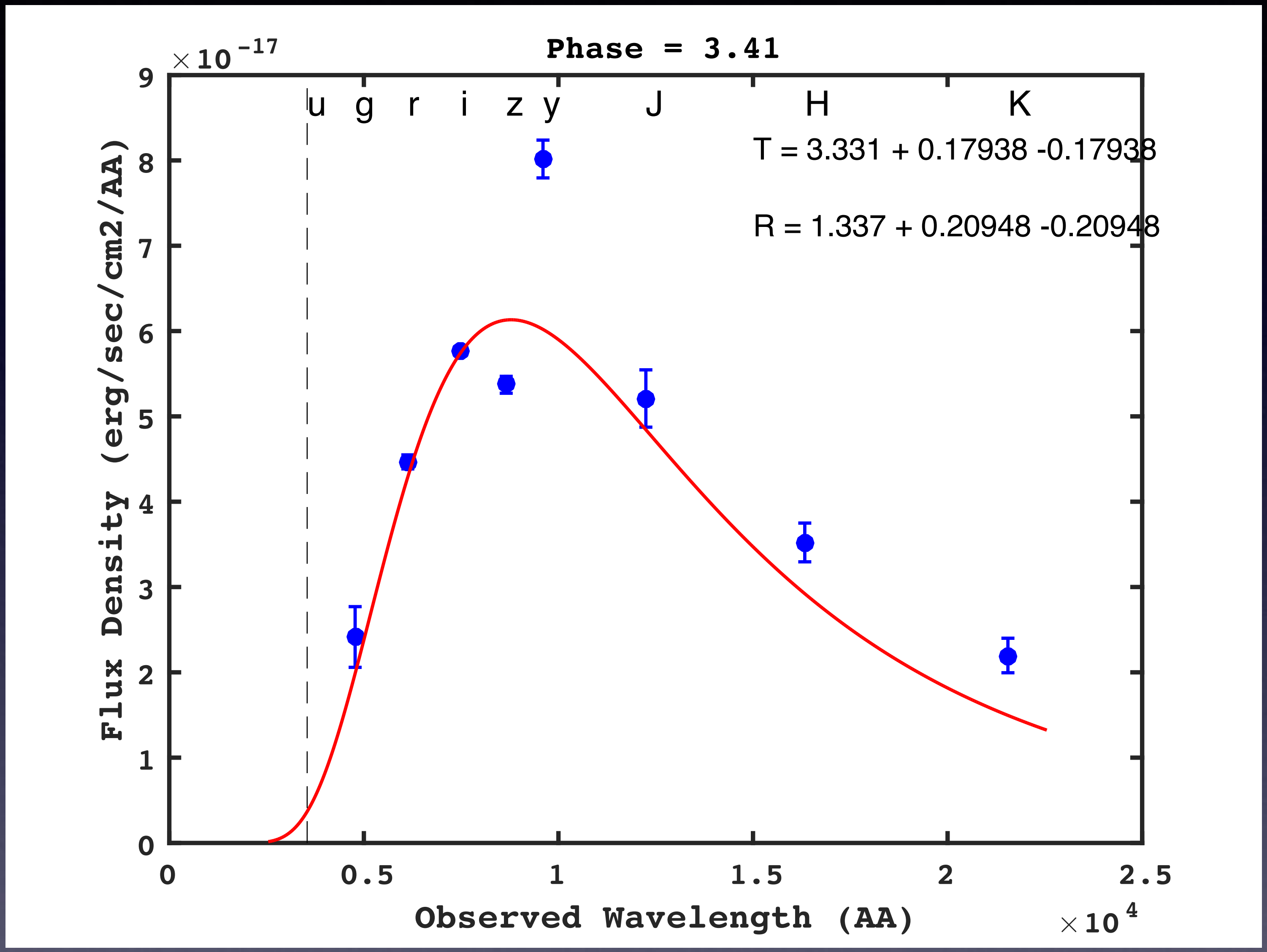

Opt: GROND, DECam

NIR: GROND

Smartt et al. 2017
Cowperthwaite et al./Soares-Santos et al. 2017

Smartt et al. 2017

+4.14d South Africa

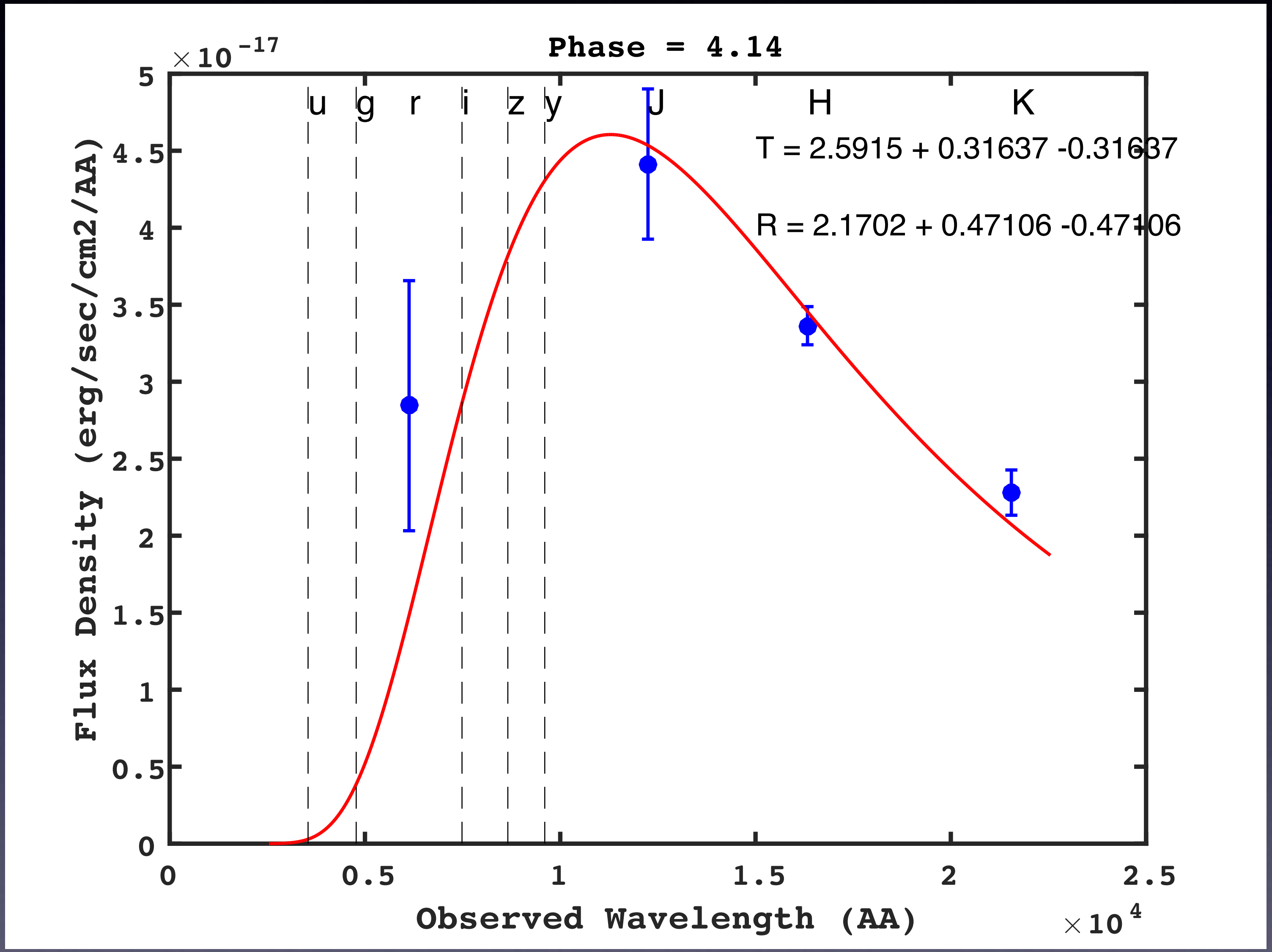

Optical : LCO

Arcavi et al, 2017

NIR: IRSF

Utomi et al. 2017

+4.4d Chile

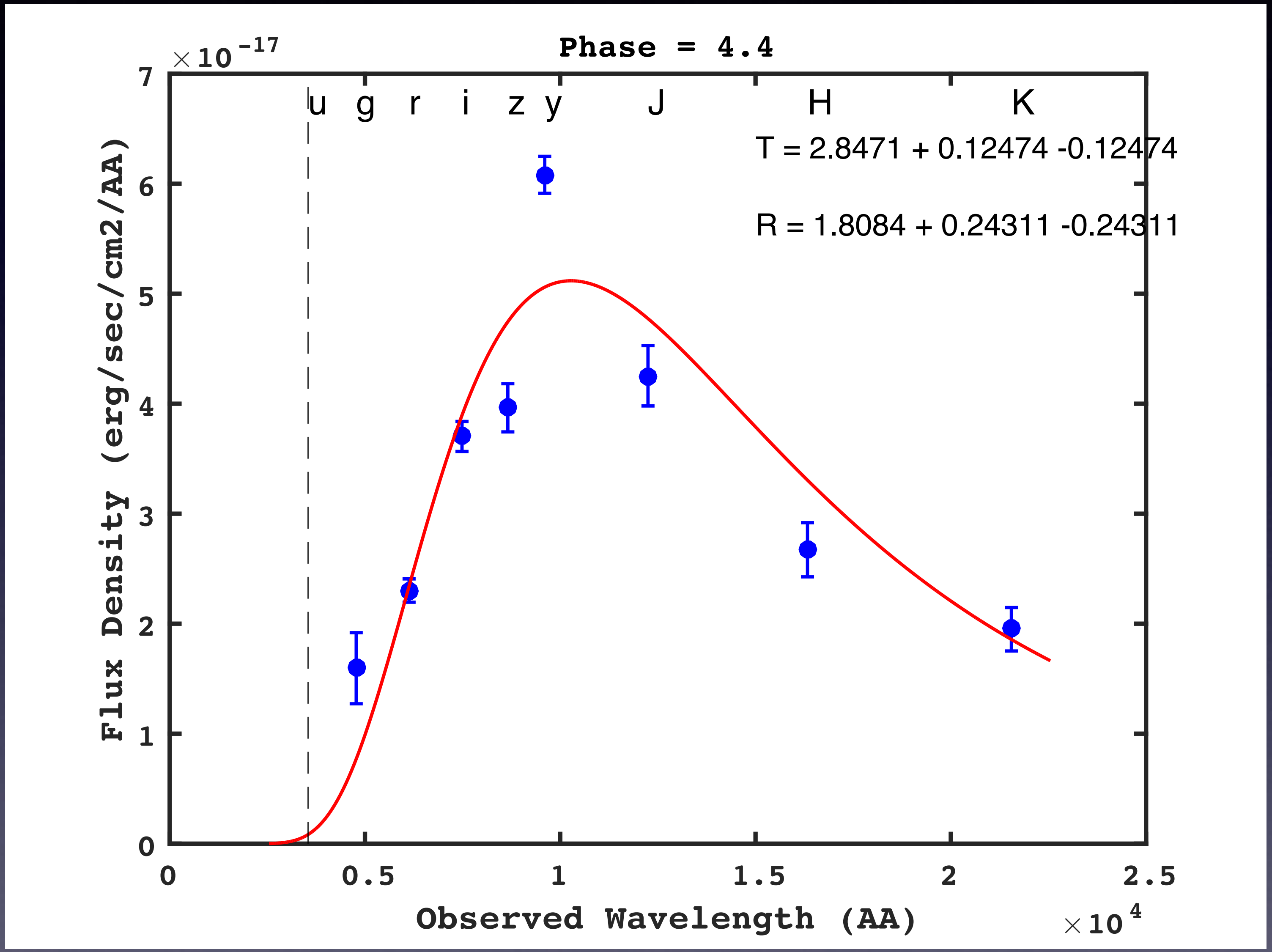

Opt: GROND, DECam

NIR: GROND

Smartt et al. 2017
Cowperthwaite et al./Soares-Santos et al. 2017

Smartt et al. 2017

+5.4d Chile

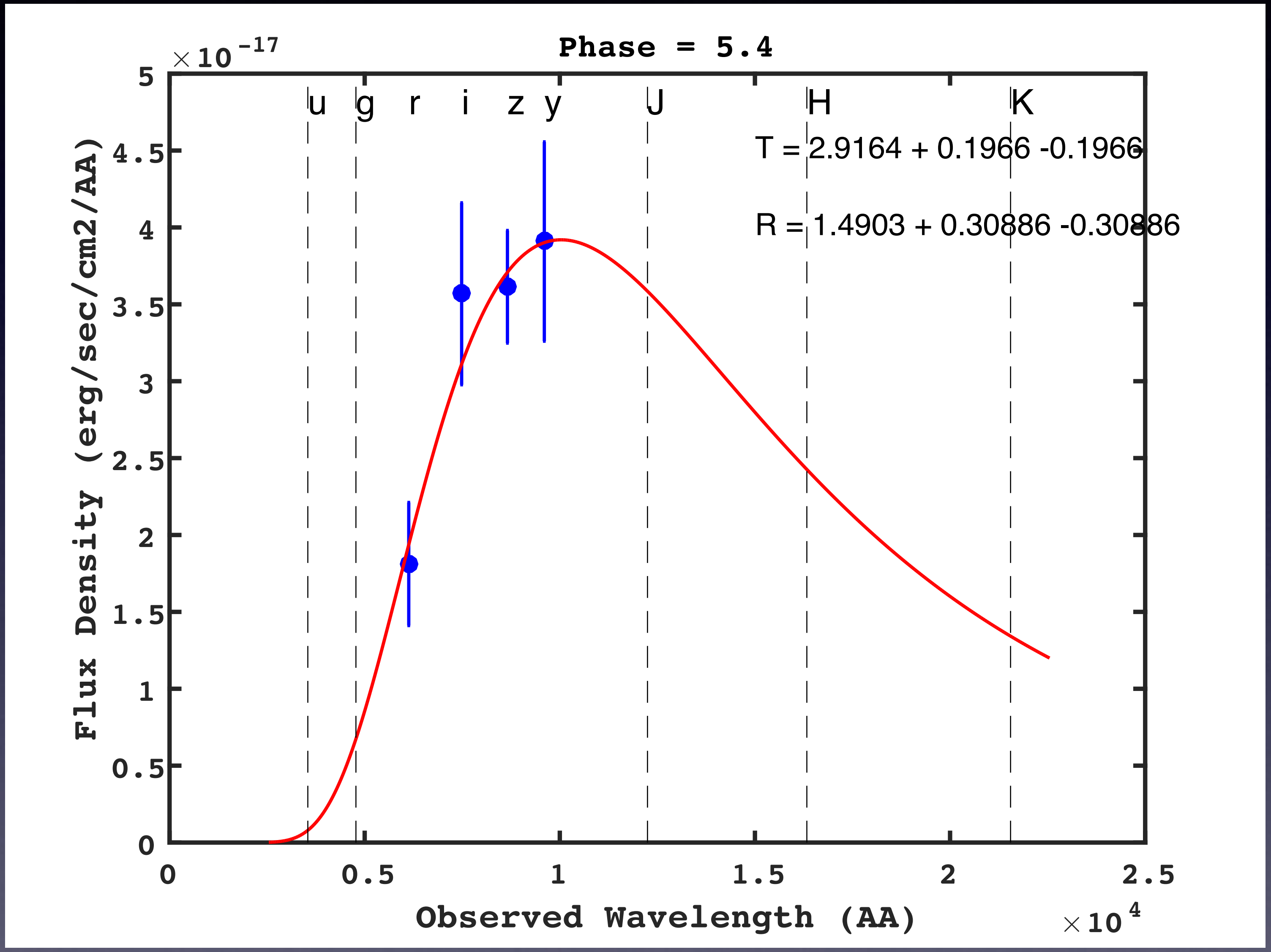

Opt: DECam

Cowperthwaite et al./Soares-Santos et al. 2017

+6.4d Chile

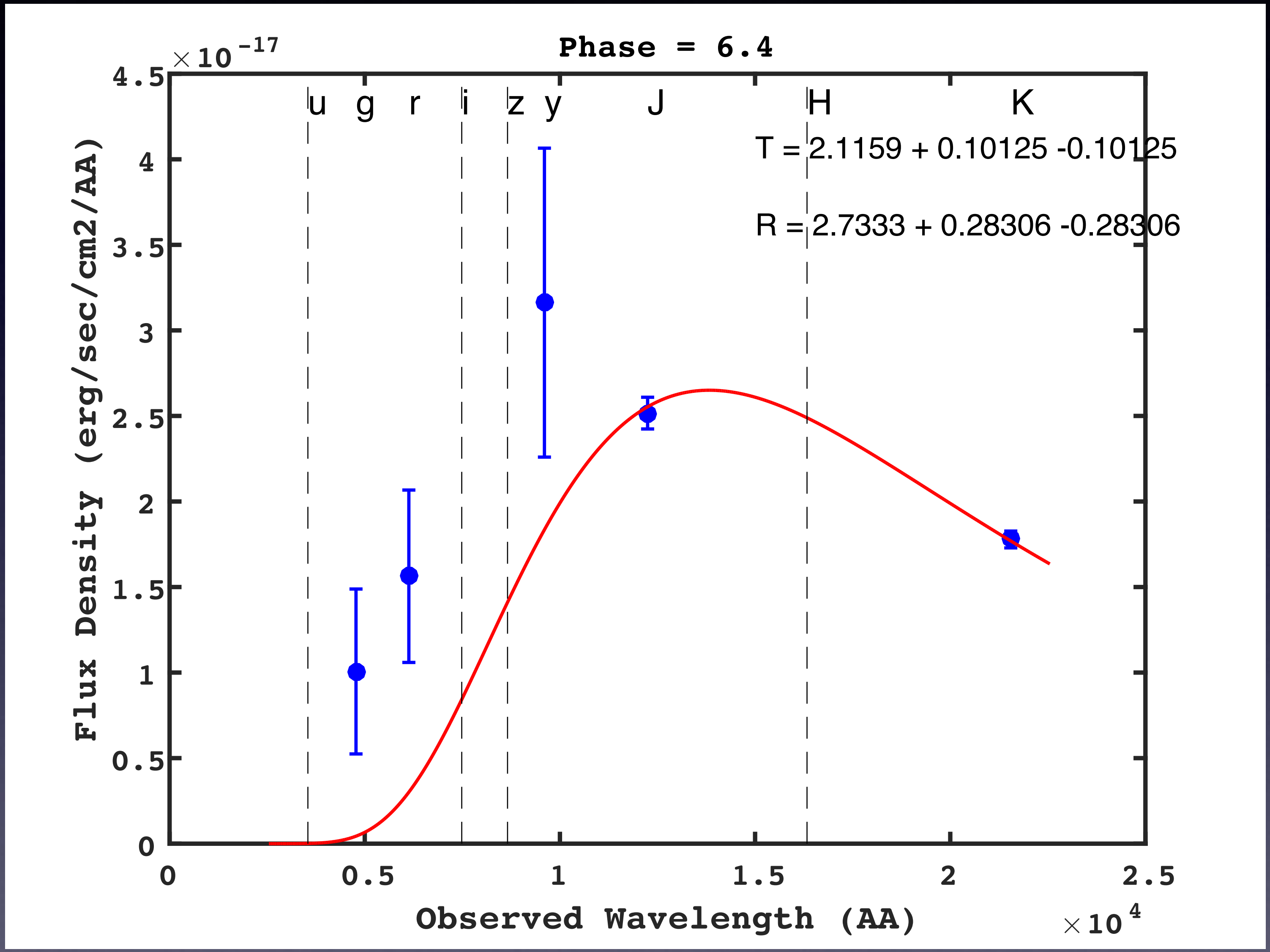

Opt:DECam

NIR: VISTA

Cowperthwaite et al./Soares-Santos et al. 2017

Tanvir et al. 2017

+7.4d Chile

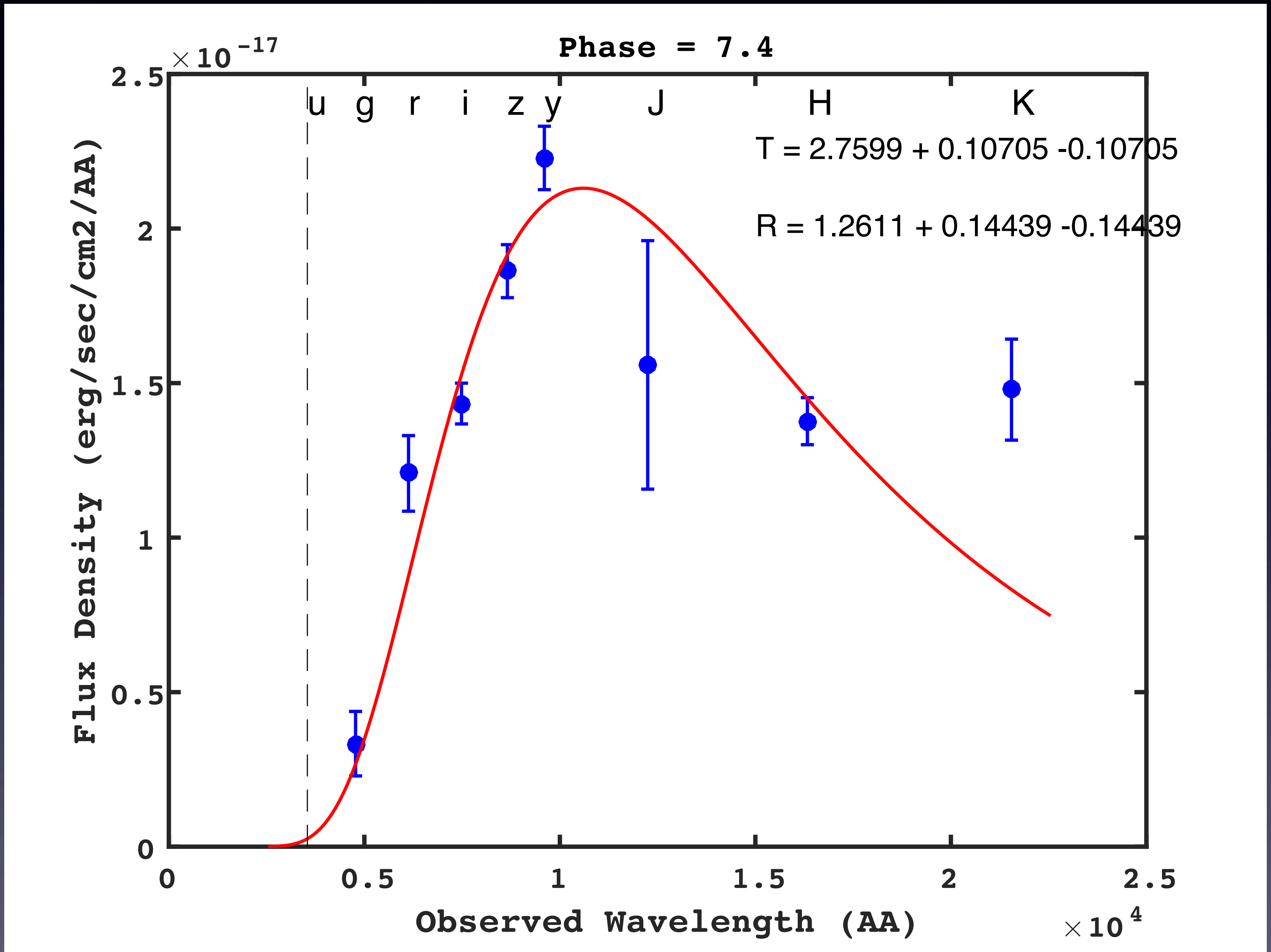

Opt:DECam

Cowperthwaite et al./Soares-Santos et al. 2017

NIR: GROND

Smartt et al. 2017

+8.4d Chile

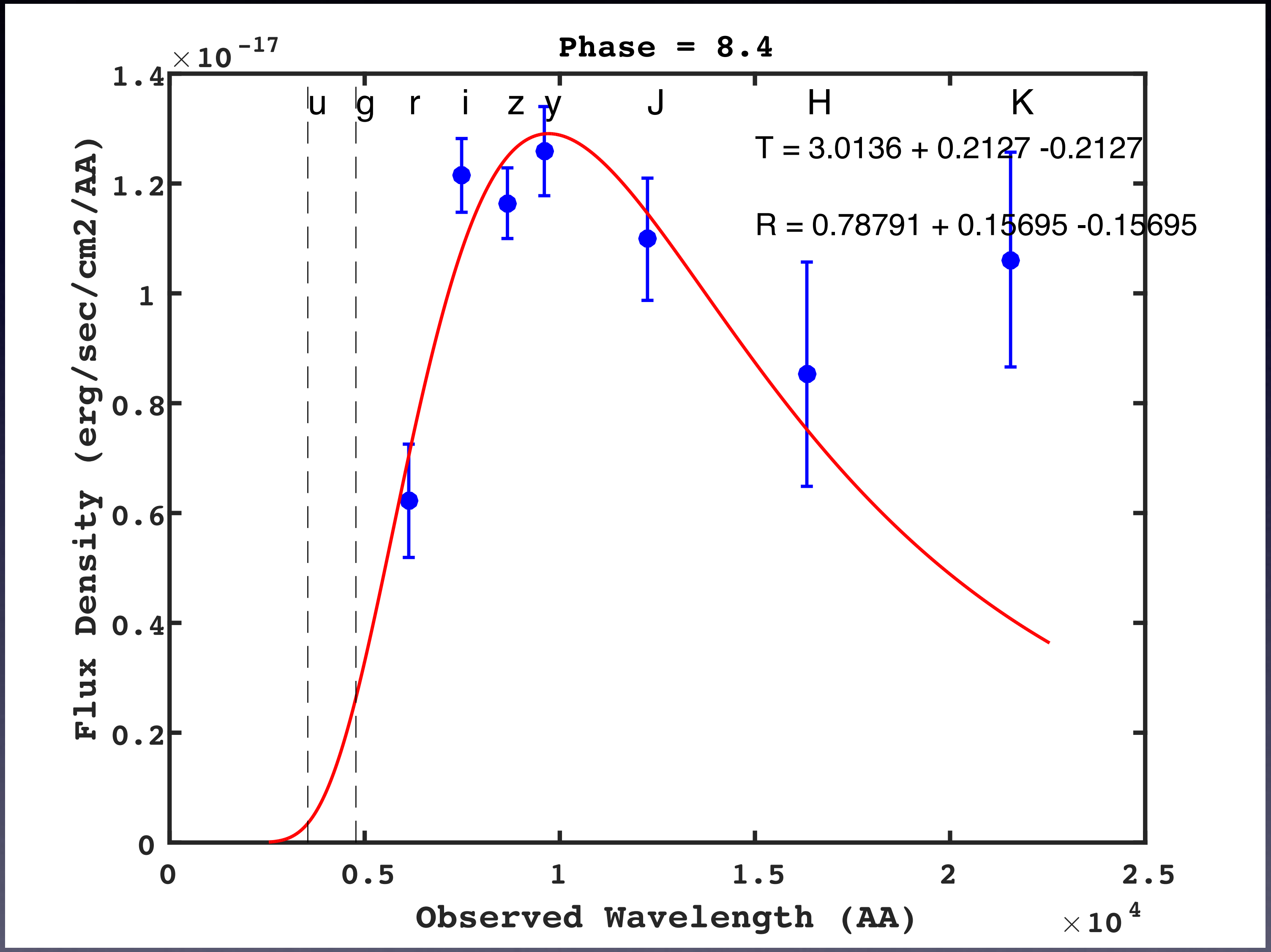

Opt:DECam

Cowperthwaite et al./Soares-Santos et al. 2017

NIR: GROND

Smartt et al. 2017

+9.4d Chile

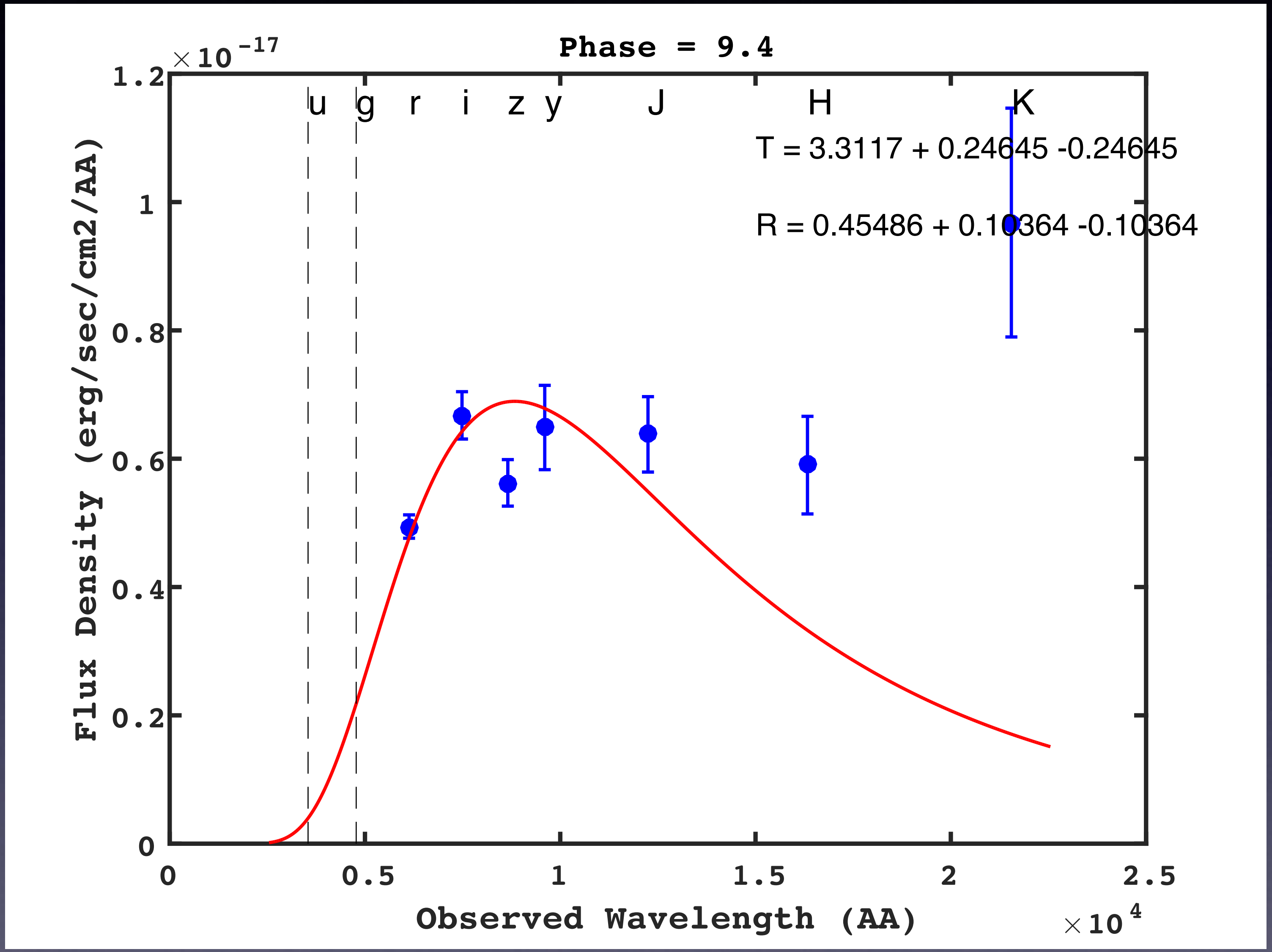

Opt:DECam, VIMOS

Cowperthwaite et al./Soares-Santos et al. 2017

Tanvir et al. 2017

NIR: GROND

Smartt et al. 2017

+10.4d Chile

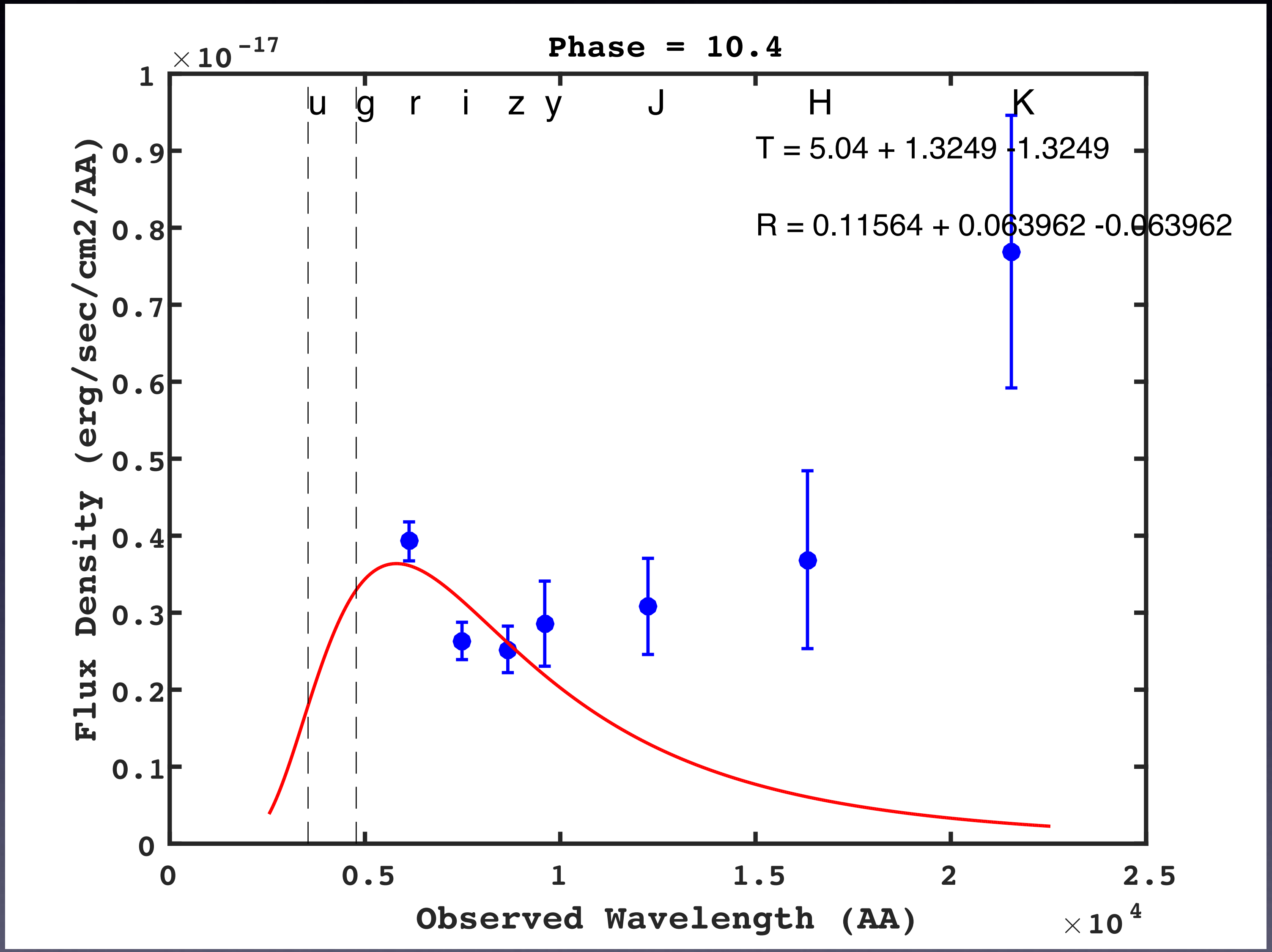

Opt:DECam, VIMOS

Cowperthwaite et al./Soares-Santos et al. 2017

Tanvir et al. 2017

NIR: GROND

Smartt et al. 2017

+11.3d Chile + Space (HST)

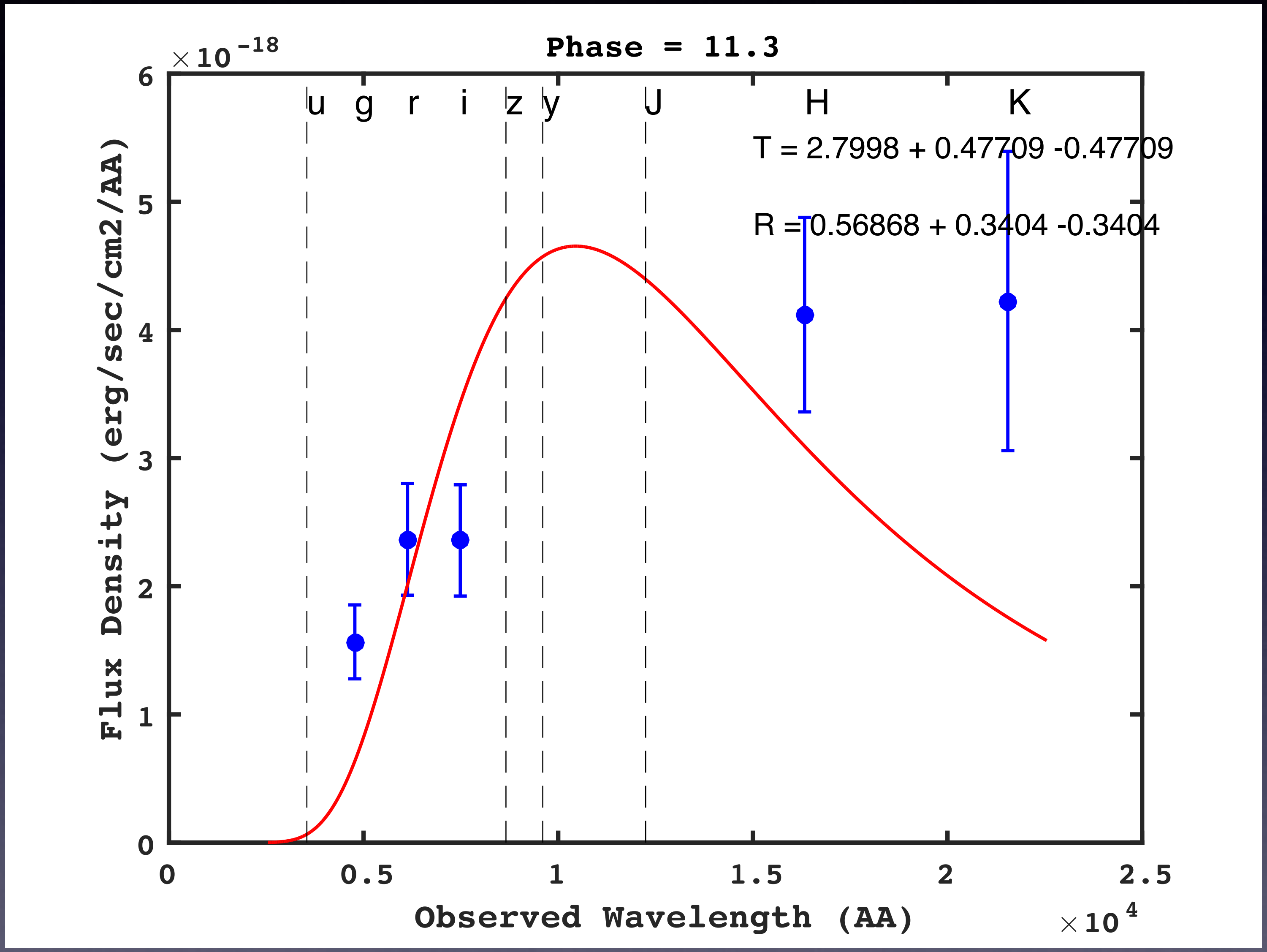

Opt: HST

Tanvir et al. 2017

NIR: GROND + NTT

Smartt et al. 2017

+13.2d Chile

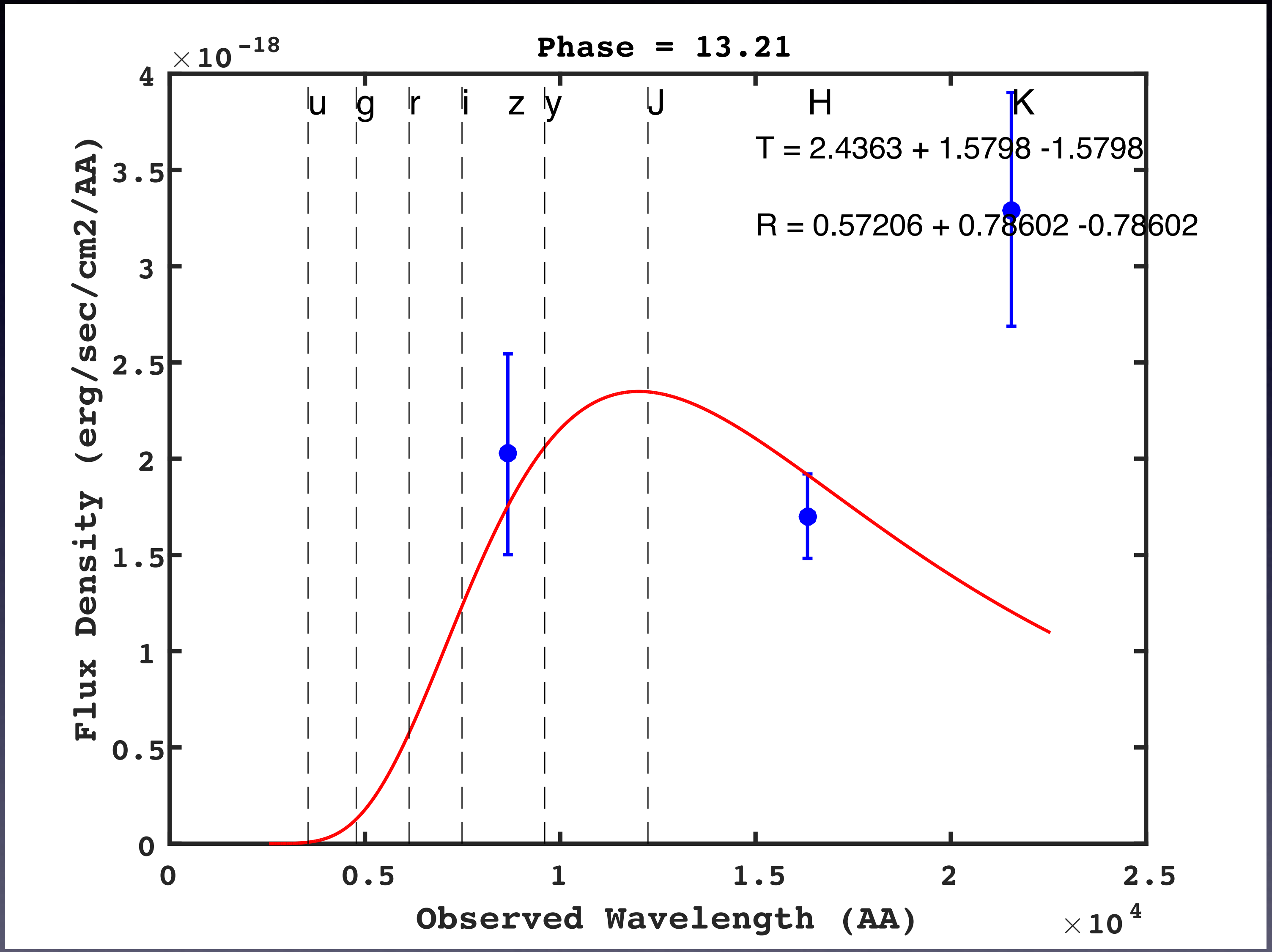

Opt: VIMOS

Tanvir et al. 2017

NIR: NTT and Gemini South

Smartt et al. 2017

Chornock et al. 2017

+14.3d Chile

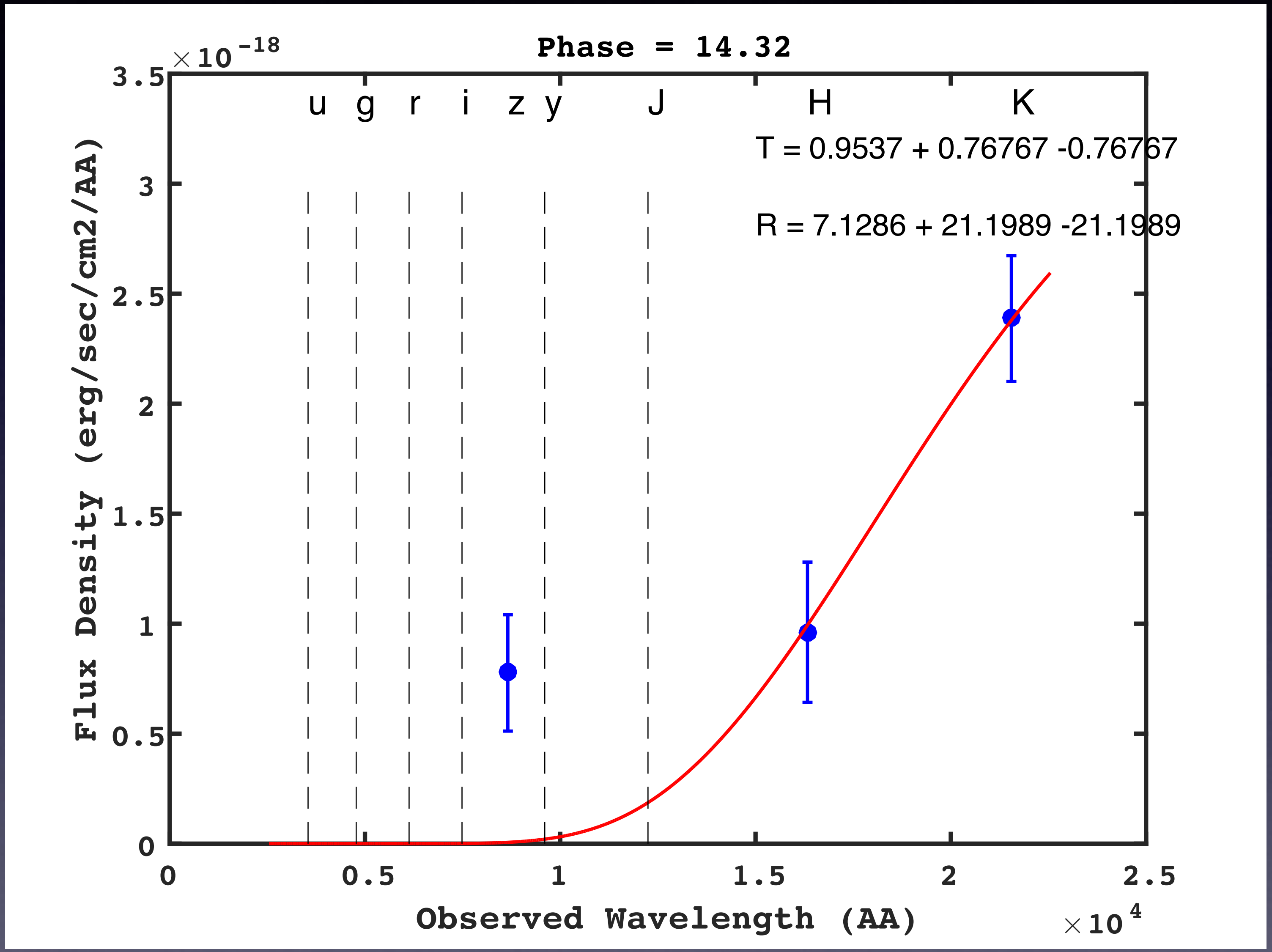

Opt: FORS2

Pian et al. 2017

NIR: VISTA and Gemini South

Tanvir et al. 2017,
Chornock et al. 2017
Kasliwal et al. 2017
Troja et al. 2017

Unconstrained beyond +15d

- K-band only beyond +15d
- SED unconstrained, can't say if it is compatible with T ≈ 2500 K

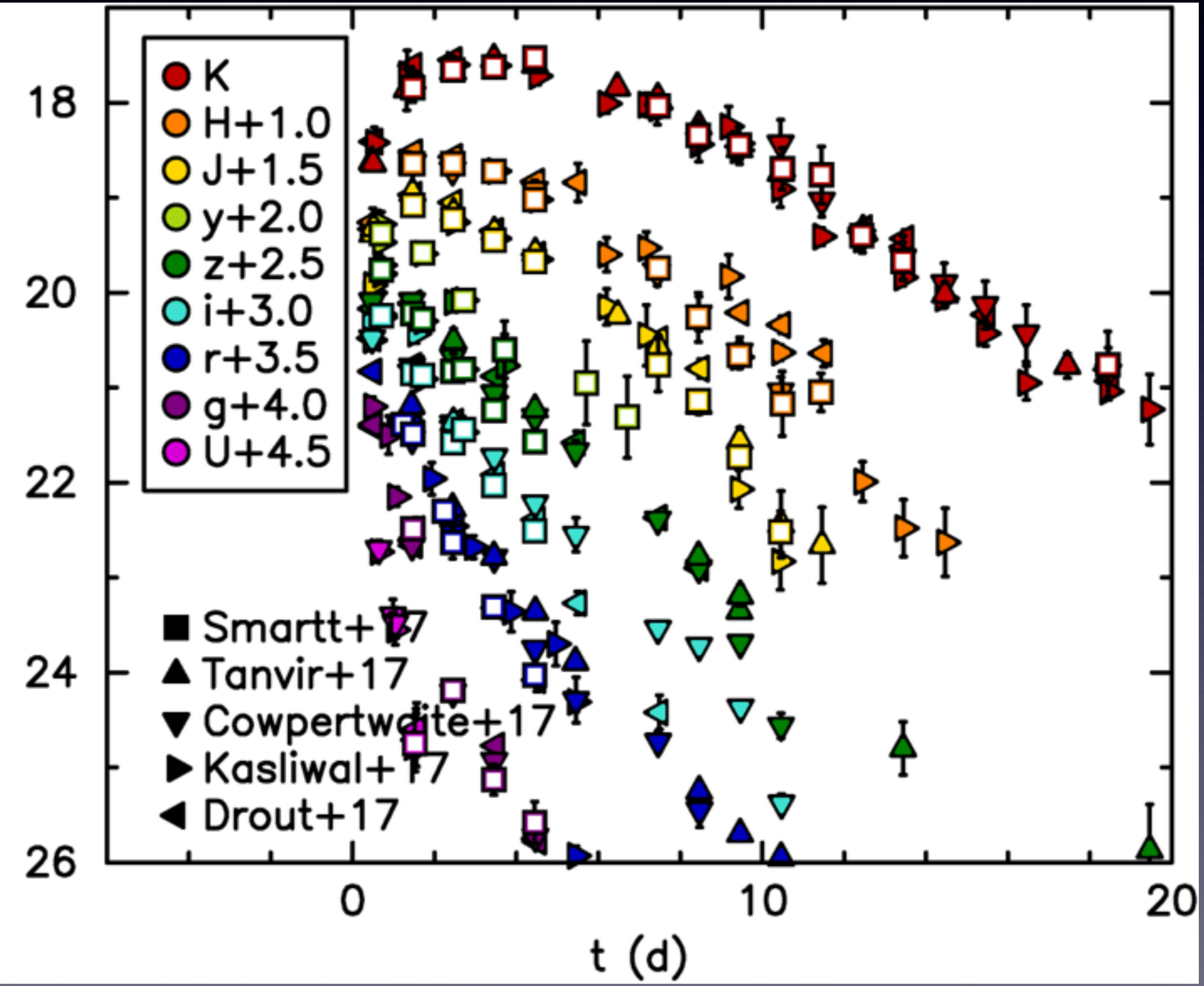

L_{bol} : reasonable agreement

Waxman et al.
arXiv:1711.09638

Beyond 2.5m
add Rayleigh-Jeans
tail ***f(λ) ~ λ^{-5}***

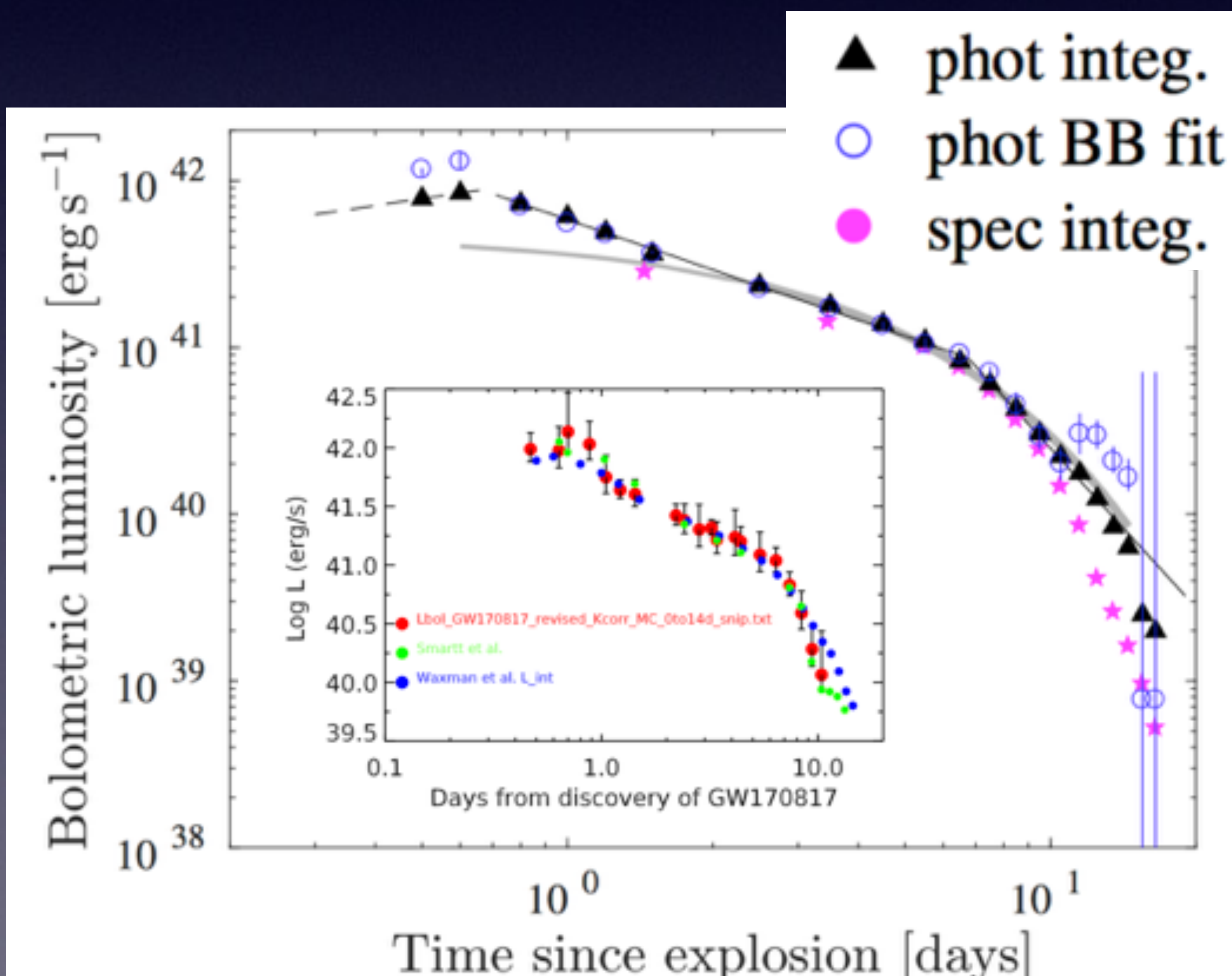

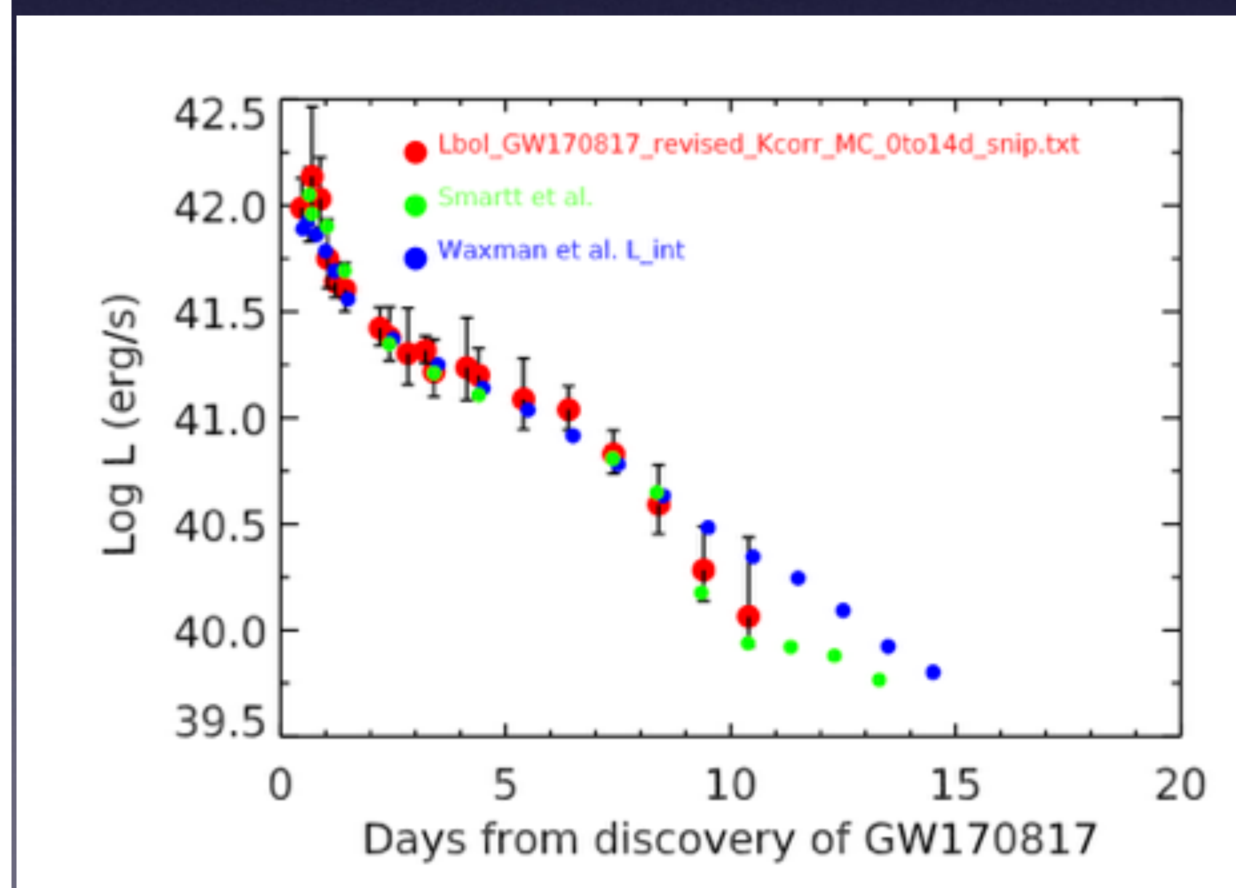

Peak luminosity

- "Peak" resolved within first 24hrs
- $0.4 < t_{peak} < 0.9$ days
- Log $L_{peak} = 42.0 \pm 0.1$
- $L = 1^{+0.26}_{-0.21} \times 10^{42}$ ergs/s

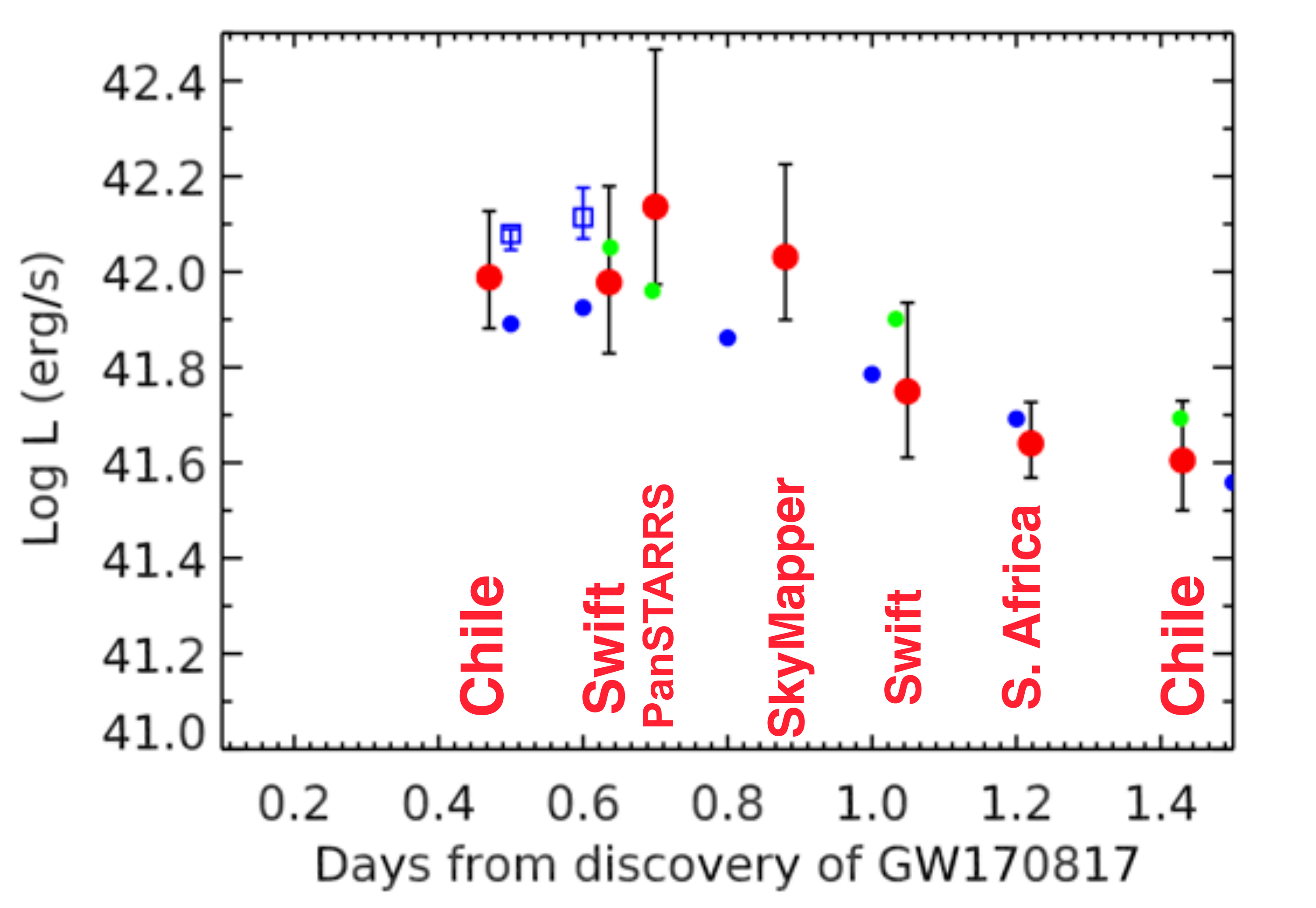

New - BB integration from all data
Smartt et al.
Waxman et al

Reasonable criticisms

- Our models are too simple - Metzger 2017 “toy model” and Arnett-Jerkstrand semi-analytic model
- We do not use the SED/spectral information available when fitting the lightcurve (L_{bol} only)
- We have underestimated K-band at > 10d. Therefore underestimated the contribution to a high opacity component
- We have only integrated our L_{bol} out to 2.5microns, there is clearly **(*some*)** flux beyond that. Therefore underestimated the contribution to a high opacity component
- **The *thermalisation function and/or heating rate* we apply for radioactive decay particles (leptons) are either wrong or unknown**

Arnett-Jerkstrand model

https://star.pst.qub.ac.uk/wiki/doku.php/users/ajerkstrand/

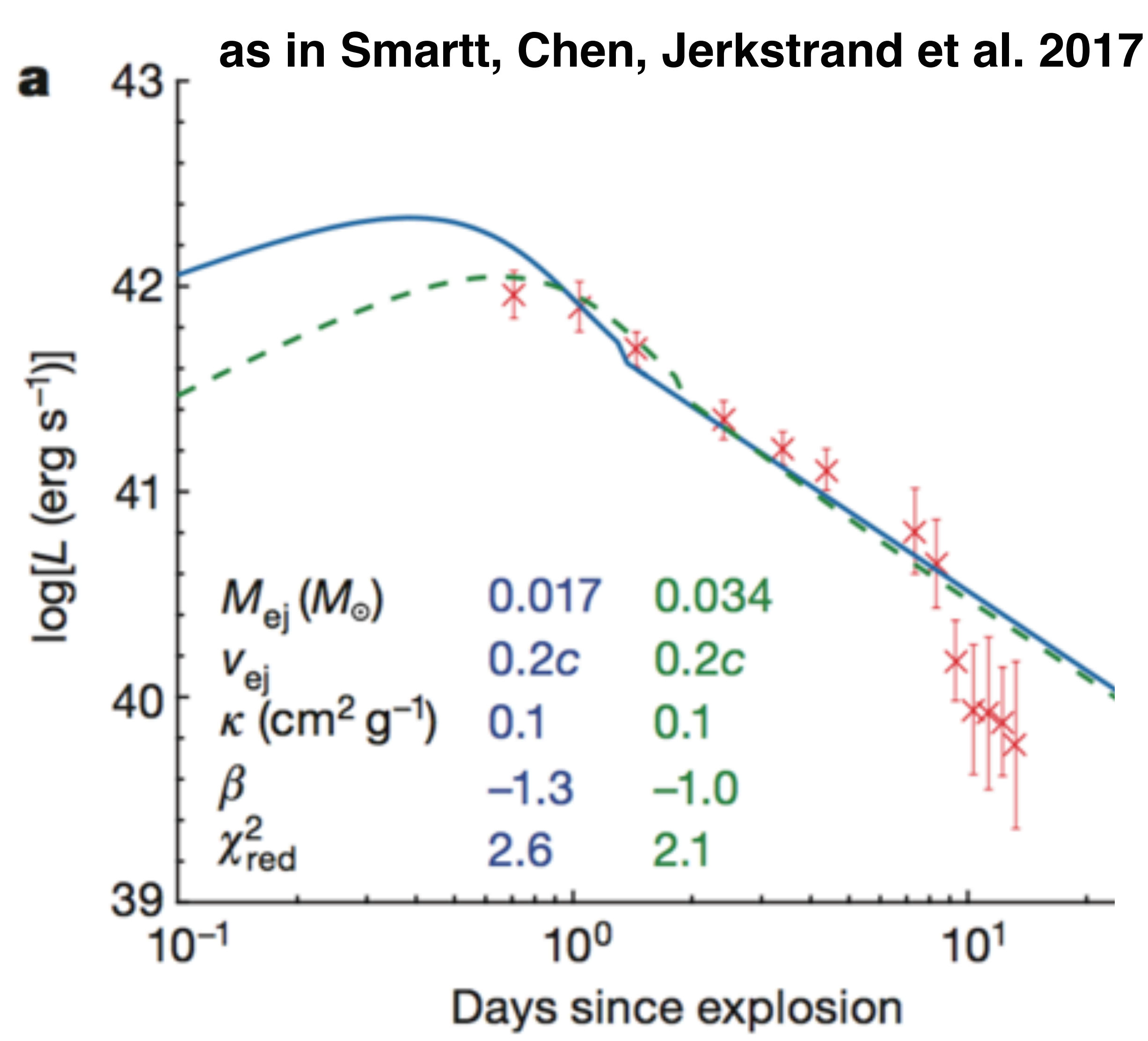

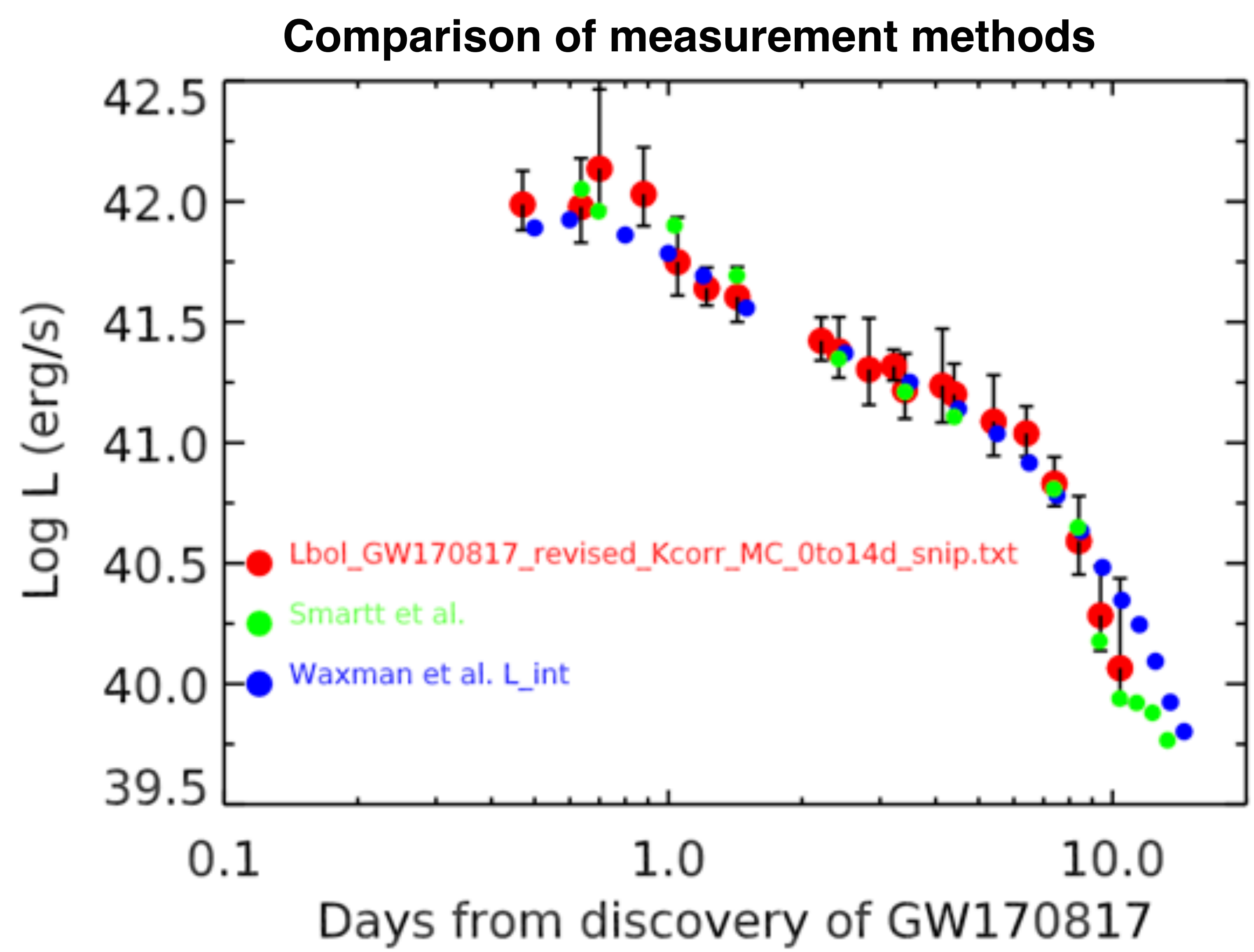

Barnes et al. : thermalisation efficiency

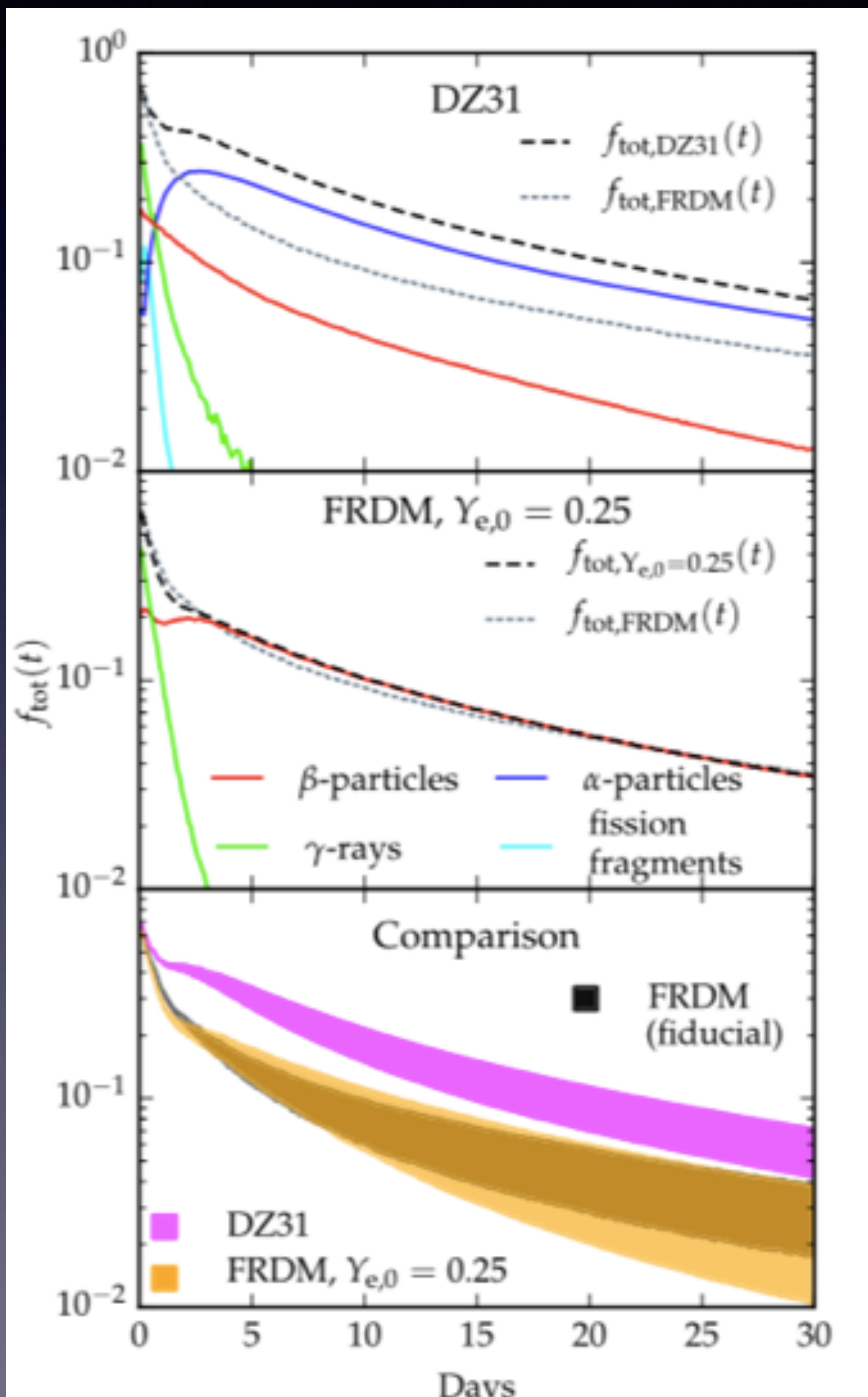

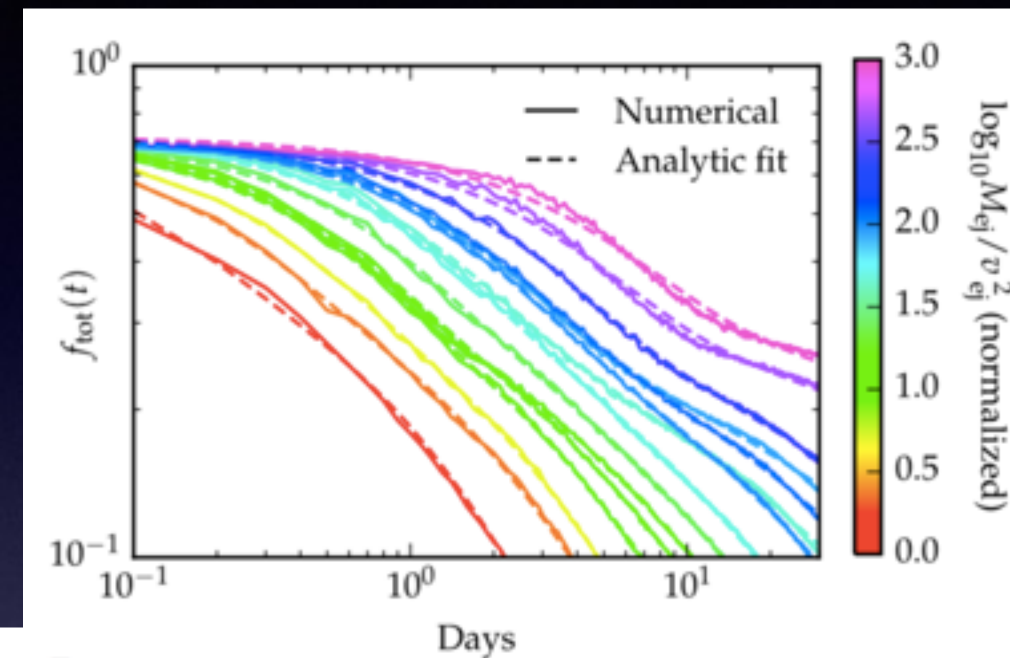

$$f_{tot}(t) = 0.36\left[\exp(-at) + \frac{\ln(1 + 2bt^d)}{2bt^d}\right],$$

Barnes et al. 2016

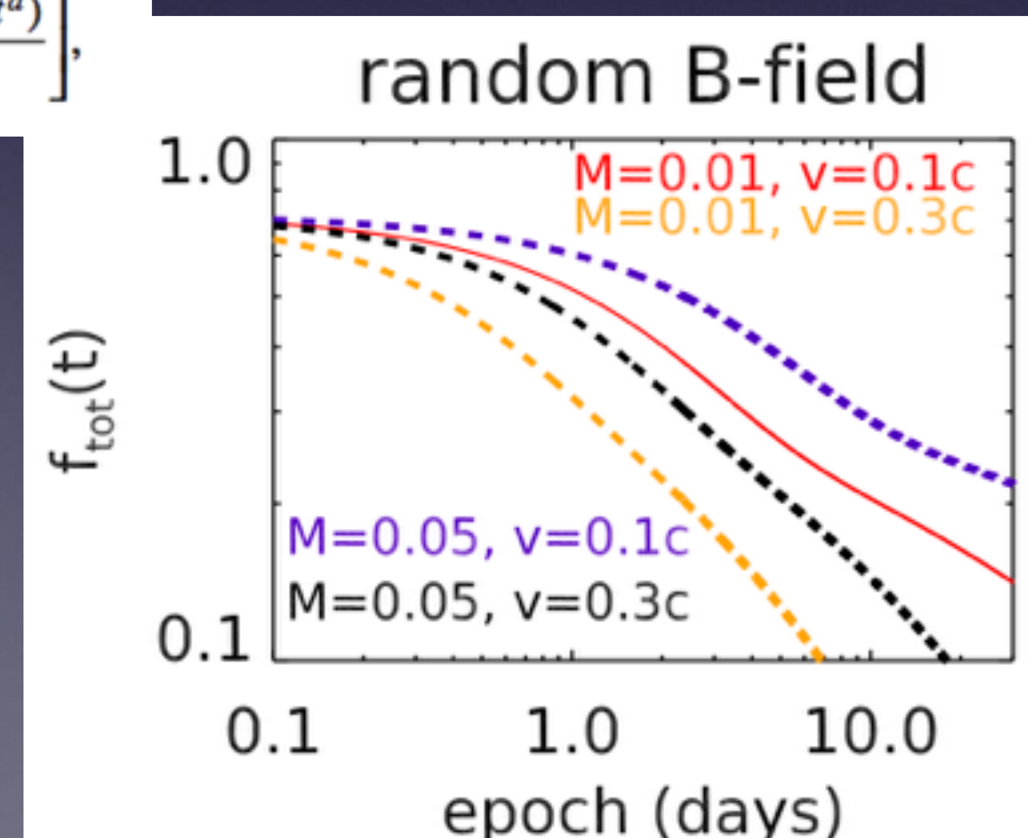

Arnett-Jerkstrand posteriors

Michael Coughlin: https://github.com/mcoughlin

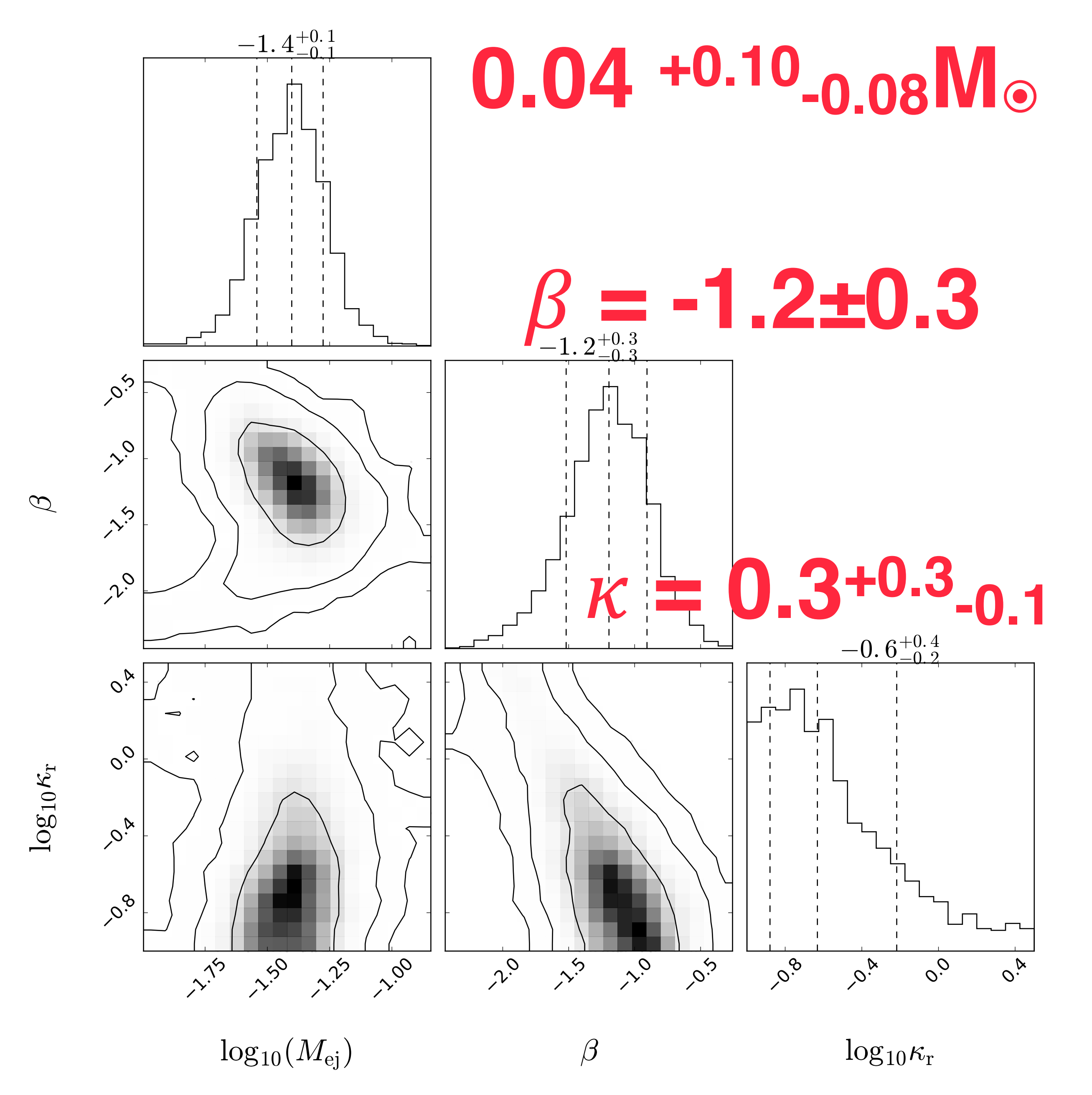

$0.04^{+0.10}_{-0.08}\,M_\odot$

$\beta = -1.2 \pm 0.3$

$\kappa = 0.3^{+0.3}_{-0.1}$

Compare with
Recent analysis by
Waxman et al. 2017

$M \approx 0.05 M_\odot$

$\kappa \approx 0.3\ \mathrm{cm^2\ g^{-1}}$

$v(m) = v_M\, m^{-\alpha}$

for $(0.1c < v < 0.3c)$

Updated Metzger posteriors

Michael Coughlin: https://github.com/mcoughlin

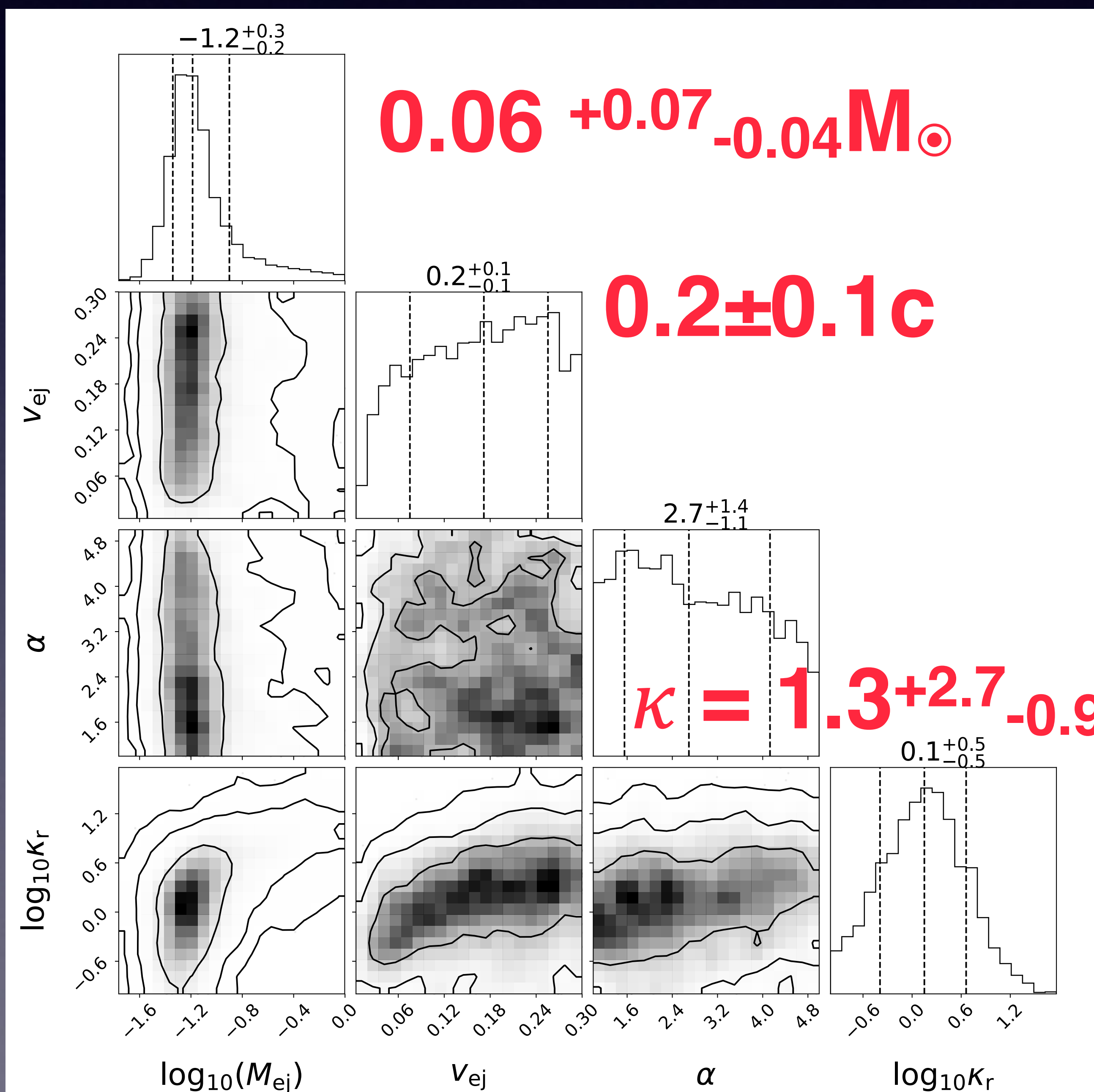

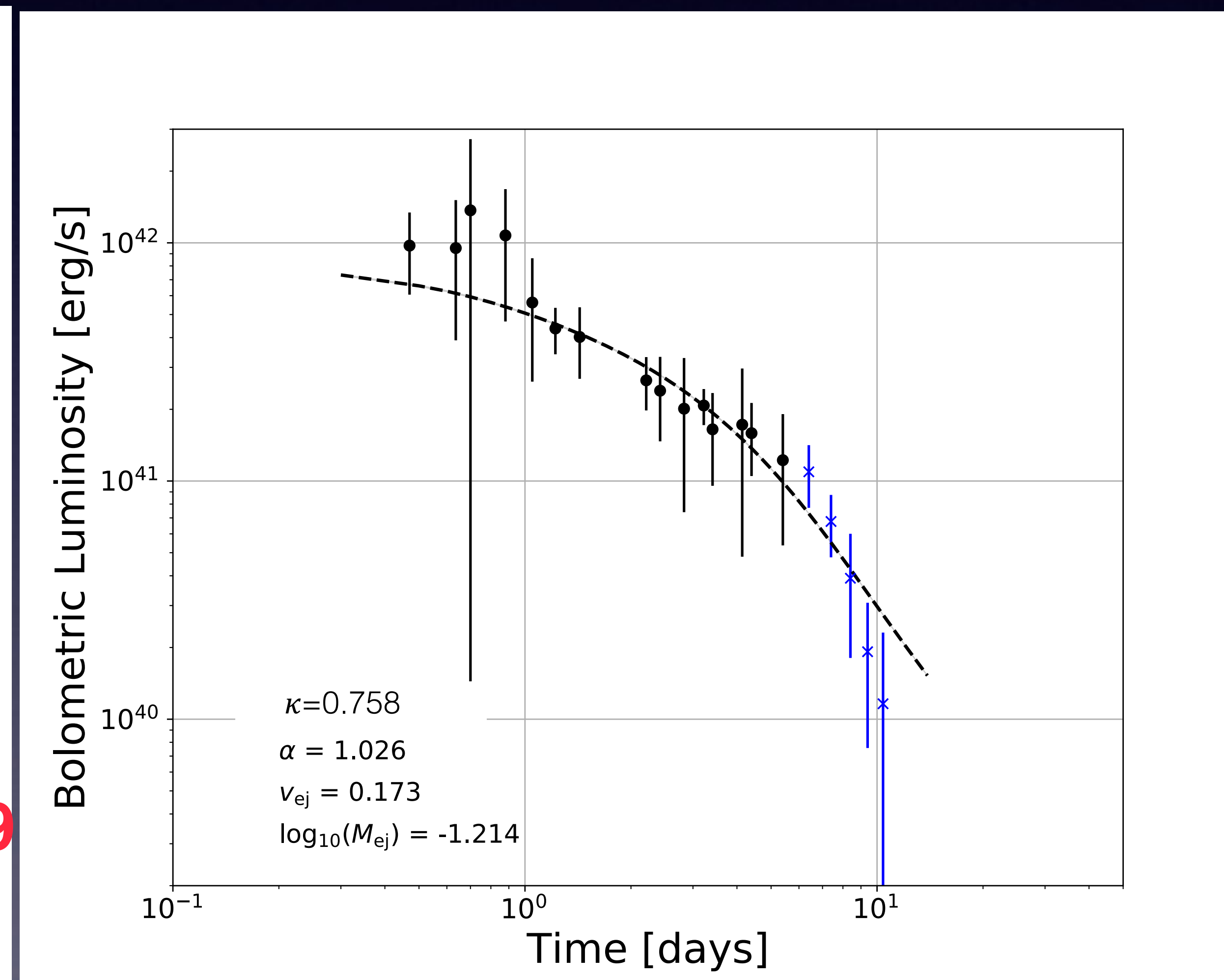

1-component fits

Data :

- Up to 6-7 days : reproduce all photometric data
- SED is (approximately) black body
- L_{bol} after that - uncertain
- No 2nd component ***required***

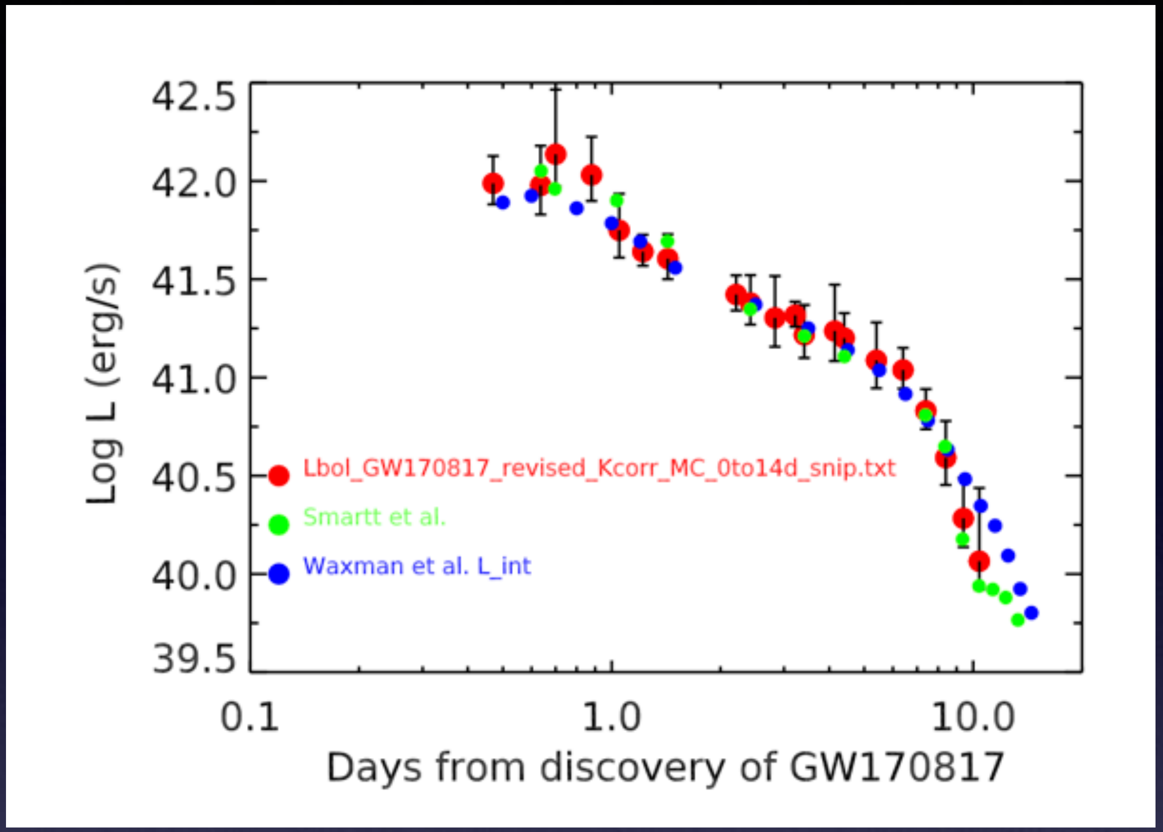

Model :

- Within the uncertainties of powering exponent (beta) and efficiency (Barnes et al.)
- Deposited energy does ***not require*** 2nd component
- Choices can allow it

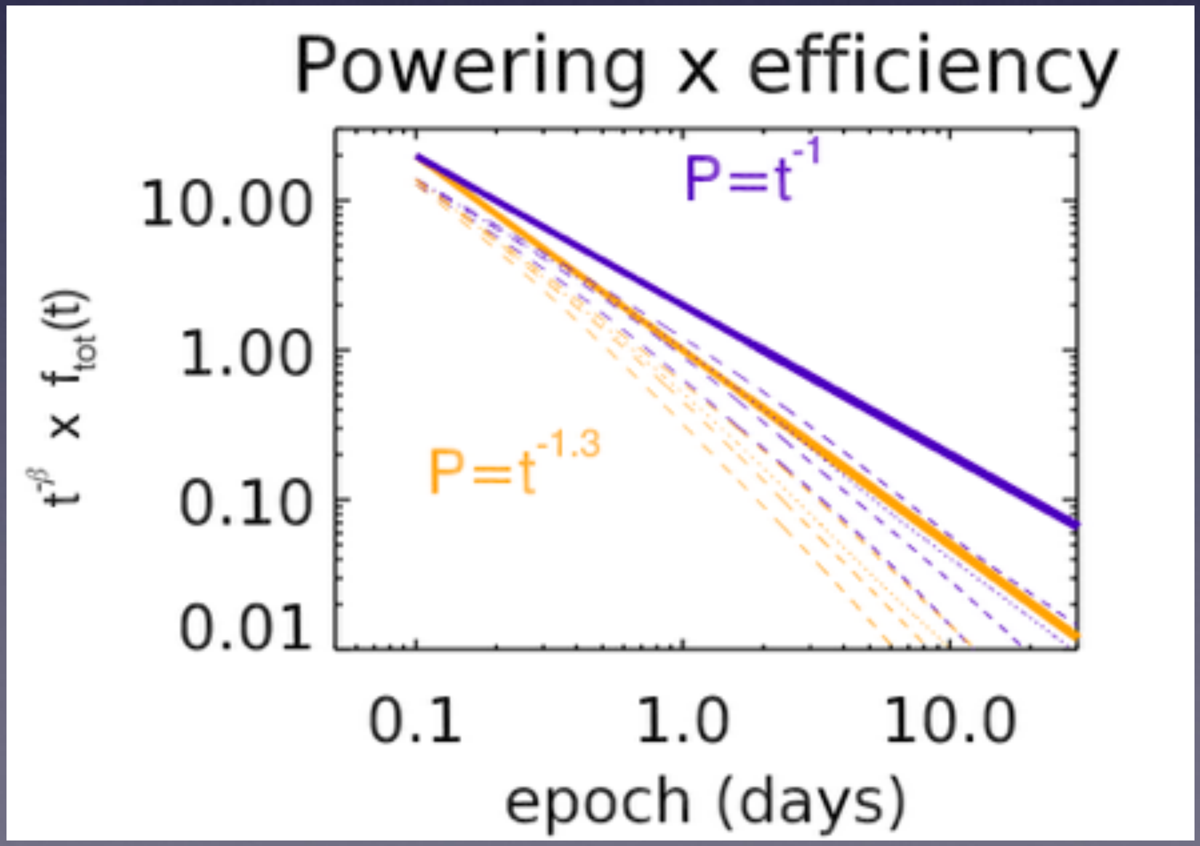

nature

Kasen, Metzger, Barnes, Quartet, Ramirez-Ruiz 2017

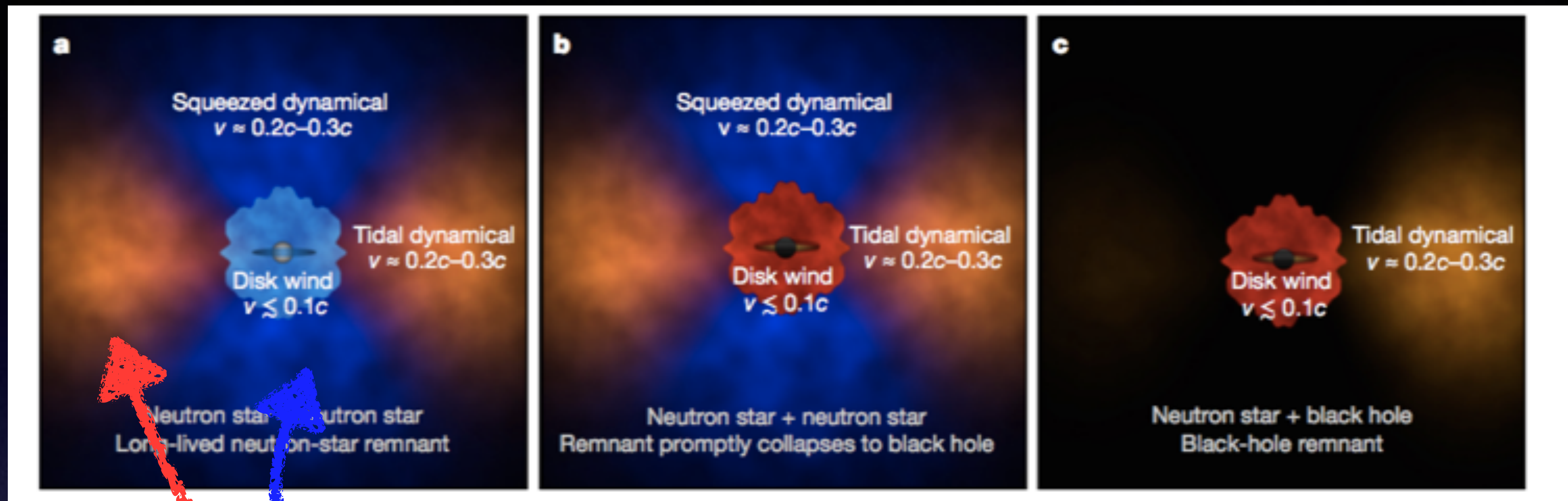

$M = 0.025 M_{\odot}$, $v_k = 0.3c$ and $X_{lan} = 10^{-4}$

$M = 0.04 M_{\odot}$, $v_k = 0.15c$ and $X_{lan} = 10^{-1.5}$

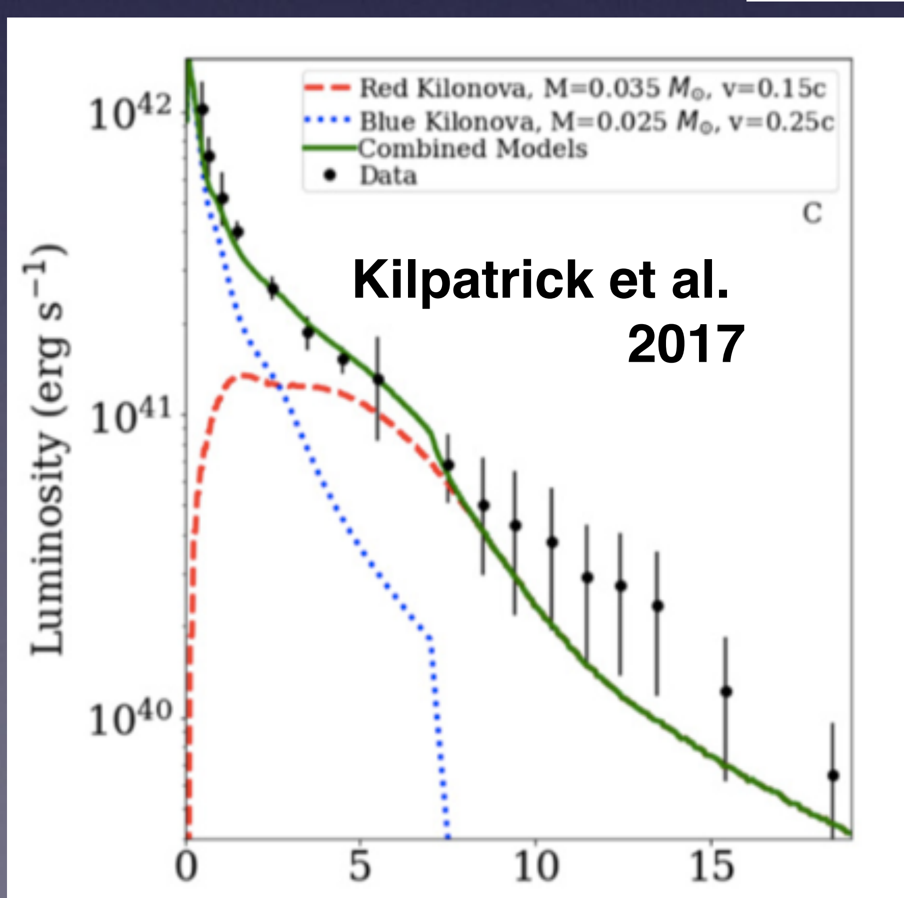

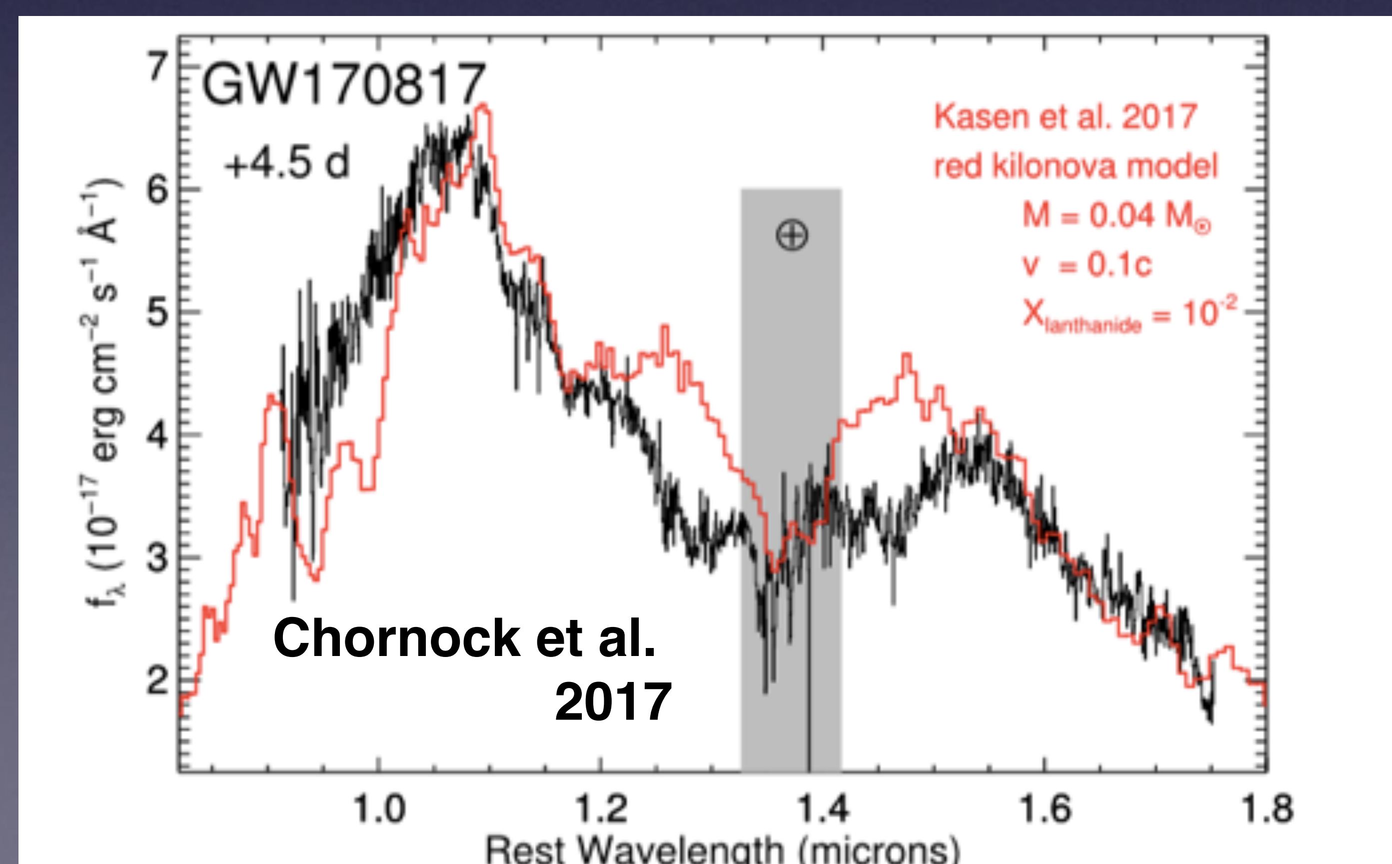

Kasen et al. vs xshooter +4.5d

- Same model - full optical and NIR
- Lacking optical
- Blue component: if thermal would dilute NIR flux

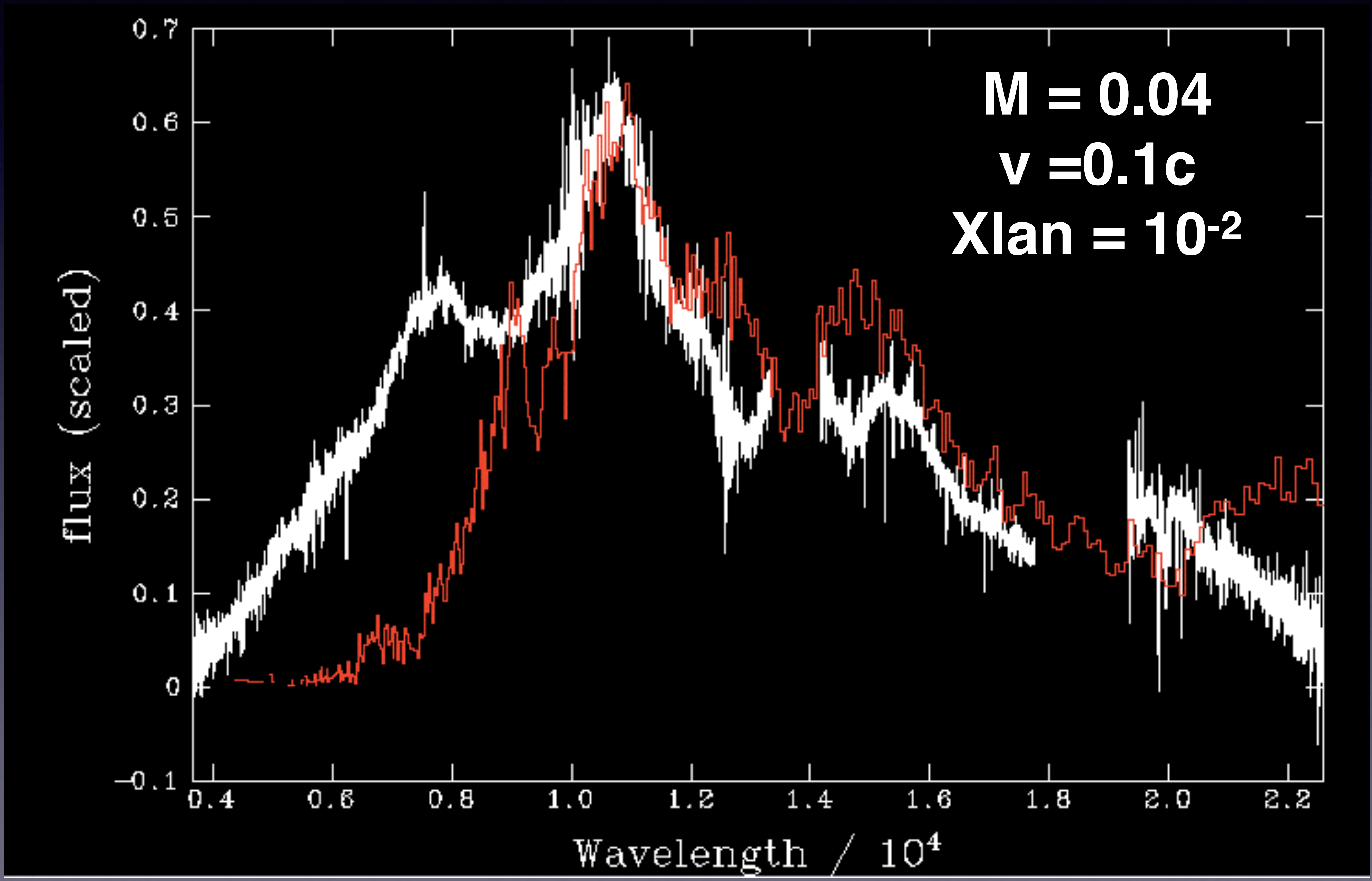

Kasen et al. vs xshooter +4.5d

- Same model - full optical and NIR
- Lacking optical
- Blue component: if thermal would dilute NIR flux

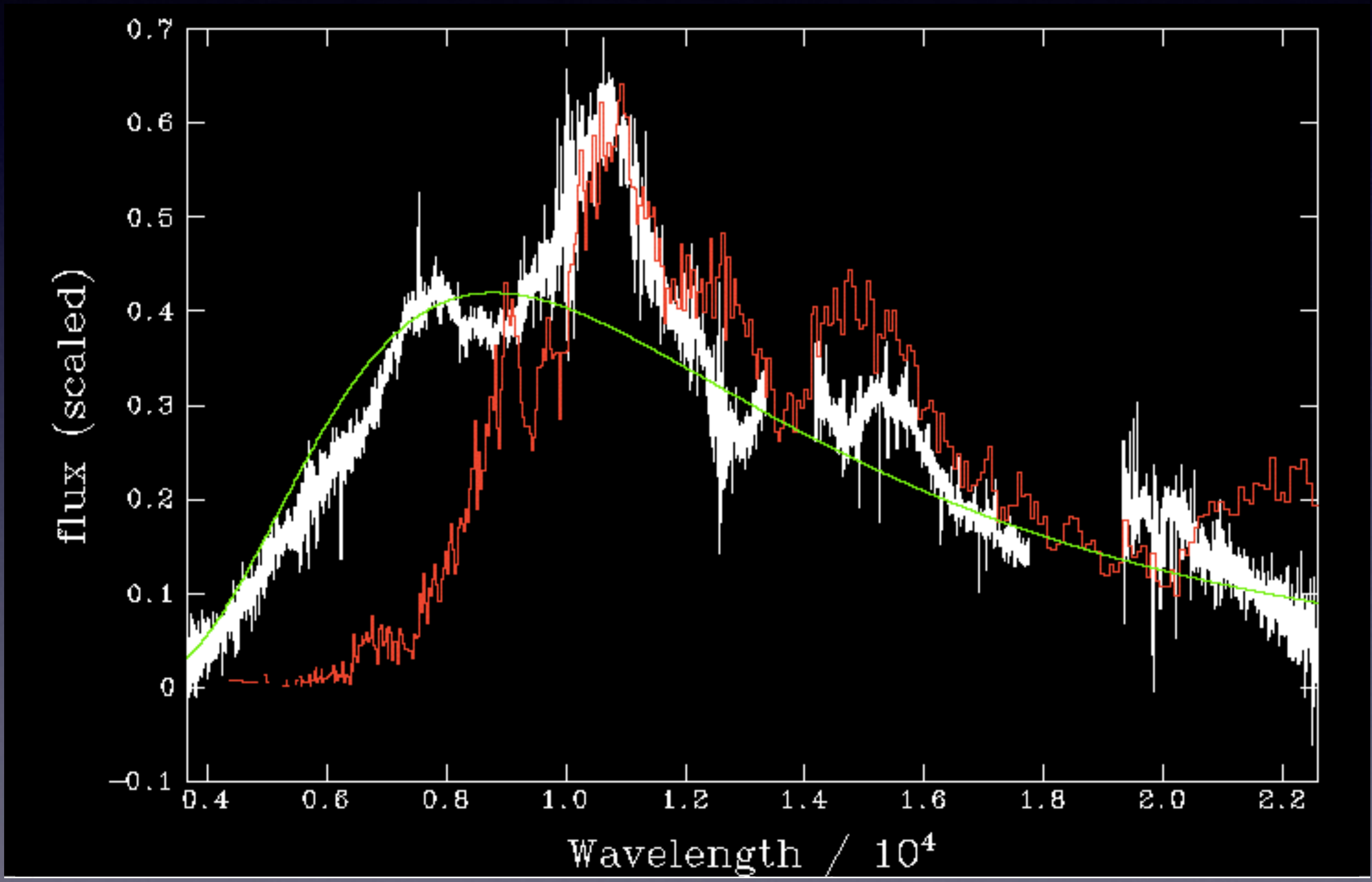

Kasen et al. vs xshooter +4.5d

- Same model - full optical and NIR
- Lacking optical
- Blue component: if thermal would dilute NIR flux

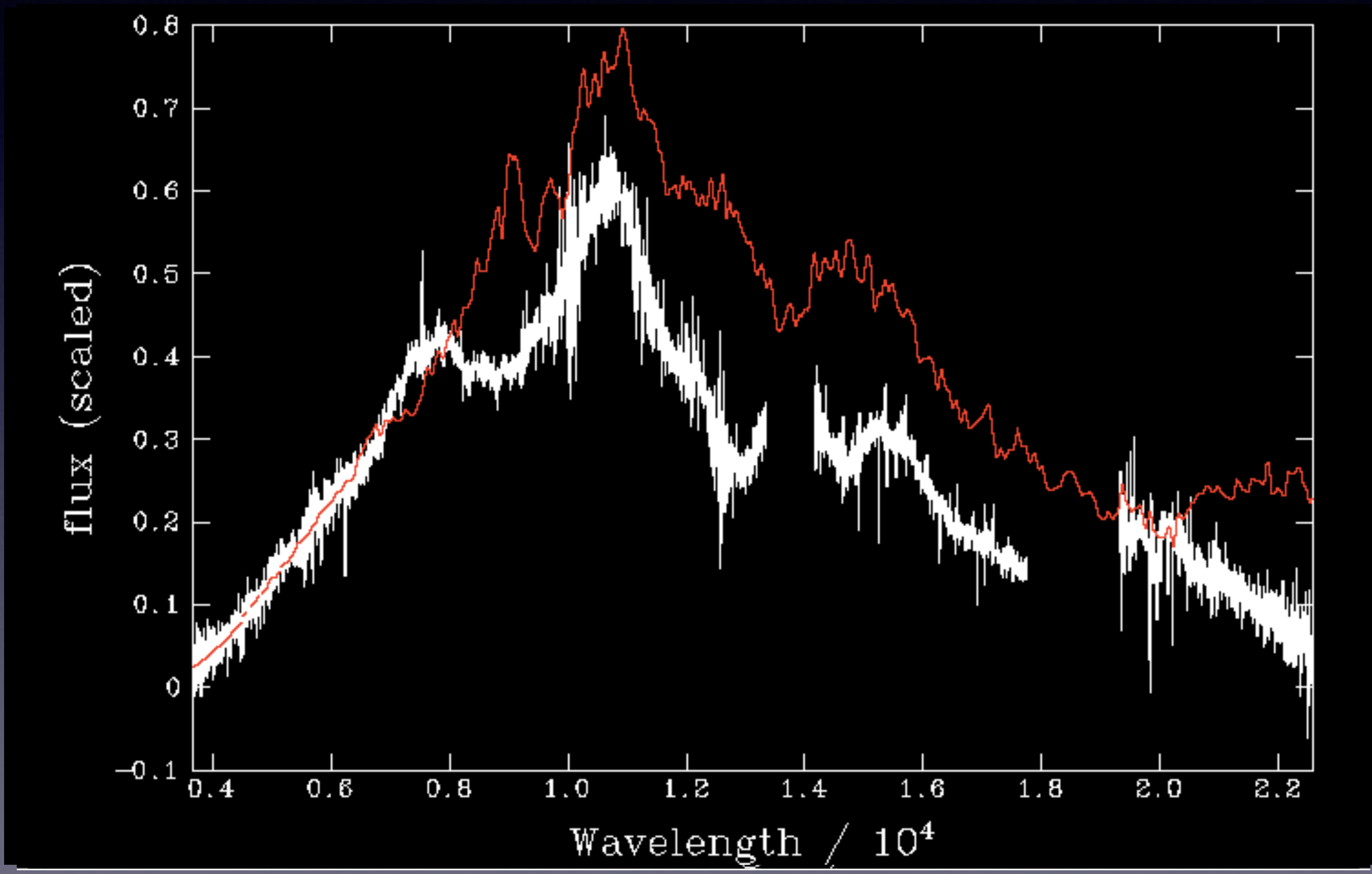

2-component fits - example at +8.4d

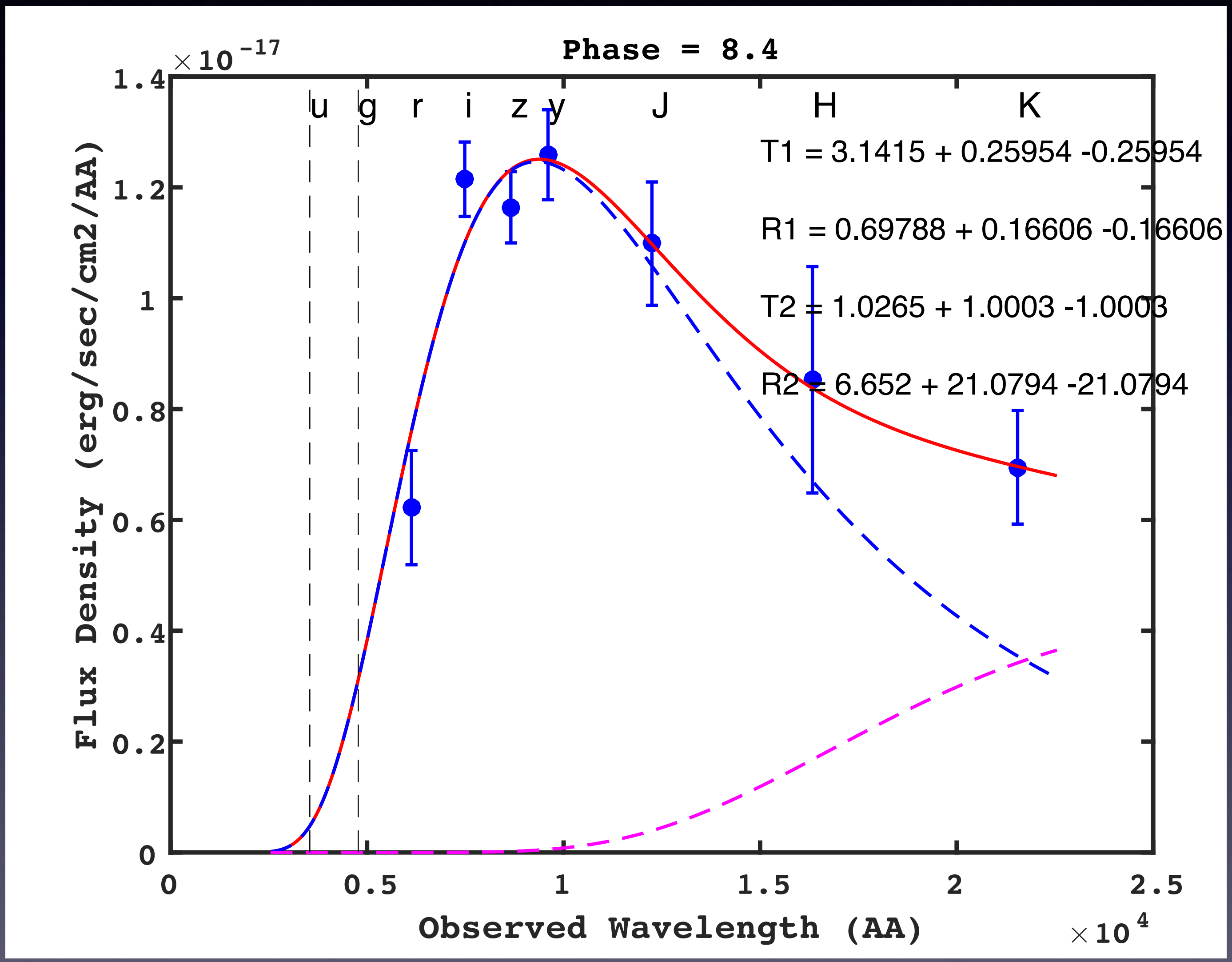

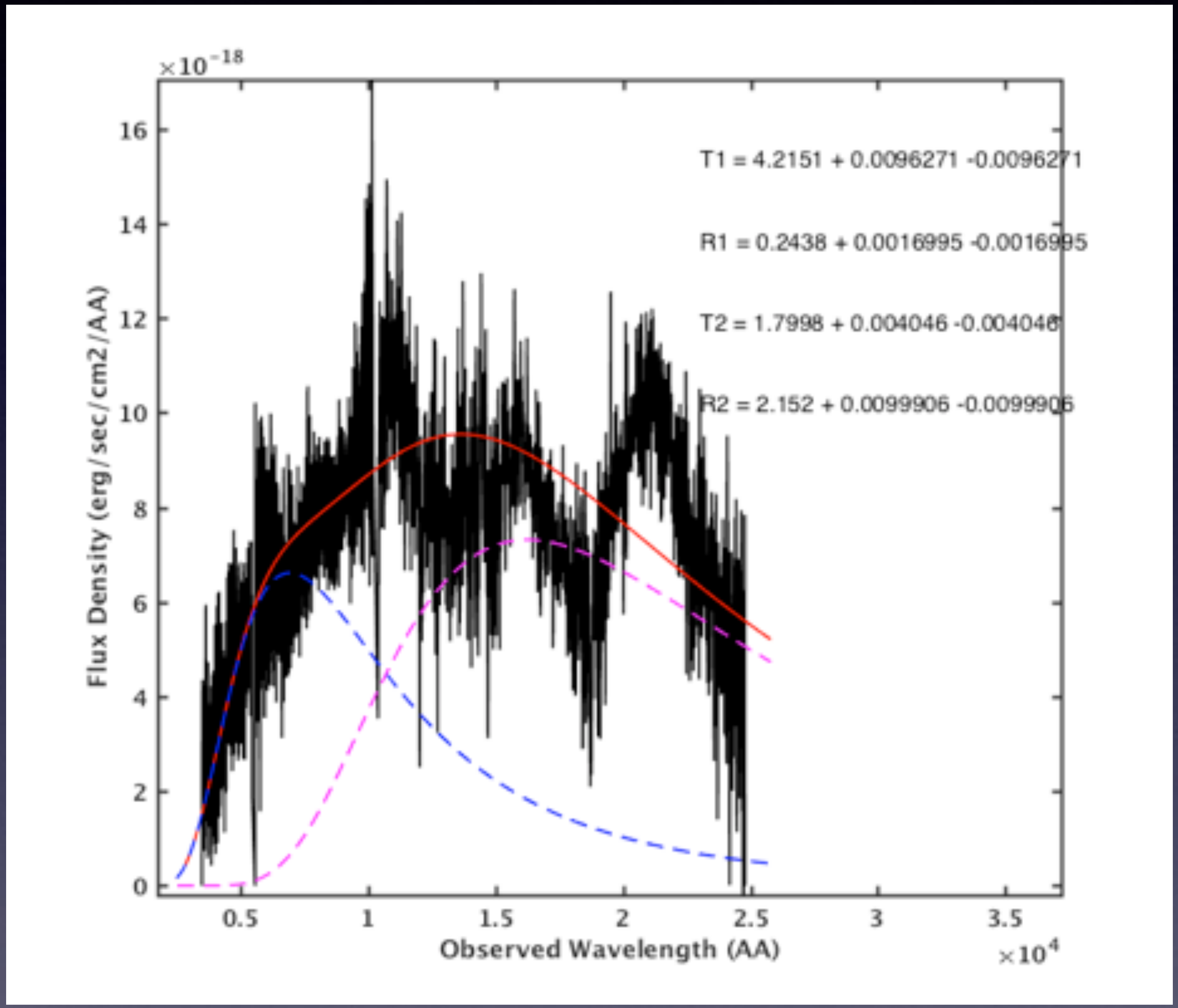

- Reasonable fits at some epochs
- But cool component is not T ~ 2500K (lanthanide recombination)
  - Consistency calculations needed for R, v_{cool}, v_{hot}, T_{cool}, T_{hot}
- Spectra do not appear photospheric after +3-4 days

Xshooter spectra - early

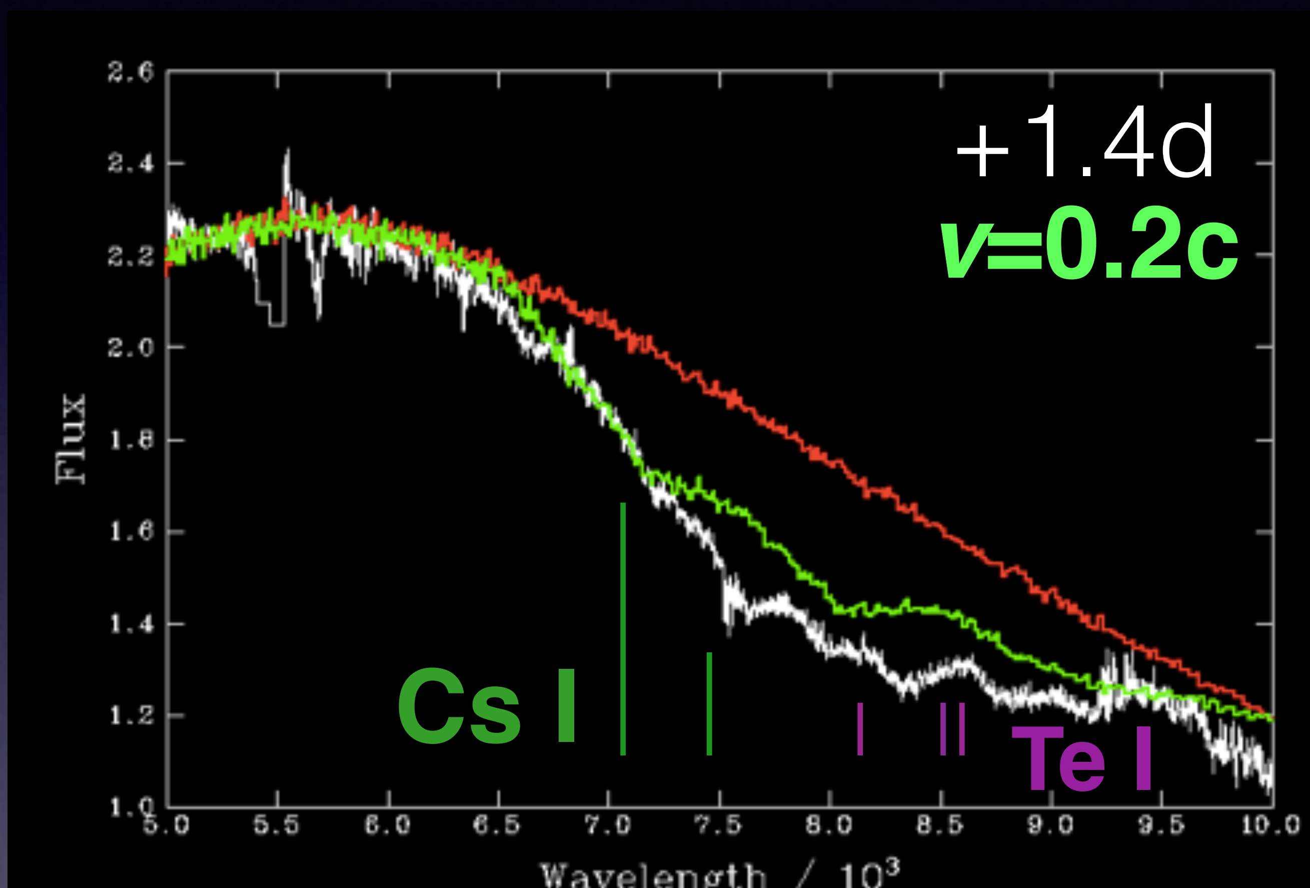

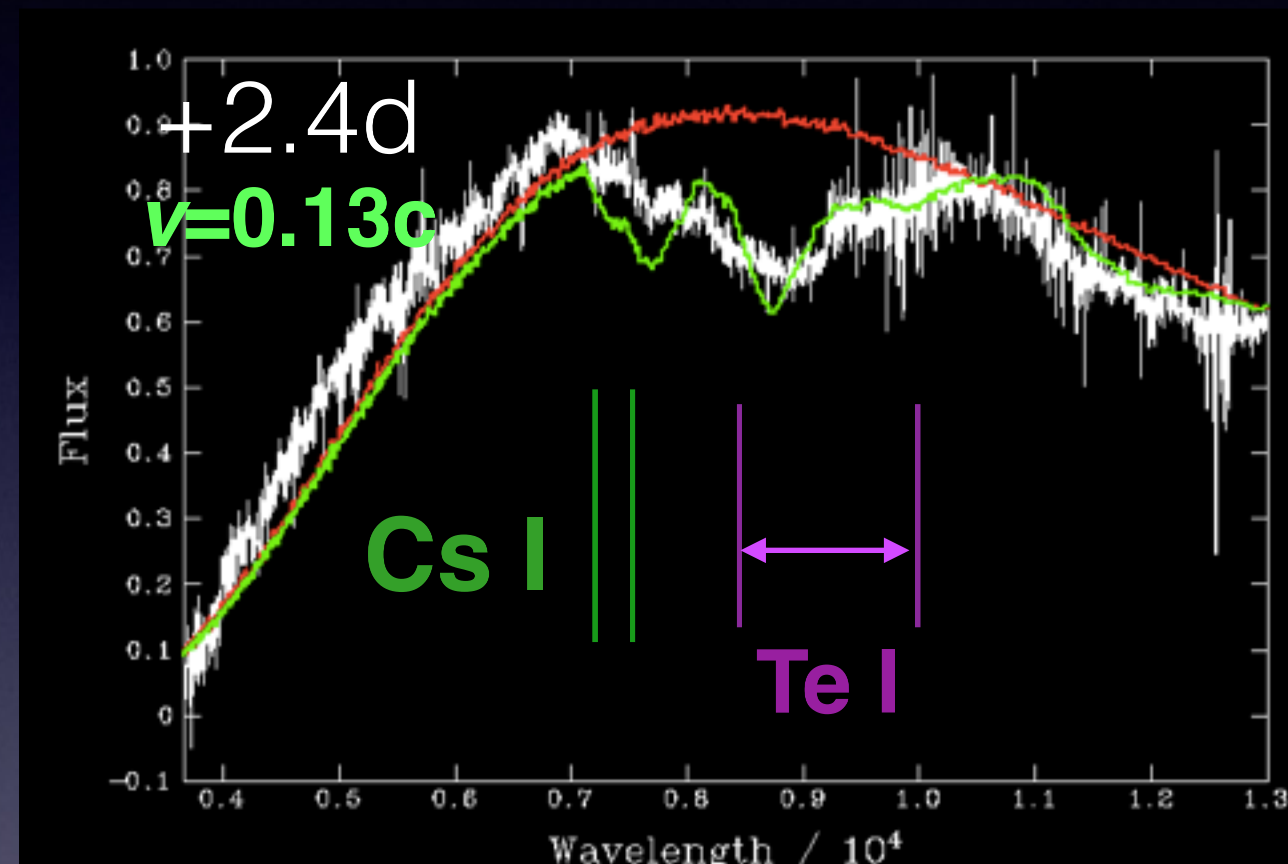

Cs I : resonance doublet 8521, 8943 Angs

Te I : log (*gf*) = 0

Pian et al. 2017, Smartt et al. 2017

TARDIS!
Exploring supernovae made easy

Diffusion phase or optically thin transition

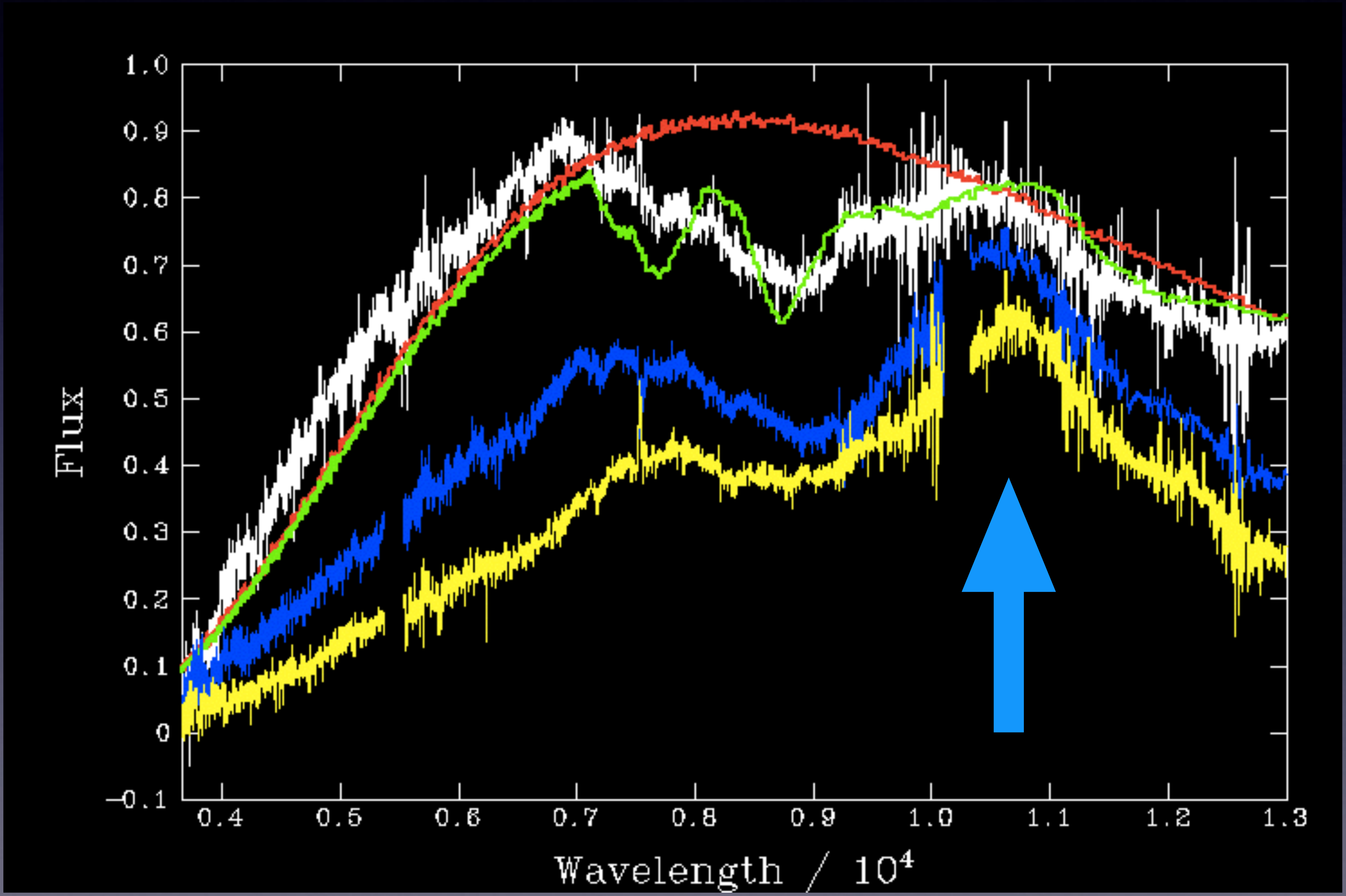

+2.4d

+3.4d

+4.4d

ESO xshooter spectra sequence

- Are all of these optically thick, diffusion phase spectra ?
- Not convincing BBody fits with single Teff beyond about 6 days
- Are we seeing “nebular” phase spectra between 6 to 10.5 days ?

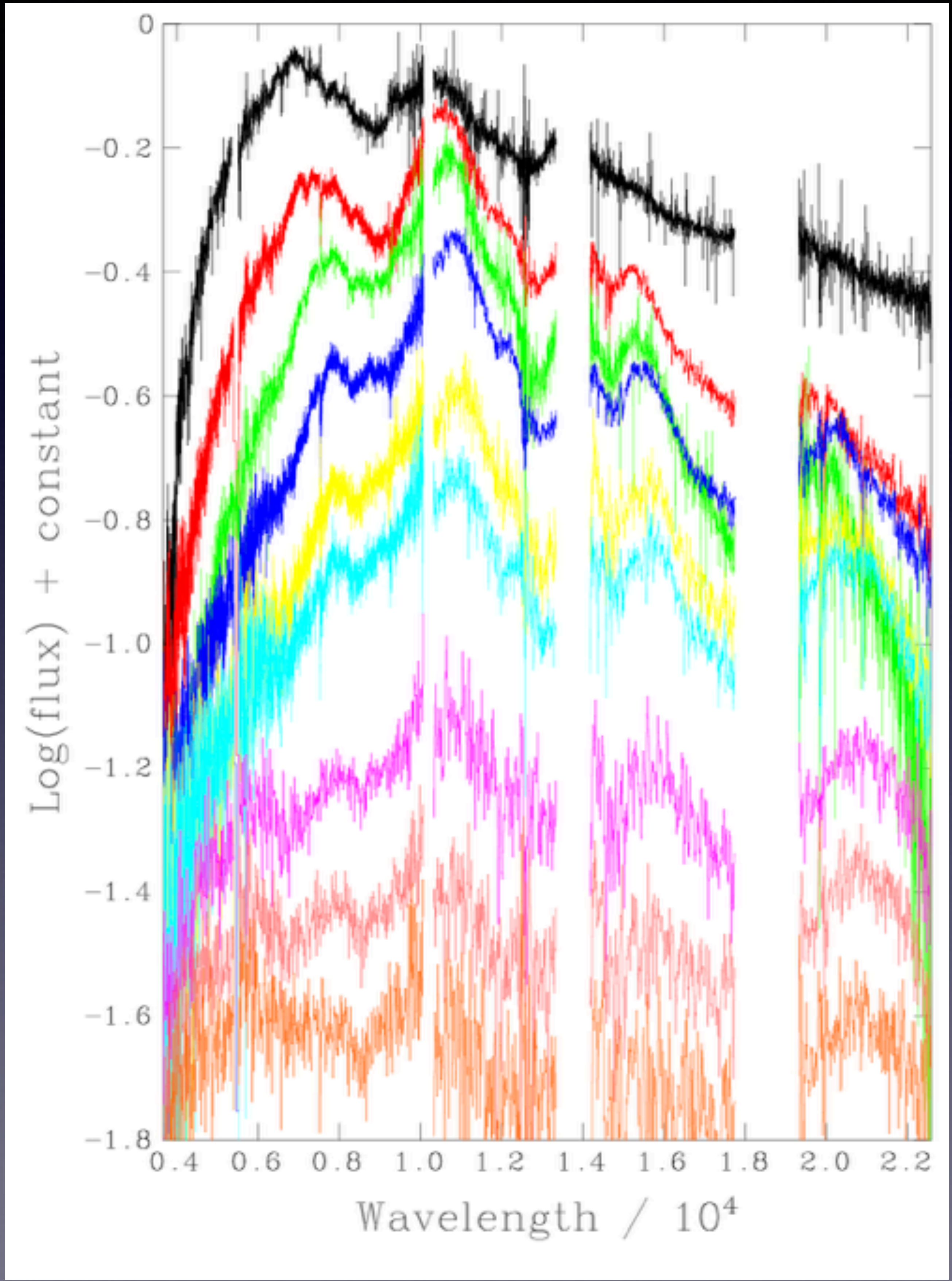

ESO xshooter spectra sequence

- Are all of these optically thick, diffusion phase spectra ?
- Not convincing BBody fits with single Teff beyond about 6 days
- Are we seeing “nebular” phase spectra between 6 to 10.5 days ?

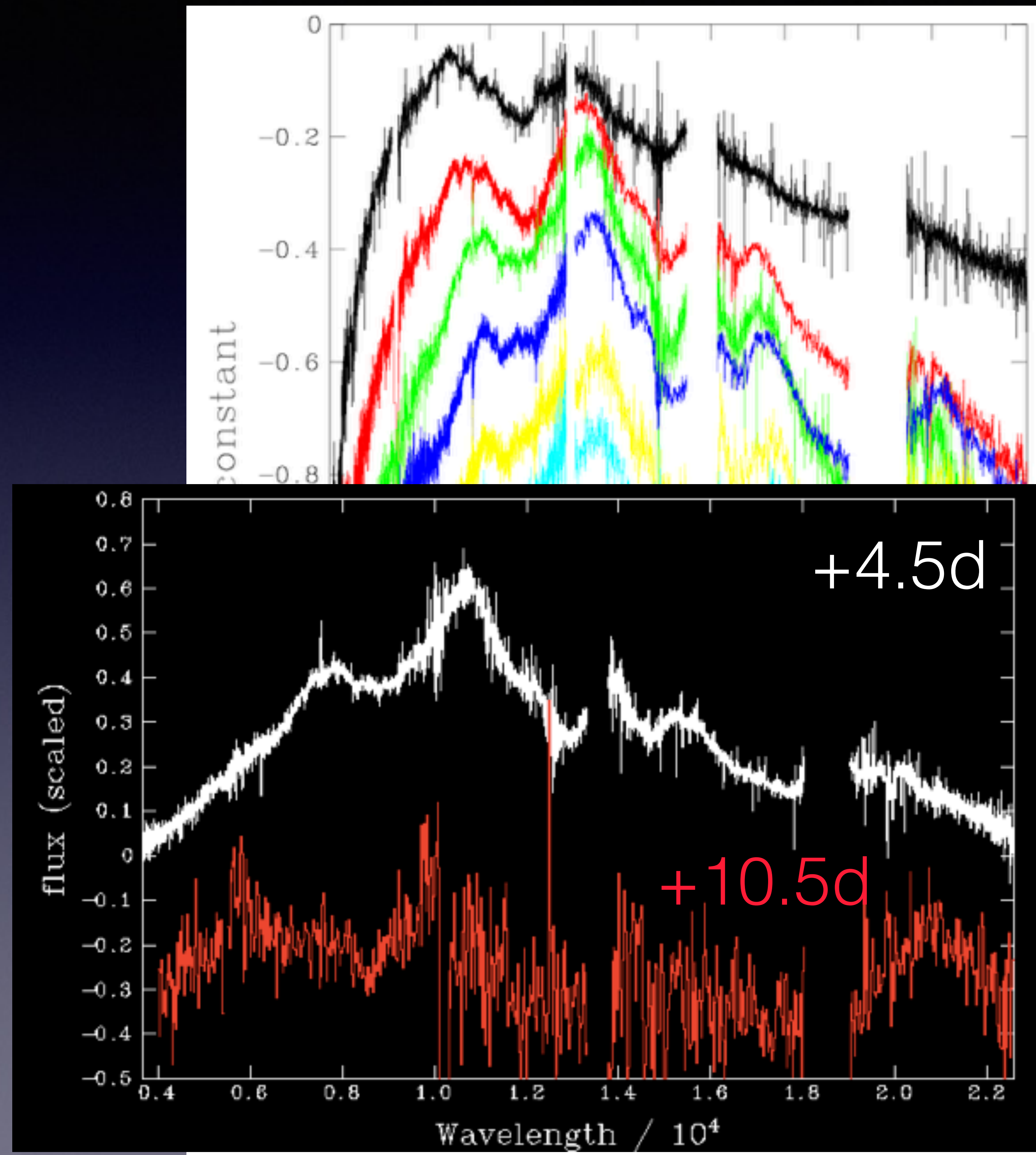

Implications for chemical evolution

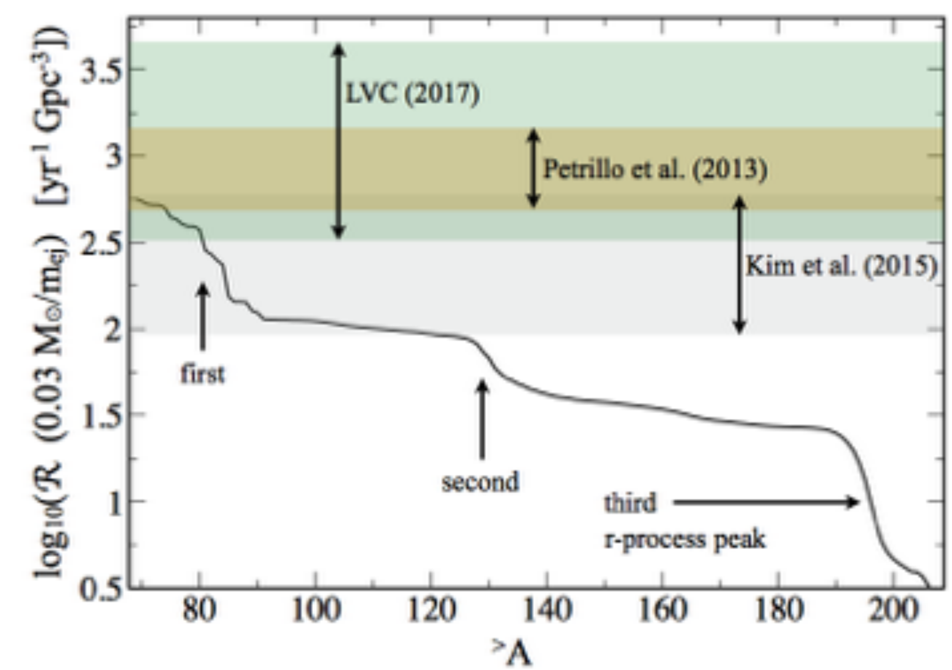

Fig. 5. Needed event rates, scaled to an ejecta mass of 0.03 $M_\odot$, if NSNS mergers are to produce all r-process (in solar proportions) *above a minimum nucleon number* $^{>}A$ (solid black line). Also shown are the estimated rates (90% conf.) for NSNS mergers from the population synthesis study of Kim et al. (2015), the sGRB rates based on SWIFT data from Petrillo et al. (2013) and the LVC estimate based on the first detected NSNS merger event.

Rosswog et al. 2017

Total mass of r-process in Milky Way

$$M_r \sim 17\,000 M_\odot \left(\frac{\mathcal{R}_{\rm NSNS}}{500\,{\rm Gpc^{-3}\ yr^{-1}}}\right)\left(\frac{\bar{m}_{\rm ej}}{0.03 M_\odot}\right)\left(\frac{\tau_{\rm gal}}{1.3\times 10^{10}{\rm yr}}\right).$$

LIGO - Virgo rate of NS-NS mergers

$$R = 1540^{+3200}_{-1220}\ {\rm Gpc^{-3}\ yr^{-1}}$$

Can account for **all** r-process abundances with AT2017gfo type objects
We may have over-production problem !

Conclusions

- L_{bol} recalculated : ok up to 10 days, very uncertain beyond
- Two component models already shown to be plausible - physically motivated, Kasen et al. models (see Monday talks)
- "Blue component" : plausible Cs I and Te I identifications. With $\kappa \sim 0.1 - 1.0$, *ejecta*
- Blue component may be the sole dominant component
- Quantitative fits (simple models) to L_{bol} account for all observed luminosity with one component which is lanthanide free, moderate opacity
- Would require spectra to be out of diffusion stage by 4-6 days - as the reason why poor BB fits

Fin